MASS TRANSFER AND COALESCENCE IN LIQUID-LIQUID SYSTEMS WITH RELEVANCE TO DISPERSION LIQUID MEMBRANE IN HOLLOW FIBER CONTACTOR

By
SMITA MISHRA
ENGG01201004017

BHABHA ATOMIC RESEARCH CENTRE, MUMBAI

A thesis submitted to the

Board of Studies in Engineering Sciences

In partial fulfillment of requirements
for the Degree of
DOCTOR OF PHILOSOPHY
of
HOMI BHABHA NATIONAL INSTITUTE

February, 2018

Homi Bhabha National Institute[1]

Recommendations of the Viva Voce Committee

As members of the Viva Voce Committee, we certify that we have read the dissertation prepared by Smita Mishra entitled "Mass transfer and coalescence in liquid-liquid systems with relevance to dispersion liquid membrane in hollow fiber contactor" and recommend that it may be accepted as fulfilling the thesis requirement for the award of Degree of Doctor of Philosophy.

Chairman – Dr. S. B. Roy		**Date:** 9. 10. 2018
Guide / Convener – Prof. V. A. Juvekar		**Date:** 09/10/2018
Co-guide - Dr. S. Mukhopadhyay		**Date:** 09/10/2018.
Examiner – Prof. S. De	Sirshendu De	**Date:** 09/10/2018
Member 1- Dr. R. N. Singh		**Date:** 09/10/2018
Member 2- Dr. G. Sugilal		**Date:** 09/10/2018

Final approval and acceptance of this thesis is contingent upon the candidate's submission of the final copies of the thesis to HBNI.

I/We hereby certify that I/we have read this thesis prepared under my/our direction and recommend that it may be accepted as fulfilling the thesis requirement.

Date: 09/10/2018

Place: Mumbai

09/10/2018
Co-guide (if applicable)

Guide 09/10/2018

---

[1] This page is to be included only for final submission after successful completion of viva voce.

DECLARATION

I, hereby declare that the investigation presented in the thesis has been carried out by me. The work is original and has not been submitted earlier as a whole or in part for a degree / diploma at this or any other Institution / University.

Smita Mishra

List of Publications arising from the thesis

Journal

1. “A Process intensified technique of Liquid Membrane employed in in-house Hollow Fiber Contactor”, Smita Dixit, S. Mukhopadhyay, K.T. Shenoy and V. A. Juvekar, Desalination and water treatment, 2017, 79, 40-48.

2. “A mathematical model for size and number scale up of hollow fiber modules for the recovery of uranium from acidic nuclear waste using the DLM technique”, S. Dixit, R. Chinchale, S. Govalkar, S. Mukhopadhyay, K. T. Shenoy, H. Rao, S. K. Ghosh, Sep. Sci. Technol., 2013, 48, 2444-2453.

3. “A mathematical model for pertraction of uranium in hollow fiber contactor using TBP”, S. Dixit, S. Mukhopadhyay, S. Govalkar, K. T. Shenoy, H. Rao, S. K. Ghosh, Desalination and Water Treatment, 2012, 38, 195-206.

4. “Extraction of zirconium from simulated acidic nitrate waste using liquid membrane in hollow fiber contactor”, G. Pandey, M. Paramanik, S. Dixit, S. Mukhopadhyay, R. Singh, S.K. Ghosh, K.T. Shenoy, Desalination and water treatment, 2017, 90, 63-69.

5. “Characterization of emulsions containing Tri-isoamyl phosphate (TiAP) and Tri-n-butyl phosphate (TBP) with regard to emulsion pertraction in hollow fiber contactor”, Smita Dixit, S. Mukhopadhyay, V.A. Juvekar, communicated in Hydrometallurgy, Manuscript no. HYDROM_2018_751.

Conferences

1. A mathematical model for recovery of uranium from acidic nuclear waste using DLM in Hollow fiber contactor; S. Dixit, R. Chinchale, S. Govalkar, S. Mukhopadhyay, K.T. Shenoy, H. Rao, S.K. Ghosh; Poster presentation in SESTEC 2012 at Mumbai, India.

2. Bench scale demonstration and strip concentration for recovery of uranium from uranium metal plant raffinate using HFDLM technique; S. Dixit, R. Chinchale, A.U. Renjith,

S. Mukhopadhyay, K.T. Shenoy and S. K. Ghosh; Oral presentation in MEMSEP-2013 at Multipurpose Hall, BARC Training School Hostel, Trombay, Mumbai during September-2013.

3. Coalescence in Liquid-Liquid systems: Experimental validation of theoretical model to predict the rate of Coalescence; Smita Dixit, Sulekha Mukhopadhyay, K.T. Shenoy, V. A. Juvekar; Poster presentation in SESTEC-2014 at Anushaktinagar 25-28 February, 2014.

4. A Process intensified technique of liquid membrane employed in in-house hollow fiber contactor; S. Dixit, R. Chinchale, S. Mukhopadhyay, K.T. Shenoy, S.K. Ghosh; Oral presentation session of Trombay Symposium on Desalination and Water Reuse 2015 held at Homi Bhabha Science Centre, Mankhurd, Jan 22-23, 2015 .

5. Extraction of zirconium from simulated acidic nitrate waste using liquid membrane in hollow fiber contactor; G. Pandey, R. Chinchale, A.U. Renjith,, S. Dixit, S. Mukhopadhyay, K.T. Shenoy, S.K. Ghosh; Poster presentation session of Trombay Symposium on Desalination and Water Reuse 2015 held at Homi Bhabha Science Centre, Mankhurd, Jan 22-23, 2015.

Others

1. “Drop-interface coalescence in liquid-liquid systems: effect of surface active agents”, S. Dixit, S. Mukhopadhyay, K.T. Shenoy, V. A. Juvekar, BARC Newsletter, 2015, July-August 2015.

2. Bench Scale demonstration of recovery of uranium from acidic nuclear waste using dispersion liquid membrane in hollow fiber contactor; S. Dixit, S. Mukhopadhyay, K.T. Shenoy and S. K. Ghosh; BARC Report External BARC/2014/E/021

Smita Mishra

Dedicated to

KAUSTUBH

ACKNOWLEDGEMENTS

The present work on *Mass transfer and coalescence in liquid-liquid systems with relevance to dispersion liquid membrane in hollow fiber contactor* has been carried out at Department of Chemical Engineering, Indian Institute of Technology, Bombay and Chemical Engineering Division, BARC, Mumbai. Here I would like to express my thankfulness to them, who have made valuable contributions to this work.

I wish to express my most sincere gratitude to my guide Prof. V. A. Juvekar at IIT, Bombay for his guidance, encouragement and support. I am also deeply indebted to my coguide Dr. S. Mukhopadhyay at Bhabha Atomic Research Centre, Mumbai for her valuable support. I am also thankful to Mr. K.T. Shenoy from Chemical Engineering Division, Bhabha Atomic Research Centre, Mumbai for his valuable suggestions during technical meetings.

Finally, I would like to thank my colleagues of chemical engineering division, BARC who have helped me in many ways to complete this work.

Smita Mishra

CONTENTS

SYNOPSIS

Processes involving facilitated transport through dispersion liquid membranes in hollow fiber contactors [1] is advantageous over conventional processes for separation of valuable metals from lean streams due to a number of reasons. These include simultaneous extraction and stripping, continuous replenishment of the organic phase immobilized in pores of polymeric membrane and fast disengagement of the loaded dispersion after the mass transport operation. In the liquid membrane based transport processes [2-3], diffusion path length inside the wetted pore is important in deciding the rate of extraction. Diffusion path length is related to the fraction of the pore length wetted by the organic liquid membrane phase. Hence, estimation of fraction of the pore length wetted by the organic phase is useful in design and scale up of this process. A mathematical model has been developed for determining the rate of transport through the membrane and the extent of extraction through the contactor as a function of the fraction of the pore length wetted by the organic membrane phase. Since, the diffusion coefficient of the metal carrier complex in the organic membrane phase is significantly lower than that of the metal ions in the aqueous feed phase, the overall rate of transport decreases rapidly as the fraction of the pore wetted by the organic phase increases. It is therefore possible to estimate the fraction of the pore length wetted by the organic membrane phase from the rate of extraction through the developed model. This estimation is also helpful to get an idea of the stability of liquid membrane phase in the pores of the given polymeric membrane. The data has been generated for extraction of uranium from nitrate medium in countercurrent once-through mode using hollow fiber dispersion liquid membrane. Effect of various hydrodynamic and chemical parameters such as carrier concentration, presence of surfactant, initial feed uranium concentration, feed acidity and varying aqueous to organic ratio in dispersion has been studied. Water-in-oil dispersion of 1 M $NaHCO_3$ in dodecane, containing 30 % v/v Tri-n-butyl phosphate (TBP), is used as extractant. For polysulfone lumen, the model estimates the fraction of the pore length wetted by the organic membrane phase as 40 %. Similarly, estimation has been made for polypropylene lumen and the entire pore length has been found wetted by the organic membrane phase. Preliminary data on liquid-liquid equilibria has been generated and utilized for model prediction. The model has been found useful for prediction of the performance of polysulfone and polypropylene hollow fiber contactors and also for scale up of these contactors.

The efficiency of mass transfer of the metal to the strip phase depends on the interfacial area of the dispersion which in turn depends upon its stability. For efficient mass transfer, the drop size should be as small as possible. However, due to coalescence, drop size continuously increases as the dispersion moves through the contactor, thereby reducing the contacting efficiency. Low rates of coalescence are desirable to achieve high stability of dispersion. The rate of drop coalescence depends on the nature and concentration of the adsorbed species at the drop-organic phase interface [4]. When the organic phase contains more than one surface active species, there would be competition among them to occupy interface. Moreover, different surface active species, depending on the structure of their hydrophobic tail, have different ability to prevent coalescence. In the present work, two different techniques have been used to study stability of emulsion. In the first, time of fall of drop of aqueous phase through an organic pool and its coalescence with its bulk phase has been studied with a typical liquid-liquid extraction system. The second technique involves use of ‘Turbiscan Online’. This is an optical instrument to characterize the liquid dispersions using multiple light scattering techniques [5]. It provides the details of back scattering and transmission through the dispersion. The intensity of the backscattered light depends on three parameters: diameter of the drop, their volume fraction and the relative refractive index between the dispersed phase and continuous phase. Therefore, any change due to a variation of the drop size is detected by the optical device. Characterization of dispersion of water in oil containing tri-n-butyl phosphate and its homologue tri-iso-amyl phosphate, has been done using Turbiscan Online to assess feasibility of this dispersion for dispersion liquid membrane extraction of U(VI) in hollow fiber contactor. Effect of carrier concentration, nature of the strip phase, power input during emulsification and effect of surfactant on stability of the dispersion has been studied using Turbiscan Online. It is observed that the carrier competes with the surfactant (SPAN80) to occupy the interface. Therefore, at high concentration of the carrier, the interface is almost fully occupied by the carrier molecules. However, carrier molecules have poor ability to prevent coalescence. Hence, high concentration of the carrier is detrimental to the stability of the emulsion, although it enhances the rate of transport. Also, among the carriers, tri-iso-amyl phosphate provides better stability to emulsion than tri-n-butyl phosphate due to its branched tail. Based on these studies, it was possible to arrive at the optimal formulation of the dispersion and method of emulsification.

The layout of the thesis is as follows,

1. Studies are conducted on drop coalescence in order to assess the stability of dispersions for the extractant, tri-n-butyl phosphate and tri-iso-amyl phosphate with aqueous phases as distilled water and 0.1 M $NaHCO_3$.
2. A model has been developed to predict the rate of transport of metal ion using hollow fiber contactor in liquid membrane mode. Model estimates the fraction of the pore length wetted by the organic liquid membrane.
3. Effect of material of construction of hollow fiber viz. polysulfone and polypropylene on rate of transport of uranium through hollow fiber dispersion liquid membrane has been studied.

4. Effect of type of extractant viz. tri-n-butyl phosphate and its homologue tri-iso-amyl phosphate on rate of transport of uranium through hollow fiber dispersion liquid membrane has been studied.
5. Scale-up aspects of hollow fiber contactor has been investigated with the help of developed model for both the contactor made of polysulfone and polypropylene.

In Chapter 1, literature review for the present work has been discussed. In Chapter 2, time of fall of drop of aqueous phase through an organic pool and its coalescence with its bulk phase has been studied with a typical liquid-liquid extraction system. Characterization of dispersion of water in oil containing TBP and TiAP has been done using Turbiscan Online to assess the stability of the dispersion for extraction of U(VI) in hollow fiber contactor. Effect of carrier concentration, nature of the strip phase, power input during emulsification and effect of surfactant on stability of the dispersion has been studied using Turbiscan Online. Based on these studies, an optimal formulation of the dispersion and method of emulsification has been arrived at.

The droplet size in the presence of TBP is found to be greater than that in TiAP. This is due to the fact that the longer as well as branched isoamyl chains of TiAP produce greater steric hindrance to coalescence than the linear butyl chains of TBP. To study the effect of carrier and SPAN 80 together on the drop size, dispersions were prepared by addition of 2% v/v of SPAN80 during the emulsification. Distilled water (DW) and 0.1 M $NaHCO_3$ were used as the dispersed phases. Different concentrations of TiAP in the range from 0 to 10% v/v in dodecane were used. It is seen that with increase in the concentration of TiAP, the drop diameter increases. This is because of possible displacement of Span 80 by TiAP due to its high concentration. Since TiAP are not as effective as SPAN 80 to prevent drop coalescence, due to their shorter hydrocarbon chains, the drop size increases as TiAP concentration in the solution increases. A similar behavior is also observed with TBP.

It is observed that the drop diameter decreases with increase in concentration of SPAN 80 until a threshold concentration is reached, beyond which increase in SPAN 80 has no effect on drop diameter. The concentration of SPAN 80 needed to reach the threshold increases with increase the concentration of the carrier. This can be understood from the fact that the carrier and the surfactant compete with each other to occupy the interface. At low concentration of surfactant, the interfacial concentration is dominated by the carrier leading to larger drop diameter. Beyond the threshold concentration, the interfacial concentration is dominated by the surfactant and hence drop size does not reduce beyond the threshold value. Higher, is the concentration of the carrier, greater is the concentration of the surfactant needed to displace it and hence the threshold value is higher. Both TBP and TiAP show similar trend.

In Chapter 3, a mathematical model has been developed for determining the rate of transport through the membrane and the extent of extraction through the contactor. Model also estimates the fraction of the pore length wetted by the organic membrane phase [6]. The model is validated for extraction of uranium from nitrate medium in recirculating and once-through mode using dispersion liquid membrane. Developed mathematical model can be used for prediction of extraction rate of other ions and other types of polymeric membrane. The data needed for the design are, the carrier mediated distribution coefficient of the ion in the organic phase, diffusion coefficient of the ion in the aqueous phase and diffusion coefficient of the ion-carrier complex in the organic phase. Along with pore diameter, pore length and pore area, fraction of the pore length wetted by the organic phase is also needed. This length will be determined by wettability of the polymeric membrane for organic liquid membrane phase. For prediction, estimation of mass transfer coefficient of feed and organic phase has been estimated with the help of empirical correlations and physical properties of the system. Effect of polymeric support on transport of uranium from lean acidic nuclear waste streams using dispersion liquid membrane in hollow fiber contactor has been studied with microporous Polysulfone, PS and Polypropylene, PP fibers. Water-in-oil dispersion of 1 M $NaHCO_3$ in dodecane containing 30 % v/v Tri-n-butyl phosphate (TBP) is used as extractant. Five different hollow fiber contactors were used. Two contactors with PS lumens, PS1 and PS2, were supplied by Desalination Division, BARC. The other three contactors, consisting of polypropylene lumens, PP1, PP2 and PP3 (make: Liqui-Cel® 2.5x8") were purchased from Membrana, Germany. Using PS1 and PS2 contactor, percent extraction of 28 % and 40 % has been achieved, respectively, in single pass of the feed solution. Similar studies have been conducted using microporous contactors with polypropylene lumen (PP1, PP2 and PP3) and percent extraction of 55 %, 75 % and 95 % has been observed, respectively. Prediction ties in well with the data.

Since the diffusion coefficient of the metal-carrier complex in the organic phase is much lower than that of the metal ion in the aqueous feed phase, mass transfer resistance inside membrane is controlling. Through model, it is found that 40 % of the pore length is wetted by the organic phase in PS2 contactor. Similarly, for PP1, consisting hydrophobic polypropylene lumen, α is estimated to be 1.1. This implies that in the case of PP membrane, the entire length of the pore is wetted by the organic phase. Value of α greater than one, implies that part of the liquid protrudes out from the pore in the form of convex meniscus. A small extent of leakage of the organic phase in the feed is also expected. It was indeed observed in PP membrane, whereas no perceptible leakage was detected with PS membrane. In spite of this drawback, PP1 module is found to exhibit greater extent of extraction than PS1 and PS2. This is because, the fiber wall thickness (L) of PP lumen is one order of magnitude less than that of the PS lumen as mentioned in Table 1. Hence, the reduction in the rate of diffusion of uranium ions due to higher value of α in PP lumen is overcompensated by its shorter pore length, L.

In Chapter 4, effect of type of extractant viz. tri-n-butyl phosphate and its homologue tri-iso-amyl phosphate has been studied on rate of transport of uranium through hollow fiber dispersion liquid membrane. TiAP is a higher homologue of TBP, which inherits its qualities of selective extraction of U(VI) and remove the limitations of chemical degradation and entrainment in aqueous phase. Through generated equilibrium distribution data of U(VI), we get the value of equilibrium constant, K_{eq} as 8.93 M^{-4}. Under the same conditions, K_{eq} for U(VI)-TBP system is also measured and found as 6.36 M^{-4}. This shows that TiAP has little bit greater affinity for U(VI), compared to TBP. The equilibrium constant for acid transport has been estimated as 0.16 M^{-2} for TBP and 0.20 M^{-2} for TiAP. So, the extent of association of nitric acid with TiAP is similar to that with TBP.

Comparison of the extraction efficiency for once through mode operation of HFDLM is shown in Figure 1 for both TiAP and TBP as the ligand.

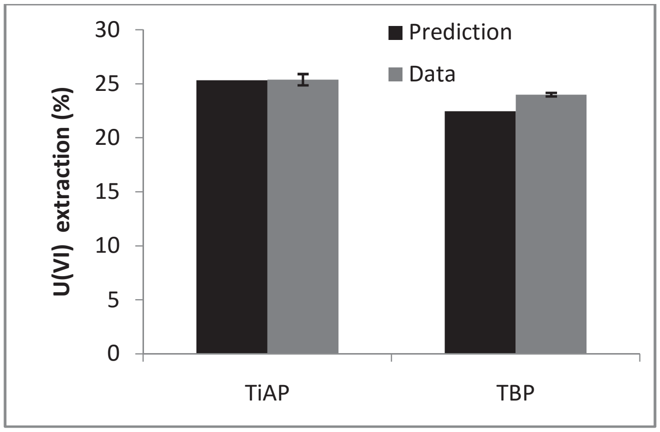

Figure 1: Comparison of transport of U(VI) in once through mode operation of HFELM using TiAP and TBP as the ligand; Feed: uranium plant raffinate; organic: 10 % v/v ligand dissolved in dodecane with 2 % v/v SPAN80; aqueous phase: 0.1 M $NaHCO_3$; W/O ratio in dispersion is 2:3 v/v; agitation rpm 4000; flow rate for HF is 400 ml min^{-1} in both the tube and shell side

HFDLM has also been operated in recirculating mode with the same conditions and observations are shown in Figure 2. U(VI) extraction of 68% has been achieved in the period of 1 hour using TiAP as the carrier. Figure 2 also shows the similar run with HFDLM in recirculating mode using TBP with similar U(VI) extraction has been achieved in 1 hour. It is seen that both the carriers are performing almost identical for U(VI) extraction. Use of TiAP for U(VI) extraction can be advantageous in view of its lower solubility in water (0.1 g L^{-1}) and greater resistance to acid hydrolysis and chemical degradation.

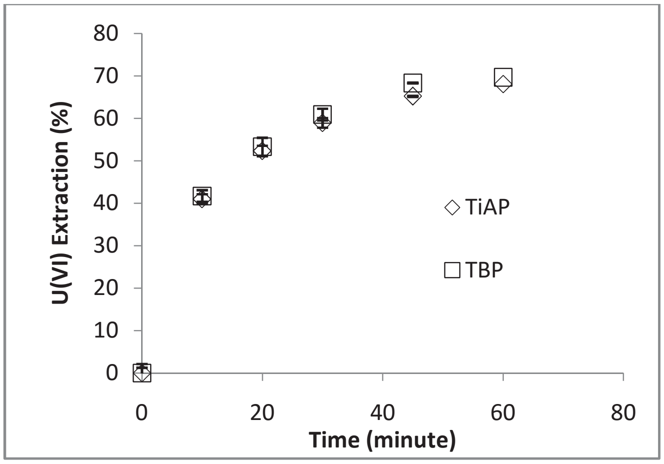

Figure 2: Transport of U(VI) in recirculating mode operation of HFELM; Feed: uranium plant raffinate; organic: 10 % v/v TiAP dissolved in dodecane with 2 % v/v SPAN80; aqueous phase: 0.1 M $NaHCO_3$; W/O ratio in dispersion is 2:3 v/v; agitation rpm 4000; flow rate 400 ml min^{-1} in both the tube and shell side; Volume in recirculation is 1L

In Chapter 5, preliminary studies, using dispersion liquid membrane in hollow fiber contactor with typical liquid-liquid extraction system, are presented. In Chapter 6, the model has been utilized to predict the performance of PS and PP hollow fiber contactors, respectively, on their scale up. Prediction made using PS1 ties in well with the data generated using PS2 and shown in Table 1 (a). Similarly, predictions made using PP1 have found in agreement with the data generated using PP2 and PP3 and shown in Table 1 (b). Hence, the present model can be easily utilized for scale up of HFDLM process with limited experimental trials.

Table 1: Effect of increase in lumen length on uranium extraction, (a) PS contactor (b) PP contactor

(a)

Length of the fiber, l (cm)	Extraction % (Prediction)	Extraction % (Data)
40	31.25	28 (generated using PS1) *
42	41.28	39.9 (generated using PS2) *
45	43.47	
50	46.94	
55	50.20	
60	53.26	

* Effective length of lumen, l in PS1 and PS2 contactors are 40 and 42 cm, respectively.

(b)

Length of the fiber (cm)	Extraction % (Prediction)	Extraction % (Data)
16	54.21	55.21 (generated using PP1) #
20	62.33	
25	70.49	73.64 (generated using PP2) #
30	76.88	
40	85.81	
50	91.29	
62	98.56	98.30 (generated using PP3) #

Effective length of lumen, l in PP1, PP2 and PP3 contactors are 16, 25 and 62 cm, respectively.

In conclusion, our study has presented a mathematical model for estimation of the wetted length of the fiber pore. Polypropylene module is found to exhibit greater extent of extraction than polysulfone. This is because, the fiber wall thickness of PP lumen is one order of magnitude less than that of the PS lumen. Hence, the reduction in the rate of diffusion of uranium ions due to higher value of α in PP lumen is overcompensated by its shorter pore length. It has also been understood that for polymeric membranes with higher ε/τ, extraction of solute will be less dependent on the fraction of the pore length wetted by the organic membrane phase. Further, efficacy of TiAP as a carrier for extraction of U(VI) from acidic plant raffinate has been evaluated in comparison to TBP. On the positive side, TiAP has a greater affinity for U(VI) compared to TBP with dodecane as solvent. On the negative side, TiAP has a higher propensity to extract nitric acid into dodecane, which reduces the driving force for extraction. These two factors appear to balance each other when the extraction is performed on a uranium plant raffinate containing 1.5 M nitric acid using hollow fiber extractor, where both TBP and TiAP perform almost identically. However, there are many lean uranium streams which have low acidity and we expect TiAP to perform better than TBP in those cases. In addition, considering the other advantages of TiAP over TBP viz. lower aqueous solubility and low rates of degradation on exposure to radiation, we can conclude that TiAP is a promising carrier in dispersion liquid membrane process for extraction of U(VI) from acidic raffinates of uranium refining plants.

REFERENCES

[1] A. Gabelman and S-T. Hwang, Hollow-fiber membrane contactors, J. Membr. Sci., 159, 1999, pp. 61-106.

[2] K.K. Sirkar, Membranes, phase interfaces, and separations: novel techniques and membranes – an overview, Ind. Eng. Chem. Res., 47, 2008, pp. 5250-5266.

[3] W. S. W. Ho and T.K. Poddar, New Membrane Technology for removal and recovery of chromium for waste waters, Environ. Prog., 20, 2001, pp. 44.

[4] G.E. Charles, S.G. Mason, The coalescence of liquid drops with flat liquid/liquid interfaces, Journal of Colloid Science, 15, 1960, pp. 236-267.

[5] O. Mengual, G. Meunier, I. Cayre, K. Puech, P. Snabre, Characterization of instability of concentrated dispersions by a new optical analyzer: The Turbiscan MA 1000, Colloids Surf., A: Physicochem. Eng. Aspects., 152, 1999, pp. 111-123.

[6] S. Dixit, S. Mukhopadhyay, K.T. Shenoy, V. A. Juvekar, A Process intensified technique of Liquid Membrane employed in in-house Hollow Fiber Contactor, Desalination and water treatment, 79, 2017, pp. 40-48.

List of Figures

List of Tables

CHAPTER 1

INTRODUCTION AND LITERATURE REVIEW

Polymeric dispersion liquid membranes

Value recovery from lean acidic streams is an important operation due to its wide applications in nuclear industry [1-2]. Raffinate containing lean values is generated from various processes in nuclear as well as chemical industry. Process intensification techniques with novel contactors and novel ligands may be utilized to treat such raffinates [3-4]. Hollow fiber module (figure 1.1) is a process-intensified mass transfer contactor with no moving parts [5]. It is ideally suited to treat such kind of lean raffinates due to its numerous advantages such as non-dispersive contact, simultaneous extraction and stripping, well defined interfacial area, easy scale up, etc. Dispersion liquid membrane immobilized in hollow fiber contactor (figure 1.2) has proved its promise in recovery of various metal ions relevant to nuclear industry. It has the advantage of simultaneous extraction and stripping, continuous replenishment of organic phase immobilized in pores of polymeric membrane and fast disengagement of loaded dispersion after the mass transport operation [6-7]. In dispersion liquid membrane (DLM), a dispersion of strip phase in a continuous organic phase is confined to one side, and the aqueous feed phase to the other side of a membrane pore. The aqueous strip phase, dispersed in the organic continuum, circulates on the shell side of the hollow fiber contactor [8]. The organic phase fills the pores of the microporous polymeric membrane and acts as a liquid membrane.

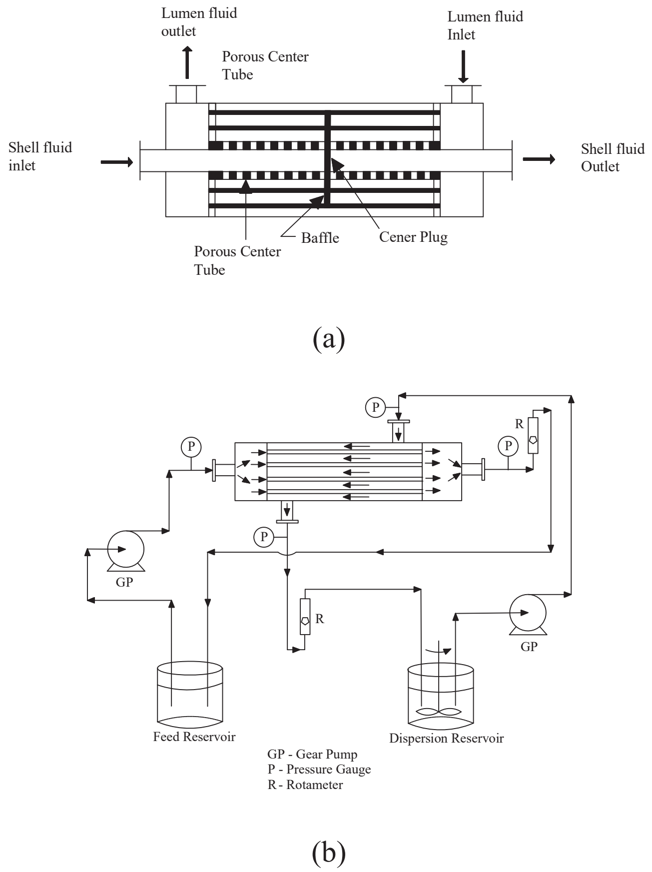

Figure 1.1: Schematic of a) hollow fiber contactor, b) experimental apparatus including hollow fiber contactor

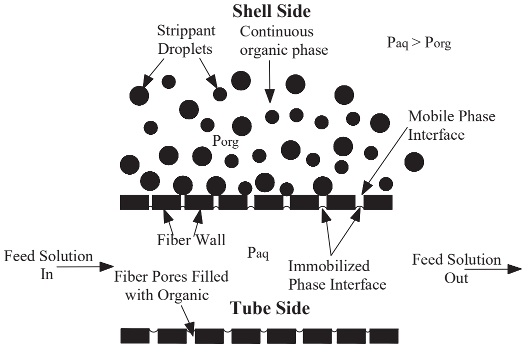

Figure 1.2: An enlarged view of the dispersion liquid membrane in hollow fiber contactor

Factors determining the efficiency of liquid dispersion membranes

The efficiency of the dispersion liquid membrane contactors depend on both the rate of transport of the metal ion across the porous solid membrane and the rate of its transport from the continuous organic phase to the strip phase drops. The efficiency of mass transfer of the metal from organic phase to the strip phase depends on the interfacial area of the strip phase-organic phase emulsion, which inturn depends upon emulsion stability. For efficient mass transfer, the strip phase drop sizes should be as small as possible. However, due to coalescence, drop size continuously increases as the emulsion moves through the contactor, thereby reducing the contacting efficiency. Low rates of coalescence are desirable to achieve high emulsion stability. Coalescence will usually occur, when two drops approach each other, where an interfacial film forms, drains to a certain thickness and then ruptures [9-10]. Film rupture is very rapid, and so the life of the interfacial film is largely determined by its rate of thinning.

One simple way to study the rate of coalescence is to measure the drop rest time. The drop rest time is defined as the time interval between arrival of the drop at a flat interface and its coalescence. It is a measure of drop stability. Drop rest time is the time required for thinning of the film of liquid, trapped between the drop and the interface (figure 1.3).

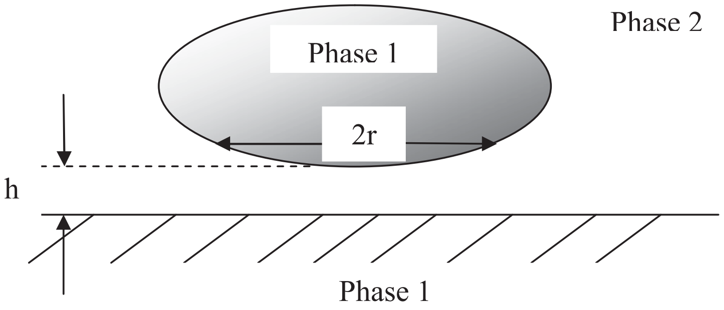

Figure 1.3: Liquid film having radius *r* trapped between the interface

Film thinning is caused by viscous drainage of the fluid contained in the film. At the critical film thickness, the attractive van der Walls force between the molecules of the drop and those of its mother phase is strong enough to overcome the cohesive force among the molecules of the film and thereby causes rupture of the film [11-12].

Characterization of emulsion is a pre-requisite before its circulation in hollow fiber contactor. There are a very few tools which can analyze stability of emulsions with high opacity. 'Turbiscan Online' is an optical instrument to characterize the liquid emulsions (figure 1.4) [13-14]. It provides the details of back scattering and transmission through the emulsion. The intensity of the backscattered light depends on three parameters: diameter of the drop, their volume fraction and the relative refractive index between the dispersed phase and continuous phase. Therefore, any change due to a variation of the drop size is detected by the optical device.

Figure 1.4: Turbiscan online apparatus using multiple light scattering technique for characterization of dispersions

The second important transport step in porous membrane based processes is diffusion through the membrane pores. Diffusion path length inside the wetted pore is important in deciding the rate of extraction [22-23]. Diffusion path length is related to the fraction of the pore length wetted by the organic liquid membrane phase (figure 1.5). Hence, estimation of fraction of the pore length wetted by the organic phase is beneficial for design and scale up of this process. This also gives idea about the stability of liquid membrane phase with reference to the given polymeric membrane.

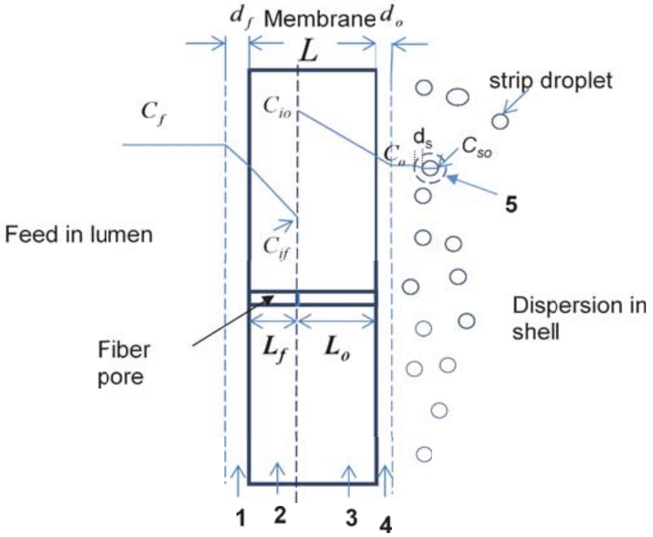

Figure 1.5: Schematic representation of transport of metal ion through the hollow fiber membrane; 1- diffusion film at the feed-membrane interface, 2-region of the pore filled with feed solution, 3-region of the pore filled with organic liquid, 4- diffusion film at the organic membrane interface, 5-diffusion film at strip-organic interface

Plan of the present work

Although, there are several studies reported in the literature on characterization of emulsion [15-18], since stability of emulsions is specific to systems, the conclusions drawn from these studies are not directly applicable to the present system. In the present work, characterization of emulsion of water in oil containing TBP and its higher homologue TiAP has been done using Turbiscan Online to assess feasibility of this emulsion for ELM extraction of U(VI) in hollow fiber contactor. Tri-iso-amyl phosphate (TiAP) is such type of ligand, which proves promising in recovery of U(VI) from lean acidic streams [19]. TiAP is the higher homologue of Tri-n-butyl phosphate (TBP) and its solubility in water is lower than that of TBP [20]. Chemical and radiolytic degradation are also minimal for TiAP due to presence of branched alkyl chain [21]. Effect of carrier concentration, nature of the strip phase, power input during emulsification and effect of surfactant on stability of the emulsion has been studied using Turbiscan Online. Based on these studies, an optimal formulation of the emulsion and method of emulsification has been arrived at. Further, the dispersion has been employed in liquid membrane mode using hollow fiber contactor to assess the performance for extraction of U(VI) from the raffinate of a uranium refining plant.

In the present work, a mathematical model has been developed for determining the rate of transport through the membrane and the extent of extraction through the contactor. A novel approach for estimation of fraction of the pore length wetted by the organic membrane phase has been suggested through developed model. This estimation is also helpful in design and scale-up of hollow fiber membrane contactors. The data has been generated for extraction of uranium from nitrate medium in countercurrent once-through mode using hollow fiber dispersion liquid membrane. Effect of various hydrodynamic and chemical parameters such as carrier concentration, presence of surfactant, initial feed uranium concentration, feed acidity and varying aqueous to organic ratio in dispersion has been studied. Water-in-oil dispersion of 1 M $NaHCO_3$ in dodecane, containing 30 % v/v Tri-n-butyl phosphate (TBP), is used as extractant. The model is validated for hollow fiber contactors made of lumens of different materials viz. polysulfone and polypropylene. Preliminary data on liquid-liquid equilibria has been generated and utilized for model validation. The model has also been found beneficial for prediction of the performance of polysulfone and polypropylene hollow fiber contactors regarding their scale up [24-27]. Process mass transfer coefficients are estimated through available correlations [28-29].

Layout of thesis

The layout of the thesis is as follows,

1. Studies are conducted on drop coalescence in order to assess the stability of dispersions for the extractant, tri-n-butyl phosphate and tri-iso-amyl phosphate with aqueous phases as distilled water and 0.1 M $NaHCO_3$.
2. A model has been developed to predict the rate of transport of metal ion using hollow fiber contactor in liquid membrane mode. Model estimates the fraction of the pore length wetted by the organic liquid membrane.
3. Effect of material of construction of hollow fiber viz. polysulfone and polypropylene on rate of transport of uranium through hollow fiber dispersion liquid membrane has been studied.
4. Effect of type of extractant viz. tri-n-butyl phosphate and its homologue tri-iso-amyl phosphate on rate of transport of uranium through hollow fiber dispersion liquid membrane has been studied.
5. Scale-up aspects of hollow fiber contactor has been investigated with the help of developed model for both the contactor made of polysulfone and polypropylene.

CHAPTER 2

STUDIES ON DROP COALESCENCE TO ASSESS STABILITY OF DISPERSIONS

Introduction

Value recovery from lean acidic streams is an important operation due to its wide applications in nuclear industry. Raffinate containing lean values is generated from various processes in nuclear as well as chemical industry. Process intensification techniques with novel contactors and novel ligands may be utilized to treat such raffinates [4]. Tri-iso-amyl phosphate (TiAP) is such type of ligand, which proves promising in recovery of U(VI) from lean acidic streams [19]. TiAP is the higher homologue of Tri-n-butyl phosphate (TBP) and its solubility in water is lower than that of TBP [20]. Chemical and radiolytic degradation is also minimal for TiAP due to presence of branched alkyl chain [21]. Batch liquid-liquid extraction studies, conducted in the present work, with uranium plant raffinate-TiAP/ dodecane reveal high partition coefficient of U(VI) with this ligand. Hollow fiber module is a process-intensified mass transfer contactor with no moving parts [5]. It is ideally suited to treat such kind of lean raffinates due to its numerous advantages such as non-dispersive contact, simultaneous extraction and stripping, well defined interfacial area, easy scale up, etc. Emulsion liquid membrane immobilized in hollow fiber contactor has proved its promise in recovery of various metal ions relevant to nuclear industry [6]. Our preliminary experiments indicated that TiAP has significantly higher affinity for U(VI) compared to tri-n-butyl phosphate. In view of this, studies were initiated on liquid membrane operation in hollow fiber contactor with the TiAP as the ligand. In this contactor, the aqueous strip phase, dispersed in the organic continuum, circulates on the shell side. Fiber material is so chosen that the organic phase wets fiber and hence fills the micro pores of the fibers. The metal-carrier complex diffuses through the pores of the membrane carrying the metal from the lumen to the shell side where it is transferred to the strip phase.

The efficiency of mass transfer of the metal to the strip phase depends on the interfacial area of the emulsion which inturn depends upon its stability. For efficient mass transfer, the drop size should be as small as possible. However, due to coalescence, drop size continuously increases as the emulsion moves through the contactor, thereby reducing the contacting efficiency. Low rates of coalescence are desirable to achieve high emulsion stability.

Characterization of emulsion is a pre-requisite before its circulation in hollow fiber contactor. There are a very few tools which can analyze stability of emulsions with high opacity. ‘Turbiscan Online’ is an optical instrument to characterize the liquid emulsions [30]. It provides the details of back scattering and transmission through the emulsion. The intensity of the backscattered light depends on three parameters: diameter of the drop, their volume fraction and the relative refractive index between the dispersed phase and continuous phase. Therefore, any change due to a variation of the drop size is detected by the optical device.

Although there are several studies reported in the literature on characterization of emulsion [13-18], since stability of emulsions is specific to systems, the conclusions drawn from these studies are not directly applicable to the present system. In the present work, characterization of emulsion of water in oil containing novel ligand TiAP has been done using Turbiscan Online to assess feasibility of this emulsion for ELM extraction of U(VI) in hollow fiber contactor. Effect of carrier concentration, nature of the strip phase, power input during emulsification and effect of surfactant on stability of the emulsion has been studied using Turbiscan Online. Based on these studies, an optimal formulation of the emulsion and method of emulsification has been arrived at. Further, the emulsion has been employed in liquid membrane mode using hollow fiber contactor to assess the performance with the new ligand for extraction of U(VI) from the raffinate of a uranium refining plant. As far as we know, these types of studies have not been reported in the literature. These studies will help in the process development of solvent extraction system using TiAP for value recovery.

Experimental

Materials

The organic phase was prepared by dissolving the required amount of TiAP (supplied by Heavy Water Board, Mumbai) in n-dodecane. Actual raffinate stream of a uranium refining plant having acidity 1.5 M, obtained from UED, BARC, was used as feed. Raffinate contains mainly U(VI) (around 200 ppm) along with some other ions in trace quantities. Aqueous solution of 0.1 M sodium bi carbonate (supplied by Merck Specialities Private Limited) was used as the stripping agent. Sorbitan monooleate (SPAN80) (supplied by S.D. Fine Chemicals Ltd.) was used as the surface active agent.

Methods

The Turbiscan analyzer (Turbiscan Online) makes use of Multiple Light Scattering by passing near infrared light (λ= 880 nm) through a cylinder filled with the emulsion sample. Two synchronous optical detectors subsequently measure the transmission and backscattering fluxes of the light from the sample. The Turbiscan analyzer enables to measure the photon transport mean free path of both the transmitted as well as backscattered photons. Photon transport mean free path is the mean penetration length of a photon in the emulsion. It is inversely proportional to the drop volume fraction, φ and proportional to the drop mean diameter, d [13]. Hence, the photon transport mean free path, measured by the Turbiscan, allows us to compute d for known φ.

Refractive indices of continuous and the dispersed phases are needed as input parameters. Refractive index of water and the sodium bicarbonate solution were taken as 1.333 and 1.343, respectively. Refractive index of TiAP, dodecane and the SPAN80 was taken as 1.4264, 1.4195 and 1.506 respectively at ambient temperature. Lorentz-Lorenz equation [31] as following was used as the mixing rule for refractive index of organic solution, containing ligand, diluent and a surface active agent.

$$\frac{n^2-1}{n^2+2}=\varphi_1\left(\frac{n_1^{\,2}-1}{n_1^{\,2}+2}\right)+\varphi_2\left(\frac{n_2^{\,2}-1}{n_2^{\,2}+2}\right)+\varphi_3\left(\frac{n_3^{\,2}-1}{n_3^{\,2}+2}\right) \tag{1}$$

Where, φ is the volume fraction of a component in the solution and n is its refractive index. In addition to refractive indices, Turbiscan also needs the transmittance of the continuous phase as the input. This was measured by pouring the organic solution into the Turbiscan cell and reading the transmittance through the acquisition unit.

Interfacial tension between the aqueous and the organic phases were measured using the Spinning Drop Tensiometer (make: KRUSS, model no.: SITE100) and OCA 20 of Dataphysics Instruments, GmBH, Germany.

The emulsion was prepared using REMI RQ-1274 CROSS BLADE emulsifier for 1L capacity and 4000 rpm speed (agitation time 20 minutes) and IKA® T25 digital ULTRA-TURRAX® for 100 ml and higher speeds of 4000-20000 rpm (agitation time 10 minutes). The impeller was kept in the organic phase and aqueous phase was slowly added to it in drop-wise manner under agitation. For preparations of emulsions, various concentrations of TiAP dissolved in dodecane have been taken with two different aqueous phase's viz. sodium bicarbonate and distilled water. External cooling was provided so as to maintain constant temperature of the emulsion because of the excessive heat produced at higher RPM. The emulsion so formed was quickly poured into the bore of the Turbiscan and analyzed for average drop size of emulsion as a function of time. The amount of light scattered is detected and send to the analyzer unit which converts analog signals to digital and then send to the computer for further processing. The software displays the values of the percent transmission, percent backscattering and photon mean free path with respect to time on a two dimensional plot. Using photon mean free path, volume fraction and the refractive indices, diameter of drops are calculated. The experiments were repeated to check the reproducibility of the results (standard deviation was ±3 %).

Liquid-liquid extraction experiments were conducted to generate the data on partition coefficient of U(VI) in the organic phase containing different TiAP concentrations. The plant raffinate was taken as the feed and the organic phase was TiAP dissolved in dodecane. The equilibrium was achieved by stirring feed and organic phase in a DBK- Digital Wrist Action Shaker for 10 minutes keeping feed to organic ratio as 1:1. After the agitation was stopped, both phases were allowed to separate and U(VI) in the aqueous phase was analyzed. Its concentration in the organic phase was estimated through material balance. To determine the extent of transport of the nitric acid along with the U(VI), acidic raffinate samples were titrated against sodium hydroxide using phenolphthalein as indicator.

The emulsion liquid membrane (ELM) experiments were performed in a hollow fiber (HF) contactor. The details of HF are presented in Table 2.1. For HFELM, feed was circulated in lumen side, while the emulsion was confined to the shell side [32]. In carrier facilitated transport through HFELM, the metal cation diffuses through aqueous feed film and reacts reversibly with the ligand at the feed-membrane interface resulting in the formation of metal carrier complex. The complex then diffuses through the membrane due to its own concentration gradient and consequently at the membrane strip interface, it releases the metal ion. The ligand thus left over diffuses back towards the feed-membrane interface and the cycle continues. The released cation diffuses through the aqueous strip film. Samples were collected periodically from both feed and strip sides and de-emulsified using EQUITRON®

Round Bath at 80 °C to recover the strip phase. Both the raffinate and the strip samples were analyzed for U(VI) through HORIBA Scientific ULTIMA 2 ICP Optical Emission Spectrometer.

Table 2.1: Characteristics of hollow fiber contactor, Liqui-Cel® 2.5x8

1.	Diameter of shell, m	$5\text{x}10^{-2}$	**7.**	Porosity, ε %	40
2.	MOC of housing (shell)	PC	**8.**	Pore diameter, m	$5\text{x}10^{-8}$
3.	Fiber MOC	PP	**9.**	No of fibers, N	$1\text{x}10^{4}$
4.	Fiber inner diameter, D_i m	$2.2\text{x}10^{-4}$	**10.**	Interfacial area for extraction, ($\pi D_i L \varepsilon N$) m^2	$4.8\text{x}10^{-1}$
5.	Fiber thickness, m	$3\text{x}10^{-5}$	**11.**	Lumen Volume, m^3	$1.5\text{x}10^{-4}$
6.	Fiber length, L m	$1.6\text{x}10^{-1}$	**12.**	Specific interfacial area (per unit lumen volume) (m^2 m^{-3})	$3.2\text{x}10^{3}$

Results and discussion

a) Studies in emulsion stability

Size of droplet in W/O emulsion plays an important role in ELM extraction. Small drop size leads to higher interfacial area and also improves emulsion stability. The latter property is important since emulsion should not break while passing through hollow fiber contactor. Smaller drop sizes can be achieved using a suitable surface-active agent (HLB 4-5 to stabilize W/O emulsion). Lower drop sizes can also be achieved in the absence of surfactant using higher energy input during emulsification. To understand the effect of energy input, water was dispersed in dodecane containing 10% carrier v/v at different speed of agitation (4000, 8000, 12000, 16000 and 20000 rpm) in Ultra-Turrax emulsifier. The ratio of the aqueous to the organic phase in the dispersion was kept constant at 2:3. These dispersions were prepared both in the presence and in the absence of the surfactant. The stable drop mean diameter observed by Turbiscan as a function of the agitator speed is shown in Figure 2.1. It was found that in the absence of the surfactant (0% v/v of SPAN80), the dispersion was not stable below the agitation speed of 12000 rpm. The drop size reduced marginally when the speed was varied from 12000 to 22000 rpm; i.e. after a certain drop diameter, the rate of coalescence of drops becomes equal to the rate of their breakage. Effect of surfactant also becomes negligible in this region.

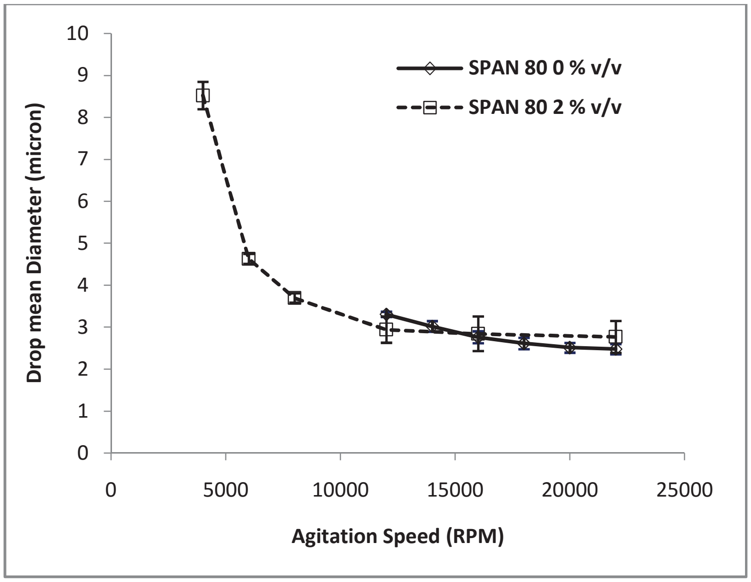

Figure 2.1: Variation of drop mean diameter of emulsion with agitation speed (RPM); organic: 10 % v/v TiAP dissolved in dodecane with or without SPAN80 v/v; aqueous phase: distilled water; W/O ratio in emulsion is 2:3 v/v

Similar data has been collected for TBP and compared with TiAP in Figure 2.2. The droplet size in the presence of TBP is found more than TiAP. Interfacial tensions of TBP and TiAP are compared in Figure 2.3. At 10% v/v loading, both ligands have the same interfacial tension and yet, TiAP produces smaller water drops. This is due to the fact that the longer as well as branched isoamyl chains of TiAP produce greater steric hindrance to coalescence than the linear butyl chains of TBP.

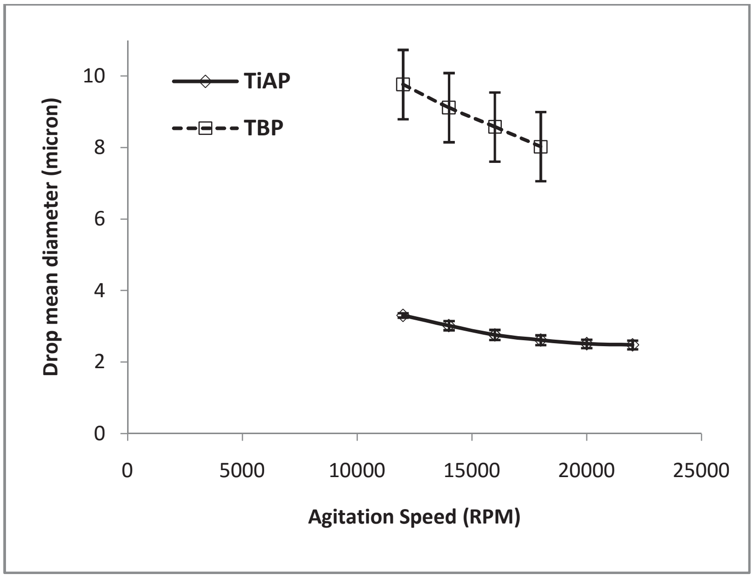

Figure 2.2: Variation of drop mean diameter of emulsion with agitation speed (RPM); organic: 10 % v/v ligand dissolved in dodecane without SPAN80; aqueous phase: distilled water; W/O ratio in emulsion is 2:3 v/v

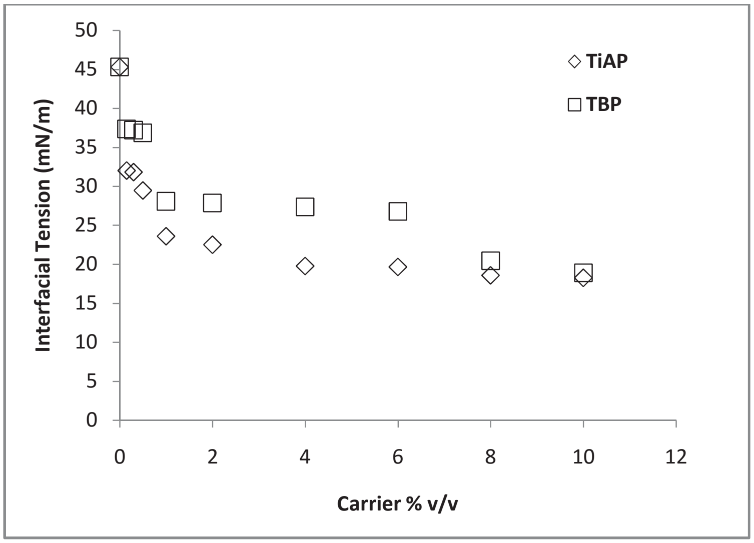

Figure 2.3: Comparison of interfacial tension of TiAP and TBP with distilled water; organic: TiAP or TBP dissolved in dodecane

To study the effect of carrier and SPAN 80 together on the drop size, dispersions were prepared by addition of 2% v/v of SPAN80 during the emulsification. Distilled water (DW) and 0.1 M $NaHCO_3$ were used as the dispersed phases. Different concentrations of TiAP in the range from 0 to 10% v/v in dodecane were used. Figure 2.4 presents the dispersed phase drop diameters obtained in these experiments. It is seen that with increase in the concentration of TiAP, the drop diameter increases. This is because of possible displacement of Span 80 by TiAP due to its high concentration. Since TiAP is not a surfactant, its ability to prevent coalescence is poor compared to SPAN 80. Also, at 20% v/v TiAP (not shown in Figure 2.4), drop diameters were found to be of the order of 100 μm and at 30% v/v TiAP, dispersion was unstable. Similar observations are made with TBP and shown in the Figure 2.4.

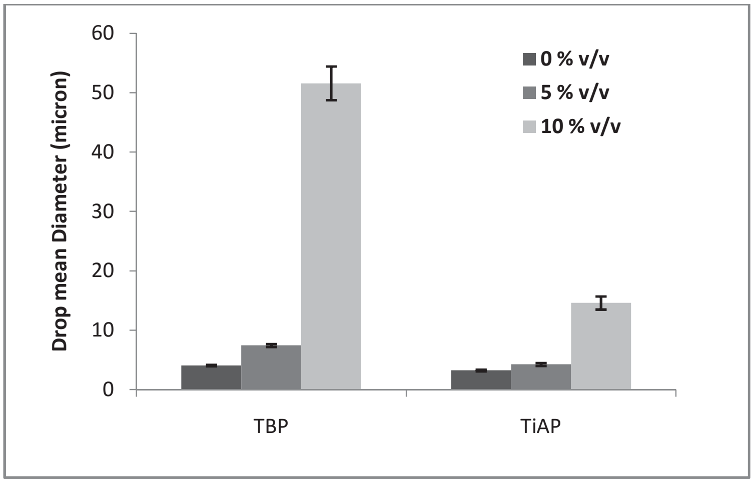

Figure 2.4: Effect of concentration of ligand on drop mean diameter of emulsion for TiAP and TBP; organic: TiAP or TBP dissolved in dodecane with 2% v/v SPAN80; aqueous phase: distilled water (DW); W/O ratio in emulsion is 2:3 v/v; agitation rpm 4000

Affinity for the interface of TiAP in comparison to SPAN80 could be judged by comparing interfacial tensions of TiAP alone and the mixture of TiAP and SPAN80 in figure 2.5. With increase in the concentration of TiAP, we find that SPAN80 has progressively lesser influence on the interfacial tension indicating that SPAN 80 molecules are progressively replaced by TiAP molecules as TiAP concentration in the solution increases. Since TiAP are not as effective as SPAN 80 to prevent drop coalescence, due to their shorter hydrocarbon chains, the drop size increases as TiAP concentration in the solution increases. A similar behavior is also observed with TBP.

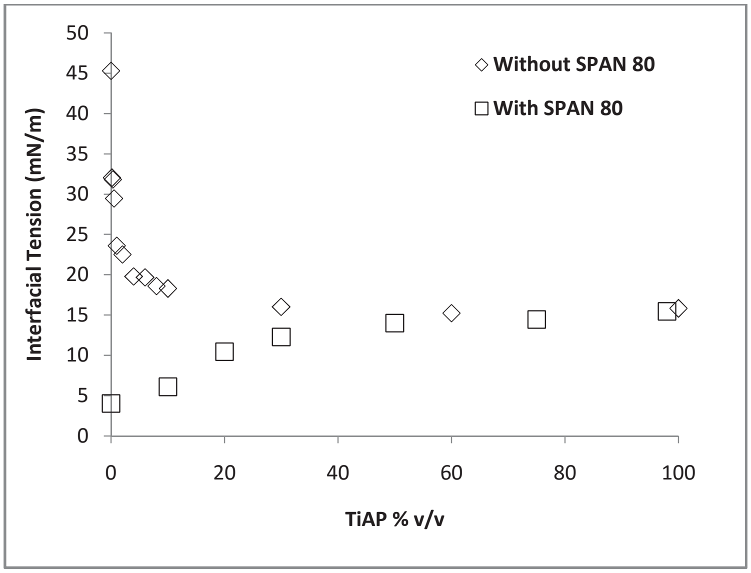

Figure 2.5: Variation of interfacial tension with distilled water; organic: TiAP dissolved in dodecane with 2% v/v SPAN80

The emulsion stability can also be judged by measuring the increase in the mean drop size with time. The effect of TiAP and TBP on variation of the normalized drop size with time is shown in Figure 2.6. In all cases 2% v/v of SPAN 80 is used.

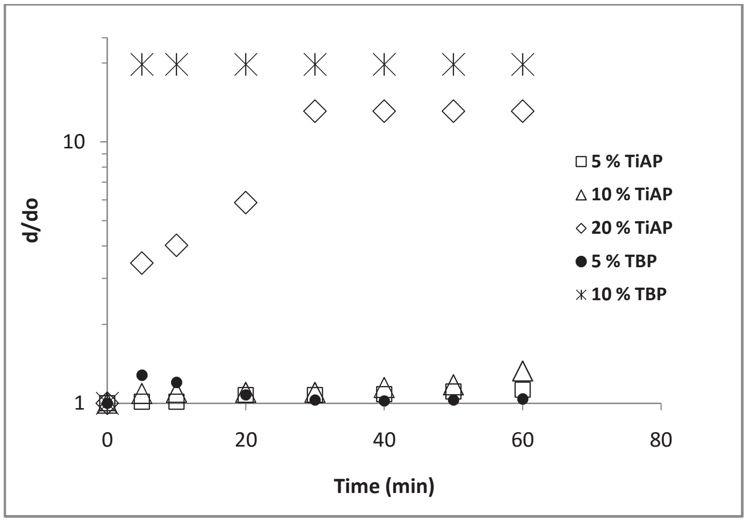

Figure 2.6: Increase of drop mean diameter of emulsion with time, *d* is diameter at a time and d_o is initial diameter; organic: TiAP dissolved in dodecane with 2% SPAN80 v/v; aqueous phase: distilled water; W/O ratio in emulsion is 2:3 v/v; agitation rpm 4000

It is seen that at low concentrations of the carrier, the drop size does not vary with time and dispersion remains stable for observation period of 1 hour. At high concentrations, the drop size increases with time and attains a larger equilibrium size after certain time. This happens at 10% TBP concentration and 20 % TiAP concentration. The time to attain the equilibrium drop size is also different in the two cases. Since, the residence time of dispersion in HFELM is much shorter, the stability period of 1 hour can be considered as acceptable.

In all the experiments described above, SPAN 80 concentration was 2% v/v. To understand the effect of surface active agent in presence of ligand, dispersions were prepared with varying concentrations of SPAN80 at different concentrations of TiAP and TBP. Resulting mean drop diameters of water in emulsion are shown in Figure 2.7 and 2.8.

It is observed from these figures that the drop diameter decreases with increase in concentration of SPAN 80 until a threshold concentration is reached, beyond which increase in SPAN 80 has no effect on drop diameter. The concentration of SPAN 80 needed to reach the threshold increases with increase the concentration of the carrier. This can be understood from the fact that the carrier and the surfactant compete with each other to occupy the interface. At low concentration of surfactant the interfacial concentration is dominated by the carrier leading to larger drop diameter. Beyond the threshold concentration, the interfacial concentration is dominated by the surfactant and hence drop size does not reduce beyond the threshold value. Higher, is the concentration of the carrier, greater is the concentration of the surfactant needed to displace it and hence the threshold value is higher. Both TBP and TiAP show similar trend.

The competition between the surfactant and carrier can also be gauged through the interfacial tension of the system in the presence of the surfactant and the carrier. In Figure 2.9, interfacial tension of dodecane-water system is plotted against the concentration of SPAN80 with the concentration of TiAP as the parameter. It is seen that in the absence of the carrier, the interfacial tension reaches a constant value beyond 2% concentration of SPAN80, where the interface is saturated with the surfactant. With increase in the concentration of TiAP, higher concentration of SPAN80 is needed to displace the carrier and attain interfacial saturation. This clearly indicates the presence of competition between the carrier and the surfactant to occupy the interface.

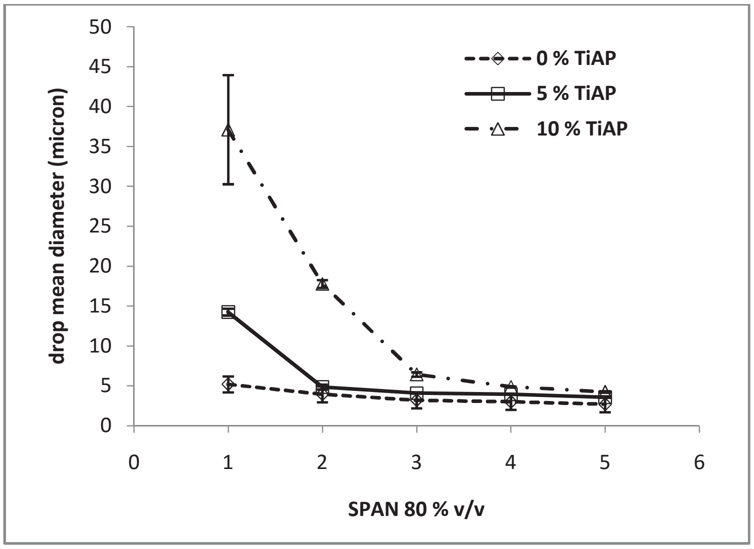

Figure 2.7: Effect of varying concentration of surface active agent on drop mean diameter of emulsion; organic: TiAP dissolved in dodecane with SPAN80; aqueous phase: distilled water; W/O ratio in emulsion is 2:3 v/v; RPM 4000

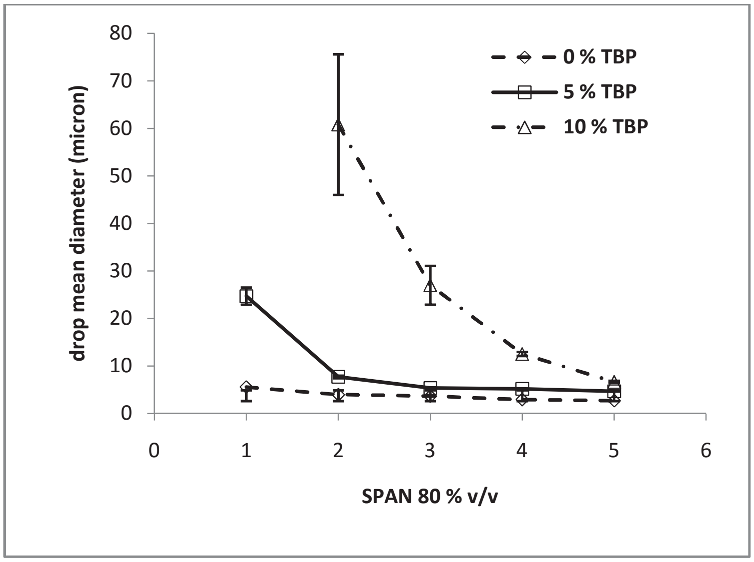

Figure 2.8: Effect of varying concentration of surface active agent on drop mean diameter of emulsion; organic: TBP dissolved in dodecane with SPAN80; aqueous phase: distilled water; W/O ratio in emulsion is 2:3 v/v; RPM 4000

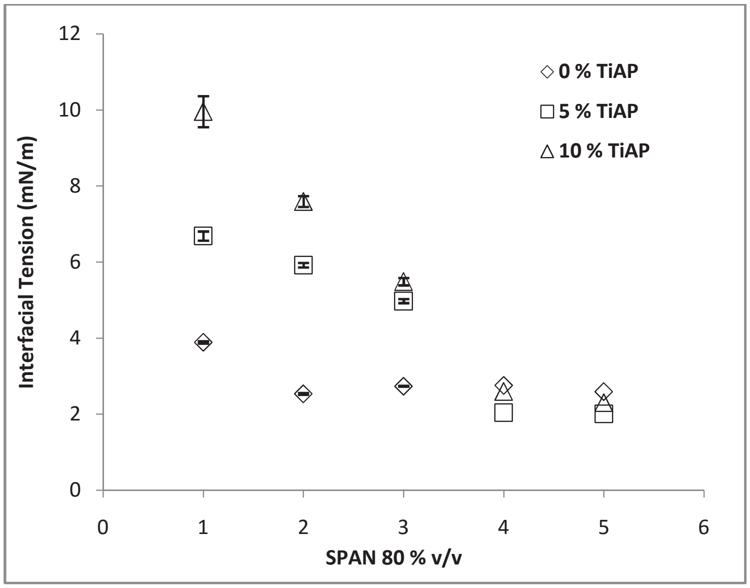

Figure 2.9: Effect of varying concentration of surface active agent on interfacial tension; organic: TiAP dissolved in dodecane with SPAN80; aqueous phase: distilled water

For recovery of U(VI) using liquid membrane operations in hollow fiber contactor, distilled water, sodium carbonate and sodium bicarbonate solutions are the promising strip phases. As the transport proceeds, there is gradual build up of nitric acid in the strippant, which does not favour the decomplexation of the metal carrier complex in the strip phase. Use of a dilute alkali like Na_2CO_3 or $NaHCO_3$ promotes decomplexation, which in turn enhances the extraction at the feed-membrane interface by generation of higher concentration of free ligand. Both Na_2CO_3 and $NaHCO_3$ as strippant have virtually the same performance, while being a milder alkali compared to Na_2CO_3, possibility of losing uranium by precipitation during stripping is less for $NaHCO_3$ and so it is used here. It has also been observed that dodecane containing TiAP with sodium bicarbonate as the aqueous phase has lower interfacial tension compared to distilled water as the aqueous phase (Figure 2.10) and thus leads to lower drop diameters (Figure 2.11). It has been seen through the batch liquid liquid extraction studies that the carbonate has the strip distribution coefficient of the order of

0.01; while for distilled water, it is of the order of 0.1 [33]. Both these reasons, lesser drop diameter (due to lower interfacial tension) and lower distribution coefficient of carbonate solutions are advantageous for stripping operations.

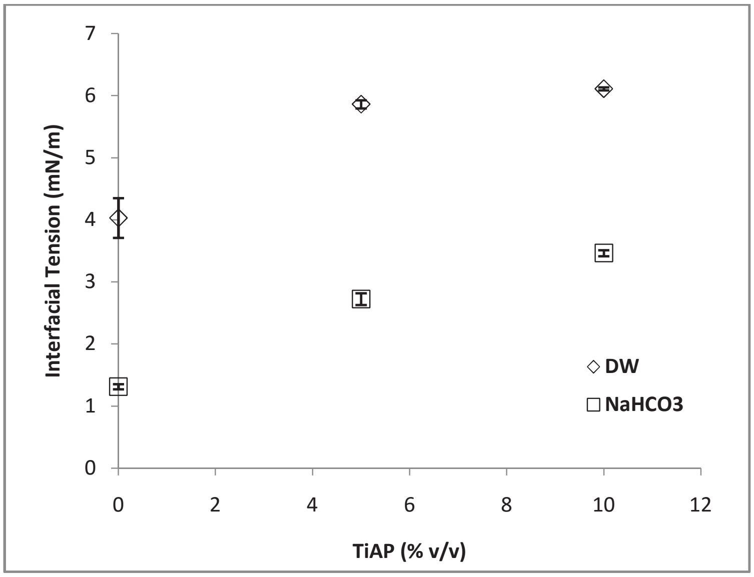

Figure 2.10: Variation of interfacial tension with distilled water; organic: TiAP dissolved in dodecane with 2% v/v SPAN80

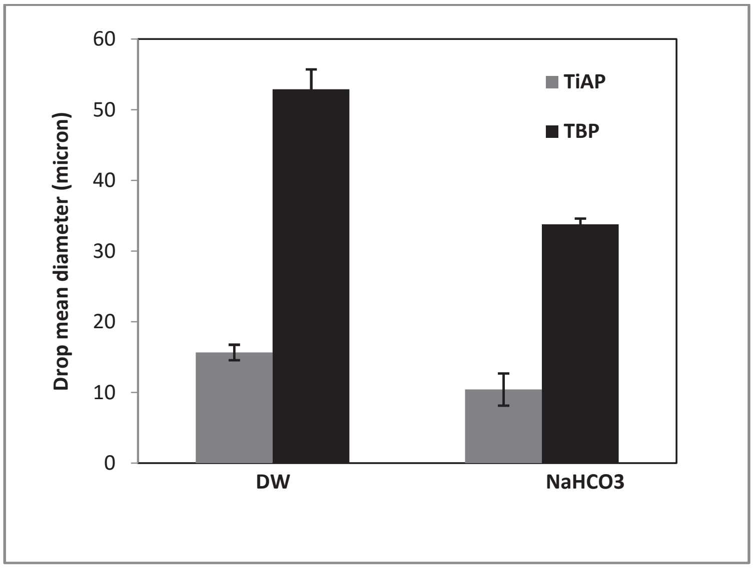

Figure 2.11: Effect of aqueous phase on drop mean diameter of emulsion for TiAP and TBP; organic: 10 % TiAP or TBP dissolved in dodecane with 2% v/v SPAN80; W/O ratio in emulsion is 2:3 v/v; agitation rpm 4000

Here, efficacy of TiAP as a carrier for extraction of U(VI) from acidic plant raffinate has been evaluated in comparison to TBP. On the positive side, TiAP has a greater affinity for U(VI) compared to TBP with dodecane as solvent. On the negative side, TiAP has a higher propensity to extract nitric acid into dodecane, which reduces the driving force for extraction. These two factors appear to balance each other when the extraction is performed on a uranium plant raffinate containing 1.5 M nitric acid using hollow fiber extractor, where both TBP and TiAP perform almost identically. However, there are many lean uranium streams which have low acidity and we expect TiAP to perform better than TBP in those cases. In addition, considering the other advantages of TiAP over TBP viz. lower aqueous solubility and low rates of degradation on exposure to radiation, we can conclude that TiAP is a promising carrier in ELM process for recovery/enrichment of U(VI) from acidic raffinates of uranium refining plants.

At carrier concentration of 10 % v/v, both the ligands TiAP and TBP have the same interfacial tension and yet, smaller water drops produced with TiAP. This is due to the fact that the branched iso amyl chains of TiAP produce greater steric hindrance to coalescence than the linear chains of TBP. It is seen that with increase in the concentration of ligand, the drop diameter increases. This is because of possible displacement of SPAN80 by ligand due to their high concentration. Since, ligand is not as effective as SPAN80 to prevent drop coalescence, due to its shorter hydrocarbon chains, the drop size increases as concentration of ligand in the solution increases.

The drop diameter decreases with increase in concentration of SPAN80 until a threshold concentration is reached, beyond which increase in SPAN80 has no effect on drop diameter. The concentration of SPAN80 needed to reach the threshold increases with increase in the concentration of the carrier. Higher, is the concentration of the carrier, greater is the concentration of the surfactant needed to displace it and hence the threshold value is higher. Both TBP and TiAP show similar trend.

b) Studies on drop-interface coalescence

Coalescence of drops, suspended in a liquid, plays a crucial role in mass transfer contactors. In a mass transfer contactor, efficient dispersification is required to enhance the transport efficiency. On the other side, adequate coalescence of drops is required to reduce emulsification and entrainment losses during phase separation. Emulsification results in poor disengagement of the two phases leading to an inefficient extraction, loss of control on phase ratio and significant entrainment losses. In the most conventional extraction systems, the interface contains interfacially active contaminants. These contaminants modify the interfacial properties, which resist the film drainage and hence retard coalescence. Effects of interfacial properties on coalescence have not been systematically studied for the relevant solvent extraction systems. In liquid membrane based mass transfer contactors, like hollow fiber modules, emulsifiers are often added to stabilize the dispersion during transport. Type and concentration of emulsifier play a crucial role in coalescence of the drops during phase separation in such systems.

A simple technique for studying the rate of coalescence is to measure the "coalescence time". When a drop of liquid 1 approaches through an immiscible liquid 2 to the interface of phases 1 and 2, it takes rest at the interface before merging with its bulk phase. The time interval, during which the drop rests at the interface, is known as the coalescence time. In the present work, time of approach of a drop of an aqueous phase through an organic phase and its coalescence time with its bulk phase have been studied using high speed camera and illumination system. Emulsifiers play an important role in modulating the coalescence time. Role of emulsifier coupled with the extractant having surface activity has also been seen.

Methodology

The experimental set-up for the present study on drop-drop coalescence under gravitational field consists of a cuvette fixture, in which organic and aqueous phases have been poured to form a liquid-liquid interface. The set-up (figure 2.12) consists of an auto syringe to release the drop of aqueous phase in organic continuum, illumination system and a high speed camera. Images are taken for drop travelling through the organic pool, sitting on organic-aqueous interface and then merging with its bulk phase. The time of approach of drop of aqueous phase through organic phase as well as the coalescence time of drop with its bulk phase has been observed for different compositions. The organic phase is taken as TBP (0%, 5%, 10%, 20% and 30% v/v) dissolved in dodecane, while the aqueous phase was distilled water.

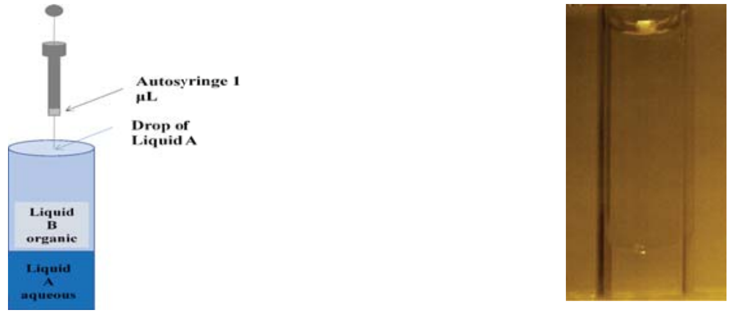

a) b)

Figure 2.12: a) Schematic of the experimental facility, b) video image of the drop resting at the interface

Theoretical

A) Deformation of a drop: The deformation of a drop under a compressive force is estimated by considering it to be contained in a fluid between two parallel planes, which are pushed together with a force F according to Charles and Mason [9]. For deformation, weight of the drop overcomes the interfacial tension force of the drop, as interfacial forces holding the drop together. At equilibrium, resultant of gravitational and buoyant force should be equal to interfacial tension force for a given distortion,

$$\frac{4}{3}\pi b^3 g\Delta\rho = \sigma\pi c^2 \frac{2}{b} \tag{2}$$

$$c = b^2\left[\frac{2\Delta\rho g}{3\sigma}\right]^{1/2} \tag{3}$$

Where, *b* is the radius of undistorted spherical drop and *c* is the radius of flat disc formed on the top and bottom, after the drop is deformed. $\Delta\rho$ is the difference in the density of the drop and the surrounding medium. From above equations, force required to produce a given distortion increases with interfacial tension σ and drop curvature *1/b*. Liquid film trapped between the interface is plano-convex in shape and is thinnest along the circumference of a circle of radius *c* according to Gillespie and Rideal [11].

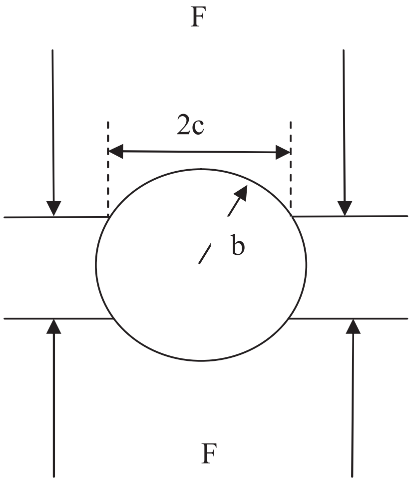

Figure 2.13: Schematic of deformation of drop

B) Thinning of the film: Following Assumptions are involved for the thinning of the film of continuous phase according to Reynolds [10]; a) Space between the drop and the two phase interface is so small that the motion of fluid is assumed to be free from eddies i.e. laminar flow. b) Forces arising from weight and inertia are altogether small compared with the stresses arising from viscosity. c) Flow is radial i.e. z-component of fluid velocity is zero.

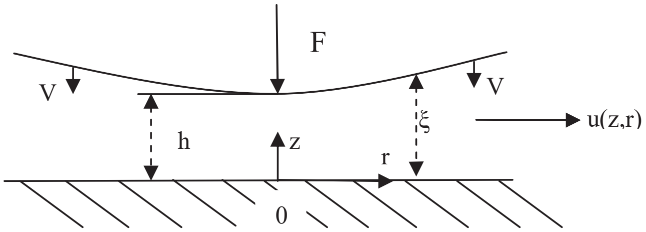

Figure 2.14: Schematic of thinning of the film

The close approach of surfaces immersed in a viscous fluid in response to a constant force F has been considered. Separation at any time t is given by $z = h$ at $r = 0$. At a distance r from the origin, separation is ξ, which is function of r. Velocity of approaching surface at time t is $V = -dh/dt$. During approach, incompressible fluid of viscosity η is expelled radially from between the two surfaces at a velocity $u\ (z,r)$. Radial velocity $u(z,r)$ is given by Eq 4. It implies a parabolic profile without slip at the adjacent surfaces, i.e. $u(z,r) = 0$ at $z = 0$ and ξ. $u(z,r)$ will be greatest half-way between the surfaces. Fluid will be pulled towards the middle by the viscosity. The volumetric flow rate across a cylindrical surface at r is represented by Eq. 5,

$$u(z,r) = z\,(\xi - z)\,\psi(r) \tag{4}$$

$$Q = \int_0^{\xi} u(z,r)\,2\pi r\,dz \tag{5}$$

By equation 4 and 5,

$$Q = 2\pi r\psi(r)\int_0^{\xi} z(\xi\text{-}z)dz \tag{6}$$

$$Q = 2\pi r\psi(r)\left(\xi\frac{z^2}{2}\bigg|_0^{\xi} - \frac{z^3}{3}\bigg|_0^{\xi} \right) \tag{7}$$

$$Q = 2\pi r\psi(r)\left(\frac{\xi^3}{2} - \frac{\xi^3}{3} \right) \tag{8}$$

$$Q = 2\pi r\psi(r)\left(\frac{\xi^3}{6} \right) \tag{9}$$

Further, by equating the change in volumetric flow rate to the volume of liquid displaced by the approaching surface in unit time,

$$dQ = 2\pi r \; dr \; V \tag{10}$$

By equation 9 and 10,

$$2\pi d\left(r\psi(r)\left(\frac{\xi^3}{6} \right) \right) = 2\pi r \; dr \; V \tag{11}$$

On integration of equation 11,

$$\psi(r) = 3rV/\xi^3 \tag{12}$$

Now, equating mechanical work to the energy dissipated due to viscosity,

$$FV = \int \tau \, (\partial u/\partial z) \, 2\pi r \; dr \; dz \tag{13}$$

$$FV = \int_0^r \int_0^{\xi} \tau \frac{\partial u}{\partial z} \, 2\pi r \; dr \; dz \tag{14}$$

Substituting for *∂u/∂z* and integrating with respect to *z* yields the relation

$$V = \frac{-dh}{dt} = \frac{F}{6\pi\mu \int_0^r \frac{r^3}{\xi^3} \, dr} \tag{15}$$

When approaching surface is flat disc of radius c, i.e. ξ = constant = h

Time required for the thinning of the film from thickness h_1 to h_2 is,

$$t_{1,2} = \frac{\mu \Delta \rho g b^5}{4\sigma^2}\left[\frac{1}{h_2^2} - \frac{1}{h_1^2}\right] \tag{16}$$

Assumptions involved in obtaining Eq 16 are as following, a) Liquid drop of radius *b* approaches a flat interface under its own weight. b) Drop undergoes a small deformation. Film does not drain regularly and it may rupture before drainage is complete, resulting in a distribution of coalescence times.

Observations

Approach velocity of drop, u_t, towards the two phase interface has been found to be in between Stokes and Newton's law regime through *K* values ($K = D_P\{g\rho\ (\rho_P-\rho)/\mu^2\}^{1/3}$). Density and viscosity have been estimated through densitymeter and viscometer for varying composition of solutions (Table 2.2). Emulsification carried out in laboratory at a speed of 3000 RPM, leads to drop diameter of dispersed phase of the order of 1 mm. Accordingly, spherical drop of 1 microlitre volume has been taken for D_P as 0.124e-02 m. u_t has been calculated through equation 17 using a value of C_D found by trial ($C_D \rightarrow u_t$ (via equation 17) $\rightarrow Re_{P,cal}$ ($=D_P u_t \rho/\mu$)), shown in Table 2.3. At chosen C_D (by trial), $Re_{P,theoretical}$ has been found through standard plot of C_D versus $N_{Re,P}$ (appendix A). If $Re_{P,cal}$ comes equal to $Re_{P,theoretical}$, corresponding value of u_t is taken, otherwise a new C_D is tried.

$$u_t = \{(4\ D_P g\ (\rho_P-\rho))/3\ C_D\ \rho\}^{1/2.} \tag{17}$$

Through u_t, time of approach of drop to interface has been estimated by taking distance of travel for the drop as 3.75e-02 m and shown in Table 2.3. Data of time of fall of drop of distill water through organic phase towards the two phase interface has been presented in Figure 2.15. With increase in the concentration of TBP, time of fall of drop towards the phase interface increases. This is because of increased density and the viscosity of the organic surrounding the drop. In presence of emulsifier (SPAN 80 2 % v/v), time of fall has larger values as shown in Figure 2.15. This is because of further rise in the density and viscosity of the continuous phase with the presence of emulsifier.

Table 2.2: Physical properties

TBP in dodecane v/v	**Density g/cm^3, ρ**	**Viscosity cP, µ**
0%	781	1.38
5%	790.585	1.38
10%	800.17	1.45
20%	819.34	1.58
30%	838.51	1.65

Table 2.3: Theoretical values of approach velocity of drop towards the Interface

TBP in dodecane v/v	C_D	u_t m/s	$Re_{P,cal}$	$Re_{P,theoretical}$	Time msec
0%	1.85	0.04955	34.775	34.8	756.81
5%	1.85	0.04817	34.217	34.8	778.49
10%	2	0.04497	30.772	30	833.89
20%	2.32	0.03924	25.231	25.4	955.66
30%	2.5	0.03533	22.26	22.5	1061.42

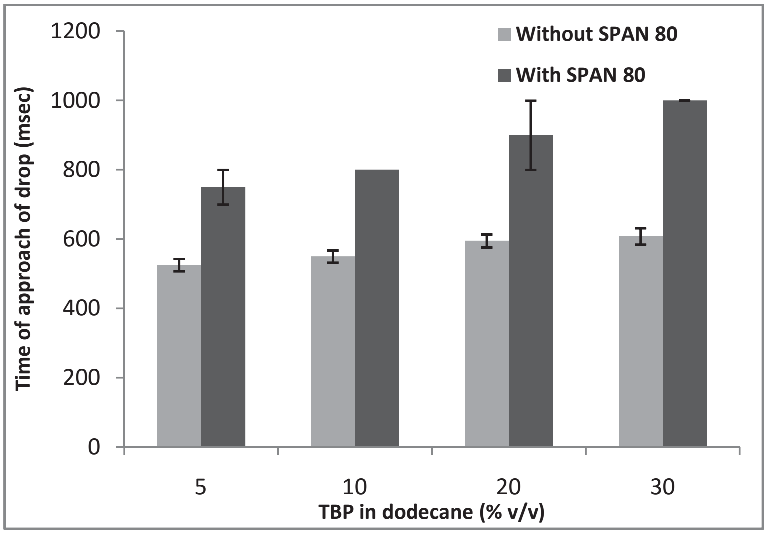

Figure 2.15: Time of approach of drop to interface: experimental data

Time for coalescence of drop [12] of distilled water to its bulk phase has been observed and presented in Figure 2.16 for TBP in absence of SPAN 80. With gradual increase in concentration of TBP, coalescence time increases. Although not shown here, similar trend has also been observed in case of TiAP. This is because of the increase in viscosity of organic and interfacial tension with the increase in carrier concentration.

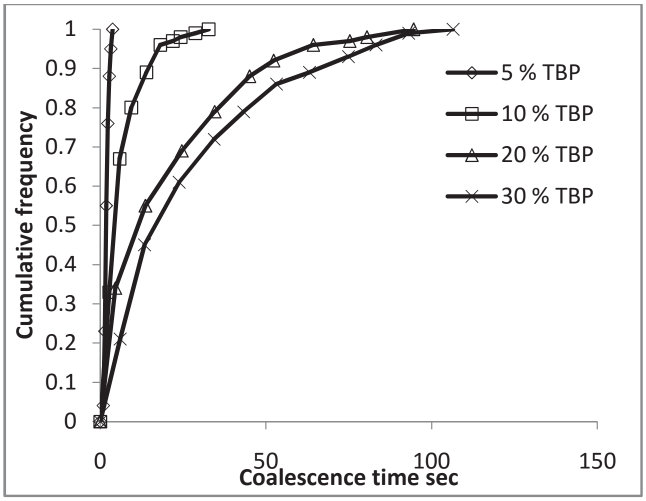

Figure 2.16*: Cumulative probability distribution of drop rest times at the oil water interface for varying concentration of carrier agent, TBP

*****data for coalescence time t_c has been collected 100 times at the same condition. This data for t_c has been divided in regular intervals like 0 - 0.5 sec, 0.5 – 1 sec, 1- 1.5 sec etc. How many numbers of t_c is coming under that particular interval is the frequency corresponding to that interval. Although not shown here, interval of coalescence time in sec (x-axis) versus its corresponding frequency (y-axis) is plotted, which comes in the form of Gaussian function. Finally, mean coalescence time for all intervals has been calculated and plotted with its cumulative frequency.

CHAPTER 3

STUDIES OF MASS TRANSFER IN LIQUID-LIQUID SYSTEMS: EFFECT OF MATERIAL OF CONSTRUCTION OF MEMBRANE

Introduction

Recovery of valuable metals such as uranium from lean acidic raffinate is a major task in nuclear industry in view of limited resources and strict environmental regulations [1]. The existing methods used for this purpose viz. solvent extraction and ion exchange have their own limitations. The solvent extraction process needs separate extraction and stripping step, multistage contactor for recovery from lean streams, large density difference between the phases (for efficient phase separation) and large solvent inventories. Moreover, there are emulsification losses. In ion exchange process, there are problems such as resin fouling, throughput limitations and poor selectivity, which limit its applicability. In addition, the driving force for mass transfer in these processes is low due to equilibrium limitations [2].On the other hand, liquid membrane process facilitates simultaneous extraction and stripping and has no moving parts. The process has low energy consumption and less entrainment losses [3, 4]. Since the organic phase is stripped as soon as it is loaded, the driving force for extraction is substantially increased and equilibrium limitation is overcome. The organic phase is, therefore, able to extract solutes from very lean solutions.

Among the major liquid membrane configurations [6, 34-36], the supported liquid membrane (SLM) comprises a micro-porous polymeric membrane in which the organic liquid is immobilized in its pores. The aqueous feed and the strip phases are confined to the two sides of a membrane pore. The organic phase immobilized in the pores, acts as a selective barrier for solute transport. Since the organic phase is confined to the pores of polymeric membrane, its total volume is limited by the pore volume of the membrane, which is very small. Moreover, any pressure imbalance on the two sides of the polymeric membrane can cause washout of the organic phase from the pores and irreversible breakthrough of one phase into the other phase [37-39]. In another configuration called dispersion liquid membrane (DLM), a dispersion of strip phase in a continuous organic phase is confined to one side, and the aqueous feed phase to the other side of a membrane pore. The organic phase fills the pores of the microporous polymeric membrane and acts as a liquid membrane. In DLM, continuous replenishment of the pores by the membrane liquid allows elimination of the problem of stability faced by SLM due to loss of the liquid membrane from the pores [22]. Due to short residence times of the dispersion in the contactor, DLM does not require the use of surfactant to stabilize the dispersion. This eases the product recovery process. The dispersion of strip phase in the organic phase is created externally in a mixer device.

Both SLM and DLM configurations can be operated in the hollow fiber modules. These are shell and tube type contactors having micro porous polymeric lumens packed in a cylindrical shell. One of the aqueous solutions passes through the lumen and the other passes through the shell side. Hollow fiber (HF) contactor provides the advantages such as non-dispersive contact, high mass transfer area per unit contactor volume and modular design for easy scale up [5, 40]. Hollow fiber dispersion liquid membrane (HFDLM) process employs DLM in HF contactor. Here, a dispersion of the strippant in the organic extractant is passed through the shell side of the hollow fiber contactor, while the feed solution is passed through the lumen side [7-8].

The interface between the organic phase and feed phase lies within the pore of the membrane. Location of this interface is important in deciding the rate of extraction. Since the diffusion coefficient of the metal cation in the aqueous feed phase is much higher than that of the metal-carrier complex in the organic phase, a higher rate of extraction can be achieved by maintaining the interface as near the shell end of the pore as possible so that diffusion path length in the organic phase is kept as low as possible. The wettability of the organic phase to the membrane material is very important. Low wettability results in shorter transport path in the organic phase and better rates of extraction. On the other hand, low wettability causes reduction of the breakthrough pressures and therefore requires more stringent control of the differential pressure across the membrane. Adequate wettability of polymeric membrane is essential for its ability to perform carrier-facilitated transport of metal species. Between the two polymeric membrane materials used in these studies, polysulfone (PS) is less hydrophobic than polypropylene (PP) [41-43], and would provide shorter path length in the organic phase. PS is a better material for working in nuclear environment due to its toughness, stability to nuclear radiation and resistance to oxidation.

In the present work, applicability of hollow fiber contactors, with micro-porous PS and PP fibers has been studied using HFDLM technique for recovery of uranium from lean acidic nuclear waste streams. Water-in-oil dispersion of 1 M $NaHCO_3$ in dodecane containing 30 % v/v Tri-n-butyl phosphate (TBP) is used as extractant. It is demonstrated here that hollow fiber contactor is a promising device for application in recovery of values like uranium from dilute streams using DLM configuration. This separation process can be applied for treatment of lean acidic streams such as raffinate from uranium refining plant. A mathematical model has been developed for determining the rate of transport through the membrane and the extent of extraction through the contactor. Model also estimates the fraction of the pore length wetted by the organic membrane phase. The model is validated for extraction of uranium from nitrate medium in once-through mode using dispersion liquid membrane employed in PS and PP contactors. The model has also been utilized for prediction of the performance of hollow fiber contactor on scale up for both polysulfone and polypropylene lumens.

Methodology

The organic phase was prepared by dissolving the 30 % v/v Tri-n-butyl phosphate (TBP) in n-dodecane. TBP and n-dodecane were supplied by Heavy Water Board, Mumbai. Pure uranyl nitrate solution (50 g/L of U^{+6}) is obtained internally from BARC. From this solution, feed of 0.5 g/L $U^{+6}$was prepared by dissolving it in 1 N HNO_3 (from Thomas Baker Chemicals Pvt. Ltd.). Raffinate stream of a uranium refining plant having acidity 1 N was also used as the feed. Raffinate contains mainly U^{+6} (around 200 ppm) along with some other ions in trace quantities. Aqueous solution of 1 M sodium bicarbonate (from Merck Specialties Pvt. Ltd.) was used as the strippant. The dispersion was prepared by adding an equal volume of strippant to the organic phase in dropwise manner, while agitating the organic phase at 3000 RPM [44]. REMI RQ-127 4 CROSS BLADE emulsifier was used as the agitator and mixing was performed in 20 minutes.

Five different hollow fiber contactors were used. Two contactors with PS lumens, PS1 and PS2, were supplied by Desalination Division, BARC. The other three contactors, consisting of polypropylene lumens, PP1, PP2 and PP3 (make: Liqui-Cel® 2.5x8”) were purchased from Membrana, Germany. Dimensional details for the contactors are presented in Table 3.1.

Table 3.1: Dimensional details for the contactors

Module	*PS1*	*PS2*	*PP1*	*PP2*	*PP3*
Diameter of the shell (cm)	5.0	5.5	5.0	8.5	8.8
Effective length, l (cm)	40	42	16	25	62
Fiber MOC	PS	PS	PP	PP	PP
Fiber OD, $2r_2$ (cm)	0.15	0.15	0.03	0.03	0.03
Fiber ID, $2r_1$ (cm)	0.125	0.10	0.024	0.024	0.024
Fiber log mean diameter, $2r_{lm}$ (cm)	0.14	0.12	0.027	0.027	0.027
Fiber wall thickness, $L\ (= r_2 - r_1)$(cm)	0.0125	0.025	0.003	0.003	0.003
Pore diameter (nm)	9	9	50	50	50
Porosity, ε %	70	70	40	40	40
Number of fibers, n_f	250	520	10,000	30,000	31800
Mass transfer area ($2\pi r_{lm} l \varepsilon n_f$) (m^2)	0.302	0.592	0.543	2.54	6.69
Contactor volume (m^3) x 10^4	7.85	9.98	3.14	14.2	37.7
Mass transfer area/contactor volume (m^2/m^3)	385	593	1729	1789	1774.5

The HFDLM system is shown in figure 3.1. It consists of a hollow fiber module, a feed and dispersion reservoirs, a feed and dispersion pumps and an agitator for dispersing the strippant into the organic phase. The feed was passed through the lumen side and the water-in-oil dispersion (1 M $NaHCO_3$ dispersed in dodecane containing 30 % v/v Tri-n-butyl phosphate) was circulated through the shell. The organic phase partially fills the micropores of the hollow fibers through capillary action. Positive pressure differential was maintained between the lumen-side of hollow fibers and the shell in order to prevent seepage of the organic phase into the lumen. At the end of the experiment, the agitator was turned off and the dispersion was allowed to separate into two phases viz. the lean organic solution and the loaded strip solution. Phase separation was rapid. Uranium content in the aqueous solutions was determined using ICP-OES. All the data are generated at least in duplicate and the standard deviation of the accepted data was within ±5%.

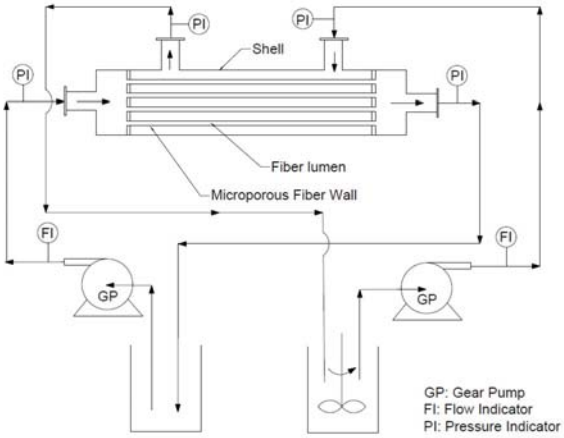

Figure 3.1: Schematic of HFDLM process in re-circulating mode

The photograph of the experimental setup is shown in Figure 3.2.

(a) Experimental set up with polysulfone contactor

(b) Experimental set up with polypropylene contactor

Figure 3.2: Experimental set up of HFDLM process; (a) PS1 contactor,(b) PP1contactor

A mathematical model of the transport process was developed for estimating the rate of transport through the membrane and the extent of extraction through the contactor. The model would be useful in optimization and scale-up of the process using a limited number of experiments.

Model development

In carrier-facilitated transport through liquid membrane in hollow fiber contactor, the metal ion, $UO_2^{2+}$is first transported from the feed phase to the interface of feed-organic phase (liquid membrane phase) located in the pores of the fiber. At the interface, UO_2^{2+}reacts with the carrier species, *TBP*, and nitrate ions, to form the metal-carrier complex, $UO_2(NO_3)_2.2TBP$. The reaction is represented by the following equation.

$$\mathrm{UO_2^{2+}(aq) + 2\,NO_3^-(aq) + 2\,TBP(org) \xleftrightarrow{K_{eq}} UO_2(NO_3)_2.2TBP(org)} \tag{1}$$

The reaction is fast enough to allow us to assume that it attains equilibrium at the interface. The equilibrium constant for this reaction can be related to the concentrations of the reacting species at the interface by the following equation.

$$K_{eq} = \frac{\left[\mathrm{UO_2(NO_3)_2.2TBP}\right]_{org}}{\left[\mathrm{UO_2^{2+}}\right]_{aq}\left[\mathrm{NO_3^-}\right]_{aq}^{2}\left[\mathrm{TBP}\right]_{org}^{2}} \tag{2}$$

The metal-carrier complex diffuses through the organic phase, till it reaches the organic-strip interface, where it releases the metal ion [34]. The regenerated *TBP* diffuses back towards feed-organic phase interface and the cycle repeats itself.

Following assumptions are involved in the development of the model,

1. The reaction is fast enough to attain equilibrium at the interface.
2. Steady state condition

3. Metal-carrier complex breaks instantaneously at the interface between the organic and the strip phase and resulting metal ions cannot be recaptured by the carrier species.
4. Stripping phase interfacial area $a_s >> a_{lm}$.

Differential mass balance for a UO_2^{2+}along a single fiber lumen, at steady state condition, gives

$$-v\,\pi\, r_l^2 \frac{dC_f}{dz} = 2\pi\, r_{lm} \varepsilon\, J \qquad (3)$$

Here, v is the linear velocity of the feed solution through the lumen, C_f is the concentration of the metal ions in the feed and z is the distance measured along the fiber. J is the flux of ions across the fiber, ε is the fraction of the fiber surface which is occupied by pores, and r_{lm} is the log-mean radius of hollow fiber, and is related to the inner radius (r_1) and the outer radius (r_2) of the fiber as, $r_{lm} = (r_1 - r_2)/ln\left(\frac{r_1}{r_2}\right)$

The rate of transport of the metal ions across unit length of the fiber bundle is $2\pi n_f r_{lm} \varepsilon J$, where n_f is number of fibers in the bundle. At steady state, these metal ions are captured by the strip phase. Hence, we can write

$$V_s \frac{dC_s}{dz} = n_f\, 2\pi\, r_{lm} \varepsilon\, J \qquad (4)$$

Here, V_s is the volumetric flow rate of the strip phase and $C_s$is the concentration of metal ions in the strip phase.

In order to obtain the flux J, we consider various transport processes occurring across the wall of a fiber. Schematic diagram of a fiber wall is presented in Figure 3.3. It shows a single pore. The interface between the feed and the organic phase lies within this pore. The total length L of the pore therefore partially filled by the feed solution on one side (length L_f) and the organic phase on the other side (length L_o).

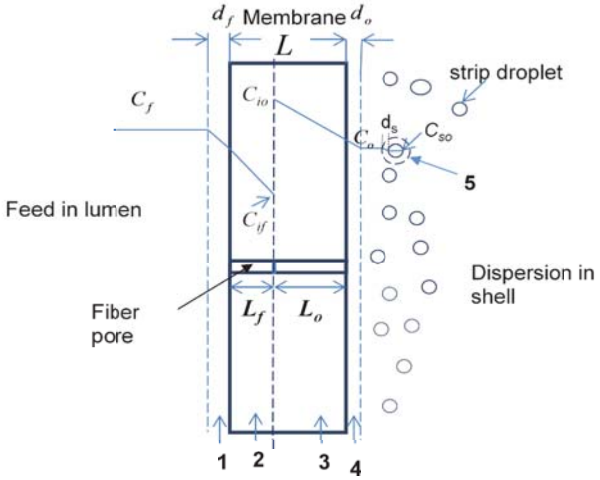

Figure 3.3: Schematic representation of transport of metal ion through the hollow fiber membrane; 1- diffusion film at the feed-membrane interface, 2-region of the pore filled with feed solution, 3-region of the pore filled with organic liquid, 4- diffusion film at the organic membrane interface, 5-diffusion film at strip-organic interface

Metal cations UO_2^{2+} are transported across the diffusion film of thickness d_f, adjacent to the inner side of the fiber wall, before they enter the pore. They are then transported through the pore until they arrive at the feed-organic phase interface. The concentration of the metal ions in the feed solution at the interface is denoted by C_{if}. At the interface, metal ions react with TBP to form the complex. The reaction is instantaneous and reversible, so that, the concentration C_{io} of the complex (i.e. $[UO_2(NO_3)_2 \cdot 2TBP]_{org}$) is in equilibrium with C_{if} $(i.e. [UO_2^{2+}]_{aq})$. The complex diffuses through the organic phase to the pore mouth on the outer surface of the fiber and then through the diffusion film into the bulk organic phase. The concentration of the complex is uniform in the bulk organic phase. It again falls in the diffusion film surrounding the drop of the strip phase, till it reaches the organic phase-strip phase interface, where its concentration drops to C_{so}. It is then captured by the strip phase. We assume that the complex breaks instantaneously at the interface between the organic and the strip phase and that the resulting metal ions cannot be recaptured by the carrier species. This allows us to assume that $C_{so} = 0$.

At steady state, all fluxes should match. This fact is depicted by the following equations

$$J = k_f\left(C_f - C_{if}\right) = k_o\left(C_{io} - C_o\right) = k_s\left(\frac{a_s}{a_{lm}}\right)\left(C_o - C_{so}\right) \tag{5}$$

Once uranyl ion enters the strip phase, it is immobilized there. Hence, it's back driving force must be zero and thus C_{so} can be taken as zero in Eq 5,

$$J = k_f\left(C_f - C_{if}\right) = k_o\left(C_{io} - C_o\right) = k_s\left(\frac{a_s}{a_{lm}}\right)C_o \tag{6}$$

Where,

$$k_f = \frac{\mathcal{D}_f}{d_f + L_f} \tag{7}$$

$$k_o = \frac{\mathcal{D}_o}{d_o + L_o} \tag{8}$$

$$k_s = \frac{\mathcal{D}_o}{d_s} \tag{9}$$

The relation between the concentrations C_{if} and C_{io} is obtained using Equation 2 as,

$$\frac{C_{io}}{C_{if}} = K_{eq}\left[NO_3^-\right]_{aq}^2\left[TBP\right]_{org}^2 \tag{10}$$

The terms on the right-hand side remain constant along the length of the fiber and hence the ratio C_{io}/C_{if} is denoted by D_f and is called the distribution coefficient.

Combining equations 6 and 10, we get

$$J = \frac{D_f C_f}{\frac{D_f}{k_f} + \frac{1}{k_o} + \frac{a_{lm}}{k_s a_s}} \tag{11}$$

Noting that the last term in the denominator of Eq. 11 is very small compared to the rest of the terms since $a_s >> a_{lm}$, we can simplify Eq. 11 to

$$J = \frac{D_f C_f}{\frac{D_f}{k_f} + \frac{1}{k_o}} \tag{12}$$

For the lumen side, from Eq. 3 and 12,

$$\frac{dC_f}{dz} = \frac{-2\, r_{lm} \varepsilon\, D_f C_f}{v r_l^2 \left(\frac{D_f}{k_f} + \frac{1}{k_o} \right)} \tag{13}$$

Similarly combining Eq. 4 and 12, we get

$$\frac{dC_s}{dz} = \frac{2\pi\, r_{lm} \varepsilon\, n_f D_f C_f}{V_s \left(\frac{D_f}{k_f} + \frac{1}{k_o} \right)} \tag{14}$$

Equation 13 can be integrated using the initial condition $C_f = C_{f0}$ at z = 0 to yield the following expression,

$$\ln\left(\frac{C_f}{C_{f0}} \right) = \frac{-2\, r_{lm} \varepsilon\, D_f z}{v r_l^2 \left(\frac{D_f}{k_f} + \frac{1}{k_o} \right)} \tag{15}$$

Combining equation 13 and 14, we get

$$\frac{dC_s}{dz} = -\pi\, n_f r_l^2 \frac{v}{V_s} \frac{dC_f}{dz} \tag{16}$$

Equation 16 on integration gives,

$$C_s = \pi\, n_f r_l^2 \frac{v}{V_s} \left(C_{f0} - C_f \right) \tag{17}$$

Where, C_{f0} is the initial uranium concentration of feed. It is assumed that strip phase is free from metal ion at the inlet. Distribution coefficients, D_f and D_s have been generated through independent liquid-liquid extraction experiments. Using Equation 15, fraction of the pore length wetted by the organic membrane phase has been estimated for lumens made of polysulfone and polypropylene.

Developed mathematical model can be used for prediction of extraction rate of other ions and other types of polymeric membrane. The data needed for the design are, the carrier mediated distribution coefficient of the ion in the organic phase, diffusion coefficient of the ion in the aqueous phase and diffusion coefficient of the ion-carrier complex in the organic phase. Along with pore diameter, pore length and pore area, fraction of the pore length wetted by the organic phase is also needed. This length will be determined by wettability of the polymeric membrane for organic liquid membrane phase.

Results

Hollow fiber dispersion liquid membrane process has been employed for transport of uranium using feed phase as pure uranyl nitrate solution containing 0.5 g/L U^{+6} in 1 N HNO_3, organic phase as 30% v/v TBP in dodecane and strip phase as 1 M $NaHCO_3$. Flow rate of feed phase through fiber lumen and flow rate of dispersion through shell has been maintained at 200 ml/min. Equal volumes of the organic and the strip phases are used for preparing the dispersion. Mass transfer coefficients for aqueous and organic phases are estimated below through available correlations in literature.

Estimation of mass transfer coefficient of feed phase

The Wilke-Chang correlation can be used for estimation of diffusivity of uranyl ion in the aqueous phase as following [28] for solute molar volume less than 0.5 m^3/kmol,

$$\mathcal{D}_f = 1.173 x 10^{-16} \frac{(\varphi M_B)^{1/2} T}{\mu_B V_A^{0.6}} \tag{18}$$

Where, M_B is the molecular weight of solvent B, μ_B is the viscosity of solvent in Pa.s, V_A is the solute molar volume in m^3/kmol and φ is an association parameter of the solvent. Substituting, M_B = 63 kg/kmol, φ = 1 for nitric acid medium, T = 298 K, $\mu_B = 1 x 10^{-3}$Pa.s and $V_A = 9.35 \times 10^{-2}$ m^3/kmol [45] in Equation 18, $\mathcal{D}_f$ is estimated as 1.15×10^{-9} m^2/s. The mass transfer coefficient inside the fibers is described by the Leveque equation (for Graetz number greater than four) considering fast chemical reaction under laminar flow as following [5],

$$\mathrm{Sh} = 1.62\,(4r_l^2 v/(l\mathcal{D}_f))^{1/3} \tag{19}$$

Where, Sh is the Sherwood number (= $2k_{fl}r_l/\mathcal{D}_f$), k_{fl} is mass transfer coefficient of aqueous feed film, r_l is the internal radius of fiber, v is the linear flow velocity of the feed solution through fiber lumen, l is the length of fiber and $\mathcal{D}_f$ is the diffusion coefficient of uranyl ion in the aqueous phase. Substituting $\mathcal{D}_f$(=1.15×10^{-9} m^2/s) along with fiber characteristic properties (r_l and l) and feed flow velocity (v) in Leveque equation, k_{fl} has been estimated for PS and PP contactors and listed in Table 3.2.

Estimation of mass transfer coefficient of organic membrane phase

The diffusion coefficient of uranyl complex, $\mathcal{D}_{oeff}$, in dodecane containing TBP has been calculated using Stokes-Einstein equation for porous medium as following [28] for solute molar volume greater than 0.5 m^3/kmol,

$$\mathcal{D}_{oeff} = \mathcal{D}_o(\varepsilon/\tau) = \frac{9.96 \times 10^{-16}\ T}{\mu V_A^{1/3}}(\varepsilon/\tau) \tag{20}$$

Where, $\mathcal{D}_o$ is the diffusion coefficient of $UO_2(NO_3)_2.2TBP$ in the bulk organic phase and μ is the viscosity of organic liquid membrane in Pa.s. Substituting $V_A = 0.64$ m^3/kmol [45], μ for Dodecane containing 30 % v/v TBP = 1.75×10^{-3} Pa.s and T = 298 K in Equation 20, $\mathcal{D}_o$ is estimated as 1.968×10^{-10} m^2/s. Calculated values of $\mathcal{D}_f$ and $\mathcal{D}_o$ are in accordance with that found in the literature [46].

Viscosity of organic liquid membrane for varying composition is measured using Ostwald viscometer and presented in Figure 3.4. Viscosity is used for estimation of mass transfer coefficient.

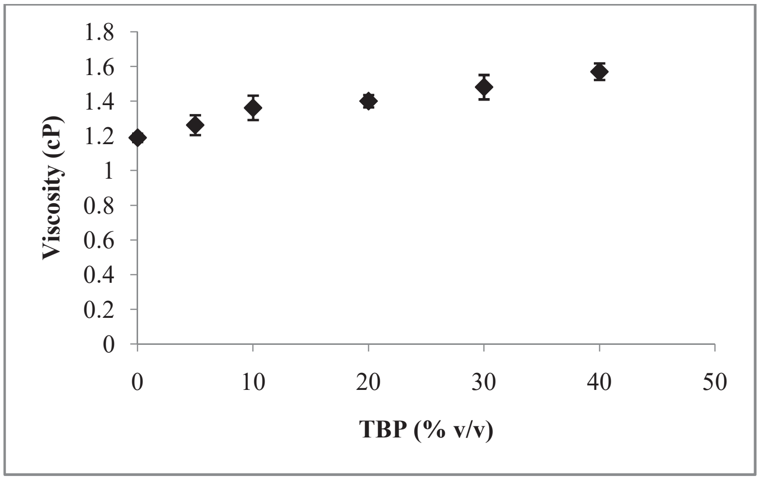

Figure 3.4: Viscosity of organic phase for varying concentration of TBP dissolved in dodecane

Estimation of mass transfer coefficient of diffusion film at the organic membrane interface shell side

Average shell side velocity, v_s is estimated using superficial velocity divided by free flow area (1- φ). Shell side equivalent diameter, d_e is estimated through 4 x flow area/total fiber circumference. Using d_e and v_s along with density and viscosity of shell side liquid, reynolds number has been calculated and shown in Table 3.2. At low reynolds number, mass transfer coefficients around a stationary cylinder can be obtained through following correlation [23, 47],

$$St\, Sc^{0.67} = 3.42\, Re^{-0.672} \tag{21}$$

Where, $St = k_{o1}/v_s$

Mass transfer coefficient of diffusion film at the organic membrane interface, k_{o1} is thus estimated for PS and PP contactors and presented in Table 3.2. All parameters along with the estimated are summarized in Table 3.2.

Table 3.2: List of parameters for contactors

Parameters	*PS1*	*PS2*	*PP1*	*PP2*	*PP3*
Fiber inner diameter, $2r_1$ (cm)	0.125	0.10	0.024	0.024	0.024
Fiber outer diameter, $2r_2$ (cm)	0.15	0.15	0.030	0.030	0.030
Fiber wall thickness, L (cm)	0.0125	0.025	0.003	0.003	0.003
Effective length of fiber, l (cm)	40	42	16	25	62
Diameter of the shell (cm)	5	5.5	5	8.5	8.8
Fiber packing fraction, φ	0.225	0.387	0.45	0.45	0.45
Feed velocity, v (cm/s)	1.087	0.82	0.74	1.23	1.16
No of fibers, n_f	250	520	10000	30000	31800
Porosity, ε	0.7		0.4		
Tortuosity, τ	1.5		2		
Diffusion coefficient in aqueous phase, D_f (cm^2/s)	1.15×10^{-5}				
Diffusion coefficient in bulk organic phase, D_o (cm^2/s)	1.97×10^{-6}				
Aqueous phase mass transfer coefficient, k_{f1} (cm/s)	9.93×10^{-4}	9.58×10^{-4}	2.05×10^{-3}	2.10×10^{-3}	7.05×10^{-3}
Average velocity shell side, v_s (cm/s)	0.219	0.229	0.38	0.40	0.55
Equivalent diameter shell side, d_e (cm)	0.517	0.24	0.036	0.058	0.039
Re_{shell} ($=d_e v_s \rho/\mu$)	8.47	4.07	1.03	1.735	1.65
Sc_{shell} ($=\mu/\rho D_o$)	6794		1163		
Organic phase mass transfer coefficient shell side, k_{o1} (cm/s)	4.88×10^{-4}	8.29×10^{-4}	3.50×10^{-3}	2.59×10^{-3}	3.68×10^{-3}

Transport of Uranium in once through mode operation of hollow fiber contactor

Polysulfone contactors (PS1 and PS2) have been employed for recovery of uranium from nitrate medium through HFDLM process using 30% v/v TBP in dodecane. Using PS1 and PS2 contactor, percent extraction of 28 % and 40 % has been achieved, respectively, in single pass of the feed solution. Prediction has been made by developed model using parameters from Table 3.2 and shown in figure 3.5 along with the data. Prediction agrees with the data.

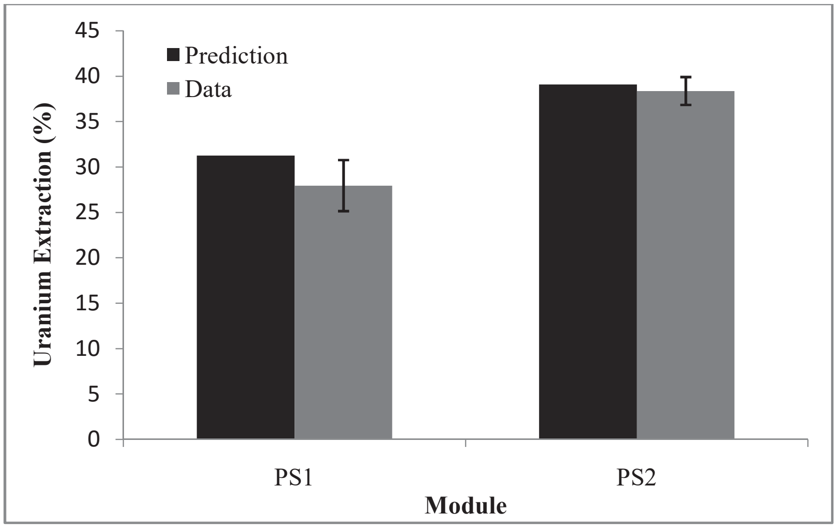

Figure 3.5: Extraction of uranium from nitrate medium using polysulfone (PS) contactors in once-through mode; organic: 30 % v/v TBP dissolved in dodecane, aqueous strip: 1 M $NaHCO_3$, W/O ratio in dispersion is 1:1 v/v; agitation rpm 3000

Similar studies have been conducted using microporous contactors with polypropylene lumen (PP1, PP2 and PP3) and percent extraction of 55 %, 75 % and 95 % has been observed, respectively. Model prediction, using parameters from Table 3.2, is shown in figure 3.6 along with the data. Prediction ties in well with the data.

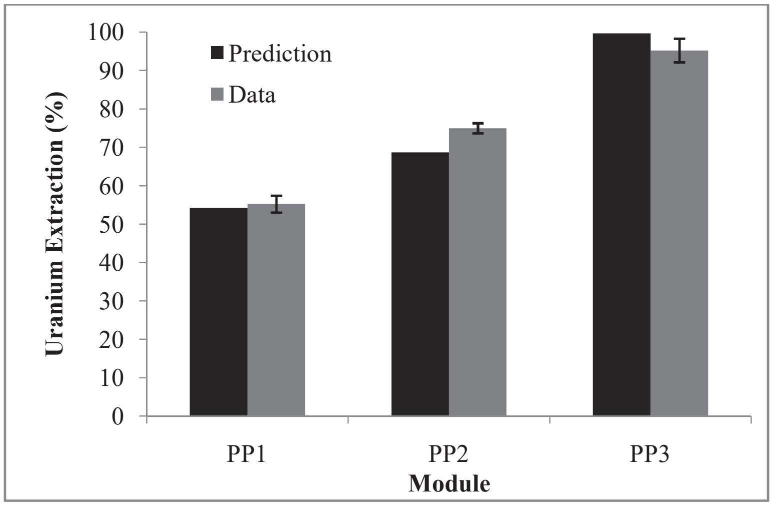

Figure 3.6: Extraction of uranium from nitrate medium using polypropylene (PP) contactors in once-through mode; organic: 30 % v/v TBP dissolved in dodecane, aqueous strip: 1 M $NaHCO_3$, W/O ratio in dispersion is 1:1 v/v; agitation rpm 3000

At $z = l$, Equation 15 can be written as,

$$\ln\left(\frac{C_f}{C_{f0}}\right) = \frac{-2\, r_{lm} \varepsilon\, D_f l}{v r_l^2 \left(\frac{D_f}{k_f} + \frac{1}{k_o}\right)} \tag{22}$$

Equation 22 can be rearranged as,

$$\frac{D_f}{k_f} + \frac{1}{k_o} = \frac{-2\, r_{lm} \varepsilon\, D_f l}{v r_l^2\, \ln\left(C_f / C_{f0}\right)} \tag{23}$$

The extraction of uranium is defined as,

$$E = \left(1 - \frac{C_f}{C_{f0}}\right) \tag{24}$$

Combining Equation 23 and 24,

$$\frac{D_f}{k_f} + \frac{1}{k_o} = \frac{-2\, r_{lm} \varepsilon\, D_f l}{v r_l^2\, \ln\left(1 - E\right)} \tag{25}$$

Substituting $L_f = L(1-\alpha)$ & $L_o = L\alpha$, Equation 7 and 8 can be rewritten as,

$$\frac{1}{k_f} = \frac{d_f + L(1-\alpha)}{\mathcal{D}_f} \tag{26}$$

$$\frac{1}{k_o} = \frac{L\alpha}{\mathcal{D}_{oeff}} + \frac{d_o}{\mathcal{D}_o} \tag{27}$$

Substituting k_f and k_o from Equation 26 and 27 in Equation 25,

$$\frac{D_f\left(d_f + L(1-\alpha)\right)}{\mathcal{D}_f} + \frac{L\alpha}{\mathcal{D}_{oeff}} + \frac{d_o}{\mathcal{D}_o} = \frac{-2\, r_{lm}\, \varepsilon\, D_f l}{v r_l^2 \ln\left(1-E\right)} \tag{28}$$

Substituting $k_{f1} = \mathcal{D}_f/d_f$ and $k_{o1} = \mathcal{D}_o/d_o$, Equation 28 can be rewritten as,

$$D_f\left(\frac{1}{k_{f1}} + \frac{L\left(1-\alpha\right)}{\mathcal{D}_f}\right) + \frac{L\alpha}{\mathcal{D}_{oeff}} + \frac{1}{k_{o1}} = \frac{-2\, r_{lm}\, \varepsilon\, D_f l}{v r_l^2 \ln\left(1-E\right)} \tag{29}$$

Simplifying Equation 29,

$$\frac{-2\, r_{lm}\, \varepsilon\, l}{v r_l^2 \ln\left(1-E\right)} = \left(\frac{1}{D_f \mathcal{D}_{oeff}} - \frac{1}{\mathcal{D}_f}\right) L\alpha + \left(\frac{1}{k_{f1}} + \frac{L}{\mathcal{D}_f} + \frac{1}{D_f k_{o1}}\right) \tag{30}$$

Since the diffusion coefficient of the metal-carrier complex in the organic phase is much lower than that of the metal ion in the aqueous feed phase (as per Table 3.2), mass transfer resistance inside membrane is controlling. Hence, estimation of fraction of the pore length wetted by the organic phase is necessary for estimation of the rate of extraction. Equation 30 has been used for estimation of the fraction of the pore length wetted by the organic phase for known extraction in PS and PP contactors. It is found that 40 % of the pore length is wetted by the organic phase in PS2 contactor. Similarly, for PP1, consisting hydrophobic polypropylene lumen, α is estimated to be 1.1. This implies that in the case of PP membrane, the entire length of the pore is wetted by the organic phase. Value of α greater than one, implies that part of the liquid protrudes out from the pore in the form of convex meniscus. A small extent of leakage of the organic phase in the feed is also expected. It was indeed observed in PP membrane, whereas no perceptible leakage was detected with PS membrane. In spite of this drawback, PP1 module is found to exhibit greater extent of extraction than PS1 and PS2. This is because, the fiber wall thickness (L) of PP lumen is one order of magnitude less than that of the PS lumen as mentioned in Table 3.1. Hence, the reduction in the rate of diffusion of uranium ions due to higher value of α in PP lumen is overcompensated by its shorter pore length, L.

It has also been understood through Equation 30 that gradient of $L\alpha$ depends upon diffusion coefficient of solute in organic liquid membrane phase sitting inside the pores, $\mathcal{D}_{oeff}$ ($=\mathcal{D}_o(\varepsilon/\tau)$). This diffusion coefficient will vary among different polymeric membranes because it depends on the characteristic properties of porous polymeric support such as its porosity, ε and tortuosity, τ. Thus, for polymeric membranes with higher ε/τ (i.e. higher $\mathcal{D}_{oeff}$), result in low gradient of $L\alpha$.Hence, for those membranes, extraction of solute (E) will be less dependent on the fraction of the pore length wetted by the organic membrane phase, L_o ($=L\alpha$).

Utilization of the model for scale up of the process

The model has been utilized to predict the performance of PS and PP hollow fiber contactors, respectively, on their scale up [48]. Parameters conserved during scale up are feed flow velocity, mass transfer coefficients of aqueous and organic phases and fiber characteristic properties. Parameters scaled up are mass transfer area and throughput. Figure 3.7 presents the schematic of the separation process showing a hollow fiber lumen of length l. Prediction of extraction made using PS1 and PP1 with parameters conserved as above has been shown in Table 3.3. PS1 predicts the performance of PS2 for increased lumen length of 42 cm. Prediction made using PS1 ties in well with the data generated using PS2 and shown in Table 3.3 (a). Similarly, PP1 predicts the performance of PP2 and PP3 for increased lumen length of 25 cm and 62 cm. Predictions made using PP1 have found in agreement with the data generated using PP2 and PP3 and shown in Table 3.3 (b). Hence, the present model can be easily utilized for scale up of HFDLM process with limited experimental trials [49].

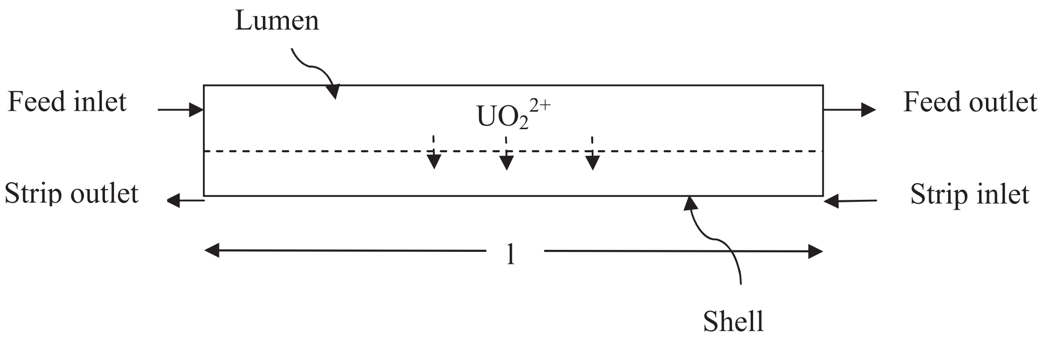

Figure 3.7: Schematic of the separation process showing a hollow fiber lumen of length, l

Table 3.3: Effect of increase in lumen length on uranium extraction, (a) PS contactor (b) PP contactor

(a)

Length of the fiber, l (cm)	Extraction % (Prediction)	Extraction % (Data)
40	31.25	28 (generated using PS1) *
42	41.28	39.9 (generated using PS2) *
45	43.47	
50	46.94	
55	50.20	
60	53.26	

** Effective length of lumen, l in PS1 and PS2 contactors are 40 and 42 cm, respectively.*

(b)

Length of the fiber (cm)	Extraction % (Prediction)	Extraction % (Data)
16	54.21	55.21 (generated using PP1) #
20	62.33	
25	70.49	73.64 (generated using PP2) #
30	76.88	

40	85.81	
50	91.29	
62	98.56	98.30 (generated using PP3) #

Effective length of lumen, l in PP1, PP2 and PP3 contactors are 16, 25 and 62 cm, respectively.

Our study has presented a mathematical model for estimation of the wetted length of the fiber pore. Developed model is not system specific and can be used for prediction of extraction rate of other ions and other types of polymeric membranes. It is found that 40 % of the pore length is wetted by the organic phase in polysulfone contactor. Similarly, for polypropylene contactor, consisting hydrophobic polypropylene lumen, α is estimated to be 1.1. This implies that in the case of polypropylene membrane, the entire length of the pore is wetted by the organic phase. Polypropylene module is found to exhibit greater extent of extraction than polysulfone. This is because, the fiber wall thickness of PP lumen is one order of magnitude less than that of the PS lumen. Hence, the reduction in the rate of diffusion of uranium ions due to higher value of α in PP lumen is overcompensated by its shorter pore length. It has also been understood that for polymeric membranes with higher ε/τ, extraction of solute will be less dependent on the fraction of the pore length wetted by the organic membrane phase. The model has been utilized to predict the performance of PS and PP hollow fiber contactor, respectively, on their scale up. Prediction is found in agreement with the data.

CHAPTER 4

STUDIES OF MASS TRANSFER IN LIQUID-LIQUID SYSTEMS: EFFECT OF EXTRACTANT

Introduction

Effect of type of extractant viz. tri-n-butyl phosphate and its homologue tri-iso-amyl phosphate has been studied on rate of transport of uranium through hollow fiber dispersion liquid membrane. TiAP is a higher homologue of TBP, which inherits its qualities of selective extraction of U(VI) and remove the limitations of chemical degradation and entrainment in aqueous phase. Liquid-liquid extraction experiments were conducted to generate the data on partition coefficient of U(VI) in the organic phase containing different TBP and TiAP concentrations.

Methodology

The plant raffinate was taken as the feed and the organic phase was ligand dissolved in dodecane. The equilibrium was achieved by stirring feed and organic phase in a DBK-Digital Wrist Action Shaker for 10 minutes keeping feed to organic ratio as 1:1. After the agitation was stopped, both phases were allowed to separate and U(VI) in the aqueous phase was analyzed. Its concentration in the organic phase was estimated through material balance. To determine the extent of transport of the nitric acid along with the U(VI), acidic raffinate samples were titrated against sodium hydroxide using phenolphthalein as indicator.

The dispersion liquid membrane experiments were performed in a hollow fiber (HF) contactor. The details of hollow fiber contactor are presented in Table 4.1. For hollow fiber dispersion liquid membrane (HFDLM), feed was circulated in lumen side, while the dispersion was confined to the shell side. In carrier facilitated transport through HFDLM, the metal cation diffuses through aqueous feed film and reacts reversibly with the ligand at the feed-membrane interface resulting in the formation of metal carrier complex. The complex then diffuses through the membrane due to its own concentration gradient and consequently at the membrane strip interface, it releases the metal ion. The ligand thus left over diffuses back towards the feed-membrane interface and the cycle continues. The released cation diffuses through the aqueous strip film. Both the raffinate and the strip samples were analyzed for U(VI) through HORIBA Scientific ULTIMA 2 ICP Optical Emission Spectrometer.

Table 4.1: Characteristics of hollow fiber contactor, Liqui-Cel® 2.5x8

1.	Diameter of shell, m	$5x10^{-2}$	7.	Porosity, ε %	40
2.	MOC of housing (shell)	PC	8.	Pore diameter, m	$5x10^{-8}$
3.	Fiber MOC	PP	9.	No of fibers, N	$1x10^{4}$
4.	Fiber inner diameter, D_i m	$2.2x10^{-4}$	10.	Interfacial area for extraction, ($\pi D_i L \varepsilon N$) m^2	$4.8x10^{-1}$
5.	Fiber thickness, m	$3x10^{-5}$	11.	Lumen Volume, m^3	$1.5x10^{-4}$
6.	Fiber length, L m	$1.6x10^{-1}$	12.	Specific interfacial area (per unit lumen volume) (m^2 m^{-3})	$3.2x10^{3}$

Batch liquid-liquid extraction studies

Figure 4.1 shows the generated data of distribution coefficient of U(VI) versus TiAP concentration. The extraction of U(VI) using TiAP as the extractant from nitric acid medium can be represented by the following equilibrium reaction [21],

$$UO_2^{2+}(aq) + 2\,NO_3^-(aq) + xTiAP(org) \xleftrightarrow{K_{eq}} UO_2(NO_3)_2.xTiAP(org) \tag{1}$$

$$K_{eq} = \frac{\left[UO_2(NO_3)_2.xTiAP\right]_{org}}{\left[UO_2^{2+}\right]_{aq}\left[NO_3^-\right]_{aq}^{2}\left[TiAP\right]_{org}^{x}} = \frac{K_d}{\left[NO_3^-\right]^2\left[TiAP\right]^x} \tag{2}$$

$$K_d = K_{eq}\left[NO_3^-\right]^2\left[TiAP\right]^x \tag{3}$$

K_{eq} stands for equilibrium constant and K_d is the distribution coefficient of uranium with TiAP, which is equal to $[UO_2(NO_3)_2.2TiAP]_{org}/\ [UO_2^{+2}]_{aq}$.

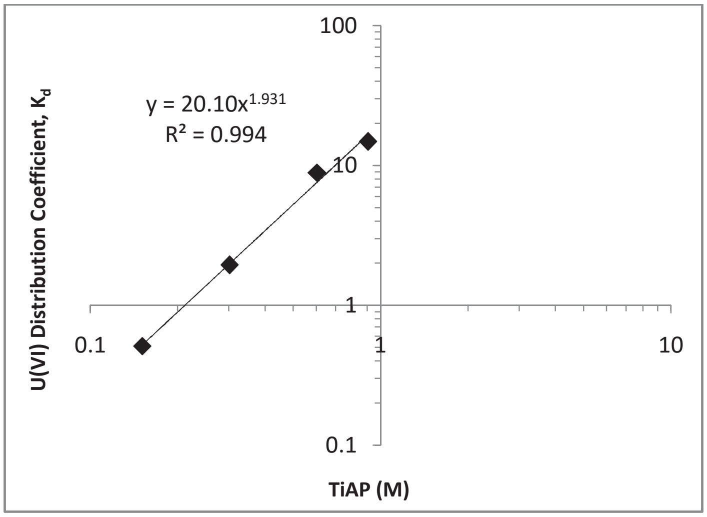

Figure 4.1: Distribution coefficient of U(VI) for different TiAP concentrations with uranium plant raffinate as the feed; feed/organic is 1

In a set of batch experiments, the K_d values are obtained at constant $[NO_3^-]$ and variable [TiAP]. A log-log plot is drawn of K_d and TiAP concentration (Figure 4.1), which can be described by the following equation,

$$K_d = 20.1\ [\text{TiAP}]^{1.93} \tag{4}$$

Comparing Eq. (3) and (4), it can be realized that around 2 molecules of TiAP are associated with one molecule of U(VI) to form the metal-carrier complex. Substituting K_d from Eq. (4) into Eq. (3) and putting $[NO_3^-] = 1.5$ M., we get the value of equilibrium constant, K_{eq} as 8.93 M^{-4}. Similarly, K_{eq} for U(VI)-TBP system is found as 6.65 M^{-4}. Corresponding to equation 4, $K_d = 6.654\ [\text{TBP}]^{1.73}$. This shows that TiAP has little bit greater affinity for U(VI), compared to TBP.

During the extraction of U(VI) from nitric acid media, HNO_3 also gets extracted by TiAP [50]. To determine the amount of nitric acid extracted into TiAP, concentration of nitric acid in the raffinate samples was titrated to assess the extent of association of the acid with TiAP in the HNO_3-TiAP complex. Observations are shown in Figure 4.2. Through regression analysis, the equilibrium constant for acid transport has been estimated as 0.20 M^{-2}. Figure 4.2 also shows the corresponding values for TBP. It has been observed that the extent of association of nitric acid with TiAP is similar to that with TBP. Using TBP, equilibrium constant for acid transport has been calculated as 0.16 M^{-2}, which is in accordance with that found in the literature [51].

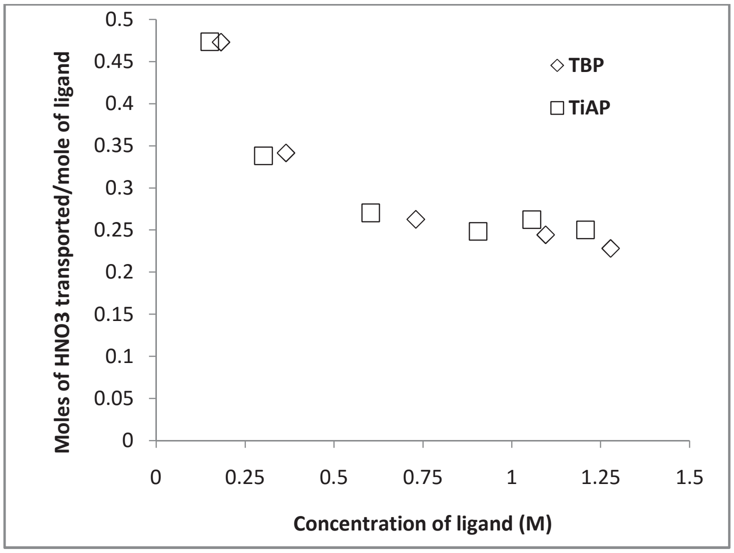

Figure 4.2: Comparison of HNO_3 transport along with the U(VI) using TiAP and TBP; feed is uranium plant raffinate; feed/organic is 1

Studies on hollow fiber contactor

ELM experiments were conducted in hollow fiber (HF) contactor having the initial U(VI) concentration 190 ppm in 1.5M nitric acid. The raffinate was circulated in lumen of HF. A dispersion of 0.1 M $NaHCO_3$ in dodecane containing TiAP (10 % v/v), stabilized with SPAN80 was passed through the shell side in countercurrent mode.

HF contactor operation in once through mode

Comparison of the extraction efficiency for once through mode operation of HFELM is shown in Figure 4.3 for both TiAP and TBP as the ligand. Extraction efficiency has been calculated through following equation.

$$\text{Extraction (\%)} = 100(1-(C/C_o)) \tag{5}$$

Where, C is the concentration of U(VI) in the raffinate and C_o is the feed initial U(VI) concentration. It has been observed that around 25% of U(VI) has been extracted in once through mode with the TiAP, while for TBP, around 24% extraction of U(VI) has been achieved.

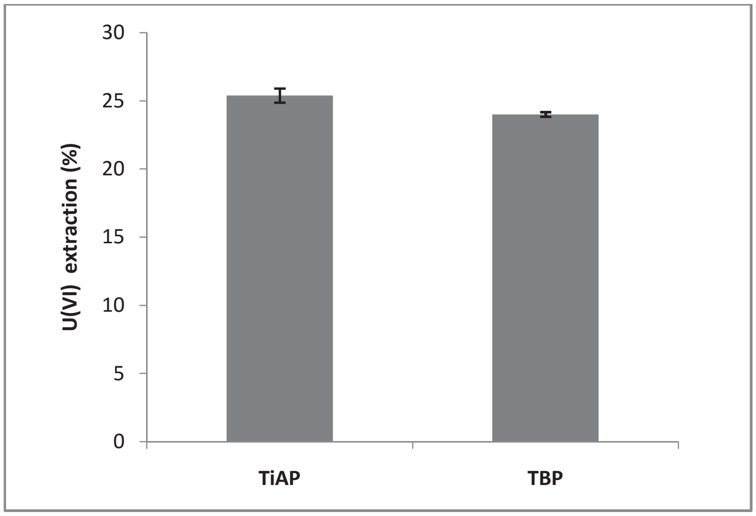

Figure 4.3: Comparison of transport of U(VI) in once through mode operation of HFELM using TiAP and TBP as the ligand; Feed: uranium plant raffinate; organic: 10 % v/v ligand dissolved in dodecane with 2 % v/v SPAN80; aqueous phase: 0.1 M $NaHCO_3$; W/O ratio in emulsion is 2:3 v/v; agitation rpm 4000; flow rate for HF is 400 ml min^{-1} in both the tube and shell side

HF contactor operation in recirculating mode

HFELM has also been operated in recirculating mode with the same conditions and observations are shown in Figure 4.4. U(VI) extraction of 68% has been achieved in the period of 1 hour using TiAP as the carrier. Figure 4.4 also shows the similar run with HFELM in recirculating mode using TBP with similar U(VI) extraction has been achieved in 1 hour. It is seen that both the carriers are performing almost identical for U(VI) extraction. Use of TiAP for U(VI) extraction can be advantageous in view of its lower solubility in water (0.1 g L^{-1}) and greater resistance to acid hydrolysis and chemical degradation.

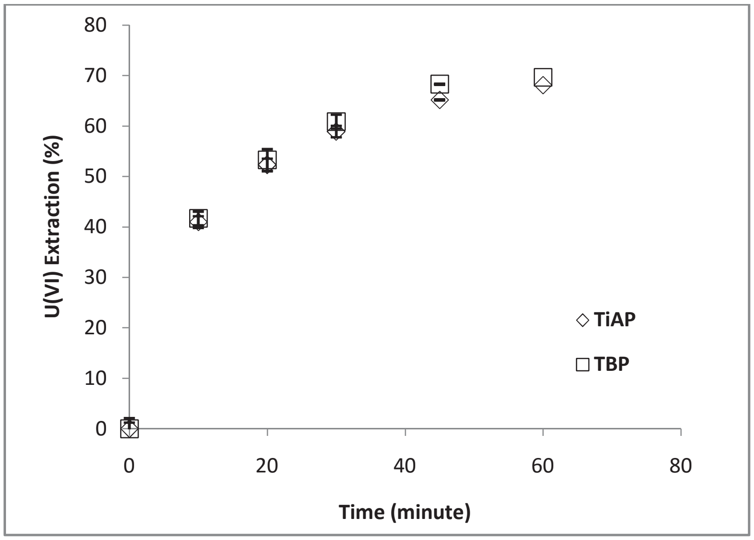

Figure 4.4: Transport of U(VI) in recirculating mode operation of HFELM; Feed: uranium plant raffinate; organic: 10 % v/v TiAP dissolved in dodecane with 2 % v/v SPAN80; aqueous phase: 0.1 M $NaHCO_3$; W/O ratio in emulsion is 2:3 v/v; agitation rpm 4000; flow rate 400 ml min^{-1} in both the tube and shell side; Volume in recirculation is 1L

CHAPTER 5

DISPERSION LIQUID MEMBRANE IN HOLLOW FIBER CONTACTOR: PRELIMINARY STUDIES

Introduction

Recovery of material like uranium, strontium, cesium, thorium etc from dilute streams is a major task in nuclear industry in view of environmental remediation and value recovery [52]. The conventional methods for these purposes, viz. solvent extraction and ion exchange have their own limitations such as solvent extraction includes the need for separate extraction and stripping steps, problems of emulsification, requirement of multistage contact for recovering solute from dilute streams, flooding and loading limits in continuous countercurrent devices, the need for density difference between the phases, use of a scrubbing agent, high solvent losses and large solvent inventories; while ion-exchange process suffers from the problem of resin fouling, capacity limitations, the requirement of more complexing material, and selectivity. Moreover, these separation processes are equilibrium-limited. Off late, liquid membrane systems are showing promise in terms of high selectivity for the strategic material, low organic and energy consumption, simultaneous extraction and stripping, moderate cost-to-performance ratios and time-effectiveness.

Among major liquid membrane configurations, one comprises an micro-porous membrane having two fluid-2 phase interfaces immobilized at the two ends of a membrane pore called supported liquid membrane (SLM); liquid layer between two immobilized fluid-2 phase interfaces acts as a selective barrier for solute transport; due to limited membrane liquid inventory, this configuration suffers from limitations such as washing out of membrane from pores and destruction of the phase interface. Another configuration is based on if one of the phase interfaces is mobile, while the other phase interface is immobilized at the end of a membrane pore mouth; here, dispersion of one liquid phase in another is created externally in a mixer/dispersion device called dispersion liquid membrane (DLM). Later configuration is beneficial in view of larger interfacial area for stripping as compared to previous and hence, higher rate of transport of solute from feed to strip can be obtained; stability issues like membrane loss from pores are also eliminated due to continuous replenishment of the membrane liquid [22].

Both of the above configurations can be operated in the hollow fiber module (figure 5.1), which are shell and tube type contactors having micro porous polymeric lumens packed in a cylindrical shell. One of the aqueous solution passes through the lumen and the other passes through the shell side. This type of contactor offers packaging large areas of membrane/ volume of module economically and efficiently; through non-dispersive contact, it avoids the mixing between the feed stream and the extracting phase; scale-up of this system is also simple due to its modular design [5]. DLM has been identified as a sufficiently stable configuration in view of providing constant supply of organic solution to the membrane pores [7]. In that a dispersion of strippant in organic extractant phase is passed through the shell side of the hollow fiber contactor, while the feed solution is passed through the lumen side. Aqueous-organic phase interface is maintained at the pore mouth on the fiber inner surface by keeping the lumen side pressure higher than that of the shell side. It does not require the use of a surfactant and thus product recovery process is very simple [53].

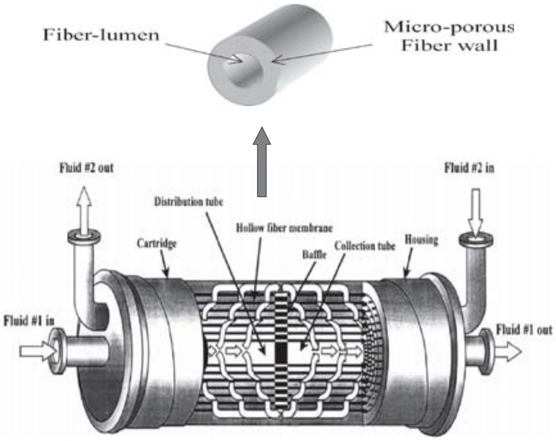

Figure 5.1: Hollow fiber contactor

Hu and Wiencek have observed that although DLM showed somewhat lower extraction rate than the configuration of strip phase emulsified in organic (because of better rate of regeneration of organic membrane due to faster stripping in the later in presence of surfactant), a good enough extraction can be accomplished in a hollow fiber contactor with DLM configuration [8]. Sonawane et al. have studied DLM configuration in hollow fiber contactor for Au (I) extraction and suggested the technique as a promising alternative to conventional processes [54]. DLM technique found to be a promising option for selective removal of Au(I) from synthetic hydrometallurgical solution; larger area for receiving due to strip dispersion aid in selective removal [55]. Alguacil et al. investigated the DLM configuration in hollow fiber module for separation of Cr (III) and suggested that technique does not allow saturation of the carrier as it is continuously regenerated in the strip dispersion [56]. Gonzalez et al. found the technology quite promising for the removal of Ni (II) from liquid effluents [57]. Further, selective separation of Cr (VI) from simulated industrial waste has been achieved effectively by this technique; optimum conditions suggested [58]. The technique is reported to be superior to other hollow fiber technologies for transport of Fe (III) from acidic media using ionic liquid as a carrier agent [59].

From the various attempts made to evaluate the DLM operation in HF contactor for different metal ions, it emerges that, this technology is an effective and economic alternative to conventional processes. In view of importance of recovery of uranium in terms of both environmental and economic point of views, this technology has huge potential for application to recovery of uranium from various streams produced in nuclear industry. Accordingly, Roy et al. have investigated removal of U^{+6} from concentrated oxalate streams (14 to 74 g/l) generated during reprocessing of spent fuel of nuclear reactor; 20 % TBP as carrier in NPH diluents and 0.01 M HNO3 as strippant has been suggested as optimal operating conditions [32]**.** In a country like India, huge quantities of waste raffinate streams are generated / ton of nuclear grade Uranium produced. Recovery of uranium from such lean raffinate streams (≈ 0.5g/l) is of immense importance in view of huge potential uranium resource. Here, efficiency of HFDLM technology for recovery of uranium from actual streams of uranium extraction plant has been studied. Also, there is need to establish the technique in a more eco-friendly and economic way with even less consumption of organic carrier and an aqueous raffinate almost free of uranium which can be recycled in the plant as process stream or disposed safely with minimum processing.

Here, DLM technique in hollow fiber is explored for uranium removal from dilute nitrate streams. Uranyl nitrate pure solution (UNPS) and Uranyl nitrate raffinate stream (UNRS) from Uranium Metal Plant were used as source stream. UNPS was used for preliminary studies with final goal of using the actual waste stream, the UNRS. The study with UNRS was carried out to observe the effect of presence of other metal ions on transport of uranium and formulation of an efficient HFDLM system for this stream. TBP is a very selective carrier agent, which only picks up uranyl ion from source stream. In uranium purification plant, uranyl nitrate impure solution is put through TBP extraction process in which only uranyl ion gets extracted in organic phase and the impurities are left behind, which remains in UNRS. Similarly, while recovering uranium from URNS using HFDLM, the TBP selectively complexes with uranyl ion and the other impurities are left behind in the raffinate stream. Sodium carbonate efficient strippant for recovery of uranium from nitrate medium, a dispersion of Na_2CO_3–TBP/ Dodecane has been used. Effect of various hydrodynamic and chemical parameters such as carrier concentration, presence of surfactant, initial feed uranium concentration, feed acidity and varying aqueous to organic ratio in dispersion has been studied. Preliminary data on liquid-liquid equilibria has been generated through batch experiments. These all may be the basis for scale up of commercial facility for treating such kind of waste.

Experimental

Materials and chemicals

The extractant solution was prepared by dissolving required amount of Tri-n-butyl phosphate in n-dodecane. UNPS (≈ 40 g/L of U^{+6}) is obtained from the product stream of Uranium Metal Plant, UED, BARC. From this solution, feed of various strengths and acidities were prepared by dissolving it in nitric acid solution of desired molarity. Uranium metal plant raffinate was also obtained from Uranium Extraction Division, BARC and used after filtration. Typical composition of the waste is given as following: Uranium(U): 0.68 g/L, Aluminium(Al): 0.6 g/L, Boron(B): 0.3 mg/L, Chromium(Cr): 50 mg/L, Iron(Fe): 0.5 gm/L, Magnesium(Mg): 50 mg/L, Manganese(Mn): 10 mg/L, Nickle(Ni): 30 mg/L, Nitric acid: 1 N. Sodium carbonate/ bicarbonate solution used as strippant was prepared by dissolving the required amount of it in distilled water. Isopropyl alcohol was used for cleaning of the membrane contactor. All chemicals used were of A.R. Grade.

Experiments were conducted in a liquid-2 extraction (LLE) system provided with Liqui-Cel® Extra-Flow 2.5x8” membrane contactor (Fig 5.1) of 1.4 m^2 contact area purchased from Membrana, Germany. It is a hollow fiber contactor having micro porous polypropylene lumens close packed in a tubular shell. Detailed characteristics of module are presented in Table 5.1. The system utilizes two stainless steel gear pumps (Make: Cole Parmer) capable of flows from 0.20 to 1.0 LPM. Chemically resistant polyolefin tubing and fittings are used throughout the system to withstand most organic hydrocarbons, acids, and bases. Two Teflon flow meters and two stainless steel pressure gauges of range 0 to 30 psig are panel-mounted to measure inlet/outlet flow and pressure respectively for both tube side and shell side streams. The dispersion was prepared by using a high speed emulsifier (REMI make: RQT-127 /D). The permeation of uranium through the liquid membrane was measured through analysis of uranium content in the aqueous solutions (non-active) using colorimetry with Chemito ultraviolet UV 2000 spectrophotometer and Jasco V-550 UV-VIS spectrophotometer.

Table 5.1: Characteristics of hollow-fiber contactor

Cartridge configuration	With Center Baffle
MOC Lumen	Polypropylene
Effective fiber length	0.15 m
ID of Lumen	240×10^{-6} m
Wall thickness of lumen	30×10^{-6} m
Average Pore size of lumen	0.05×10^{-6} m
Number of fibers	10,000
Porosity of lumen	40 %
Average cartridge i.d.	0.022 m
Average cartridge o.d.	0.050 m
Fiber packing fraction	0.45

Membrane surface area	1.4 m^2
Maximum shell side working temperature/ pressure	40 ^{0}C, 7.4 kg/cm^2
Maximum lumen side liquid temperature/ pressure	25 ^{0}C, 4.9 kg/cm^2
Priming Volume Shell side	0.40 L
Priming Volume Lumen side	0.15 L
Potting Material	Polyethylene
Housing Material	Polypropylene

Studies on UO_2^{2+}-TBP equilibrium

Extraction equilibrium of U^{+6} using TBP as carrier agent can be represented as [60],

$$UO_2^{2+}(aq) + 2\ NO_3^-(aq) + 2\ TBP(org) \xleftrightarrow{K_{eq1}} UO_2(NO_3)_2.2TBP(org) \quad (1)$$

Considering fast chemical reaction between the metal species and the membrane carrier, local equilibrium at interface is reached and concentrations at interface are related as per equation 2 [61],

$$K_{eq} = \frac{K_d}{\left[NO_3^-\right]^2 \left[TBP\right]^2} \quad (2)$$

where, K_d is the distribution coefficient of metal at feed-membrane interface. Liquid-liquid extraction (LLX) experiments have been conducted to generate the equilibrium data for U^{+6}–TBP system both with UNPS and UNRS.

a) *UNPS as source stream*: Feed is taken as 0.4 g/l (400 ppm) uranium as uranyl nitrate in 1 N nitric acid, membrane as tri-n-butyl phosphate in n-dodecane and strippant is 1 M Na_2CO_3. Extraction data is collected by stirring feed and organic phase for different agitation times keeping aqueous to organic ratio (A/O) 1:1. After that agitation is stopped, both phases are disengaged and uranium is analyzed in raffinate. For generation of stripping data, loaded organic is mixed with fresh strippant keeping A/O 1:1 for varying agitation times. Then, after phase disengagement uranium is analyzed in loaded strip. Distribution coefficient data for extraction is presented in Table 5.2. It has been observed that for LLX system, 3 min is the equilibration time. Distribution coefficient of stripping for 10% and 30% TBP (with 0.4 g/l U in 1 N nitrate and 1 M sodium carbonate as strippant) is 0.148 and 0.088, respectively; which shows that stripping is better with 30 % TBP.

b) *UNRS as source stream*: Feed is taken as uranium metal plant raffinate (composition is given above), membrane as tri-n-butyl phosphate in n-dodecane and strippant is 1 M $NaHCO_3$. Extraction data is collected by stirring feed and organic phase keeping aqueous to organic ratio (A/O) 1:1. After that agitation is stopped, both phases are disengaged and uranium is analyzed in raffinate. For generation of stripping data, loaded organic is mixed with fresh strippant keeping A/O 1:1. Then, after phase disengagement uranium is analyzed in loaded strip. Distribution coefficient data for extraction and stripping is presented in Table 5.3.

Table 5.2: Equilibrium data of extraction generated with UNPS

0.4 g/l U^{+6} in 1 N nitrate	*TBP (v/v) in dodecane*	K_d (C_{org}/C_{aq})
	5%	0.34
	10%	1.25
	30%	7.66
10 % v/v TBP in dodecane; feed acidity 1 N	*Feed uranium concentration (g/l)*	K_d
	0.4	1.25
	1.3	0.915
	4.0	0.624
	13.2	0.318

	Feed Acidity (N)	*Kd*
0.4 g/l U^{+6} with 10 % v/v TBP in dodecane	1	1.25
	2	2.10
	3	3.40

Table 5.3: Equilibrium data generated with UNRS

Carrier conc. Variation ***Feed***: Uranium Waste; ***Carrier***: TBP in Dodecane; ***Strippant***: 1 M $NaHCO_3$	*TBP (v/v)*	*K_d extraction (C_{org}/C_{aq})*	*K_d stripping (C_{org}/C_{aq})*
	5%	0.4	0.04
	10%	1.17	
	30%	4.99	
Strippant Variation ***Feed***: Uranium Waste; ***Carrier***: **10 %** TBP in Dodecane	*Strippant*	*K_d extraction (C_{org}/C_{aq})*	*K_d stripping (C_{org}/C_{aq})*
	1 M $NaHCO_3$	1.17	0.04
	0.01 N HNO_3		0.34
	Distill Water		0.29

Experiments with hollow-fiber contactor

Experiments have been conducted with strip-organic dispersion is re-circulated on the shell-side with the feed on the tube-side. Shell-side reservoir containing strippant and organic is agitated throughout the experiment to avoid phase disengagement; aqueous to organic ratio of dispersion was kept as 1:1 unless otherwise stated. Volume of feed and dispersion is kept as 500 ml unless otherwise stated. Tube-side pressure is kept a little higher ($\Delta P = 2$ psig) than the shell-side to maintain the aqueous-organic interface at inner wall of fiber and prevent organic entrainment in tube-side. Owing to pores in fiber wall are of the order of 0.05 micron and strippant droplets are of the order of 0.1 mm (Appendix 1), only organic phase of the dispersion can be present in fiber pores. Thus, organic phase will fill the hydrophobic pores and stripping droplets will stay in shell (Fig 5.2). Parametric studies have been conducted by varying carrier concentration, feed metal ion concentration, feed acidity and A/O ratio in dispersion to see the effect on metal transport. HFDLM has the following obvious advantages - *a)* preparation of emulsion, a separate unit operation, is not needed, which saves additional time and cost *b)* demulsification step, required to recover the solute, is also eliminated (owing to immediate separation of aqueous and organic as agitation is stopped) *c)* viscosity of the membrane is reduced due to the absence of surfactant *d)* in absence of surfactant, recycling of organic phase becomes easier *e)* reduced viscosity of shell side fluid may lead to faster stripping.

Amount of uranium transported from feed to strip is estimated by periodically sampling the feed solution and analyzing uranium using colorimetry (for uranyl nitrate pure solution, wavelength was kept as 375 nm using peroxide as a coloring agent; while for uranium raffinate, it was 578 nm with bromo-PADAP dye as a coloring agent). Percent transport of U^{+6} is calculated as 100* (1-C/Co)), where, *C* is the concentration of uranium in feed solution at time *t* and *Co* is the initial feed concentration. The dispersion was prepared by mixing the stripping solution with the organic membrane phase at 3000 rpm; sauter mean diameter of drops is around 0.1 mm. Aqueous to organic ratio of 1:1 and flow rate was maintained as 400 ml/min unless otherwise stated. Stripping agent was 1 M sodium carbonate/ bicarbonate.

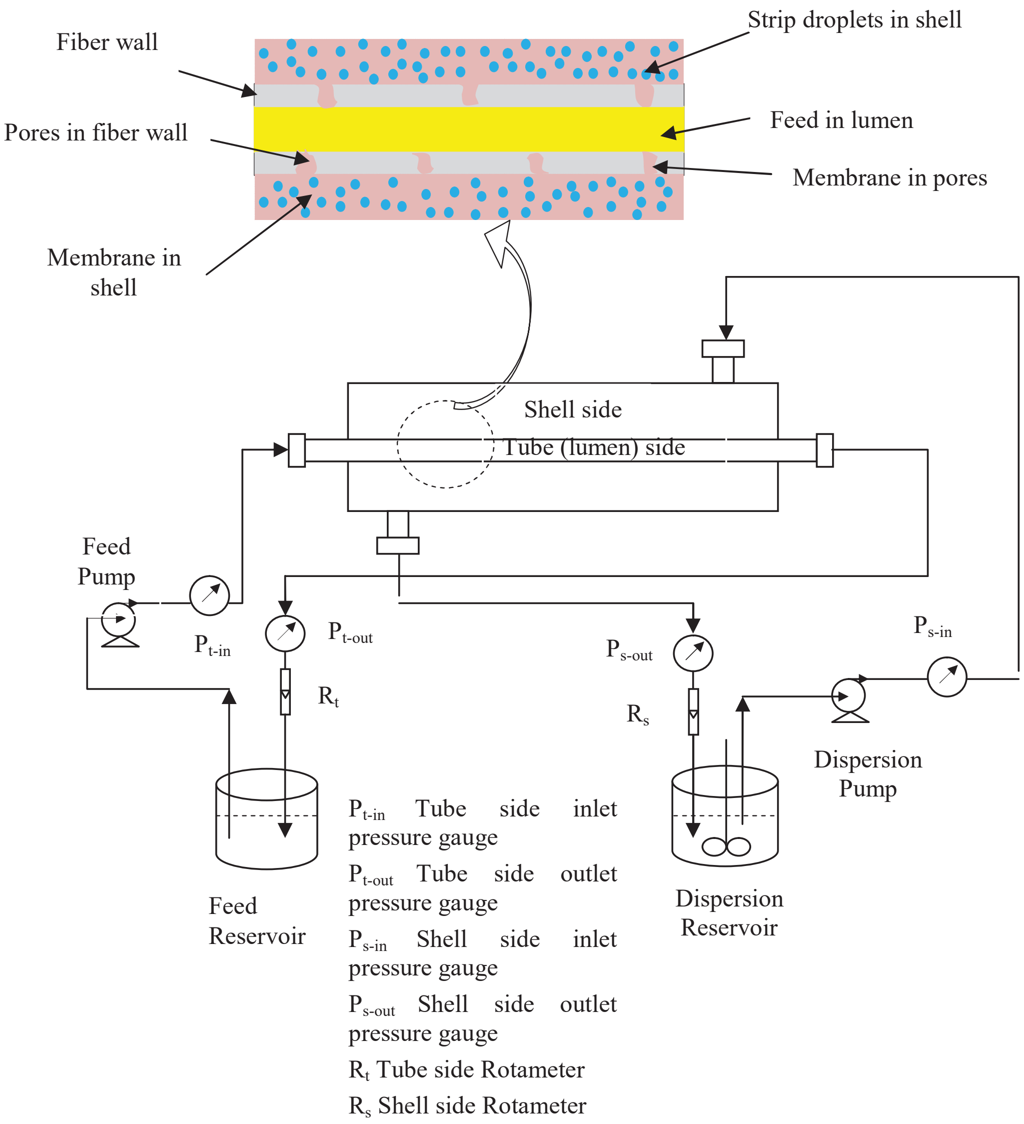

Figure 5.2: Schematic of DLM with flow diagram of experimental apparatus

Results and Discussion

Effect of variation in system parameters on transport rate of uranium has been presented as following.

Effect of varying carrier concentration

Experiments were conducted with different concentrations of TBP in dodecane. Fig 5.3 shows percentage transport of uranium as a function of time for varying carrier concentrations. It is seen that the rate of U^{+6} transport increases with increasing carrier concentration. Increase of the carrier concentration enhances the formation of U-TBP complex at the feed-membrane interface, resulting in increased rate of extraction of uranyl ion. Although 30 % TBP is showing fastest rate of transport, 10% TBP gives good enough extraction in DLM mode with the advantage of reducing the organic input in the system.

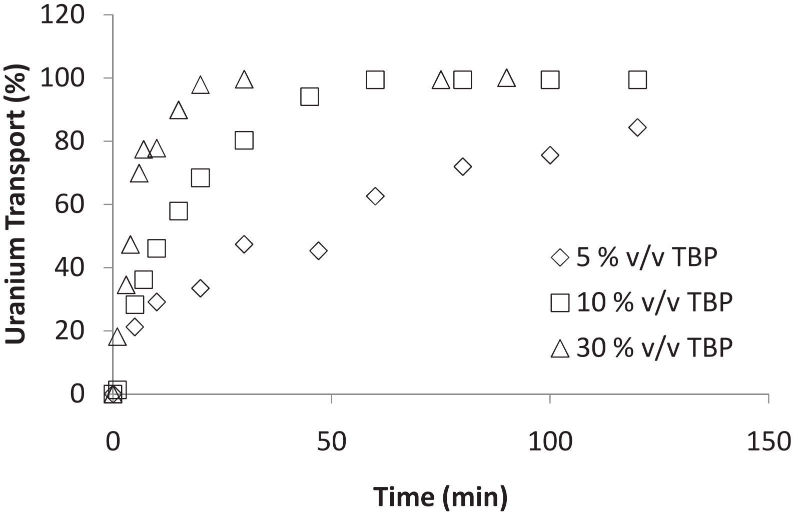

Figure 5.3: Effect of varying carrier concentration on extraction of uranium; feed: 0.4 g/L U^{+6} in 1 N nitric acid medium; dispersion: aq/org 1:1, aq (1 M Na_2CO_3), org (TBP in dodecane)

Effect of varying initial feed uranium concentration

Fig 5.4 shows time-variation of uranium transport for different initial feed uranium concentrations. It is observed that rate of transport decreases with increase in feed metal ion concentration. This observation points to the fact that equilibrium limitation dominates the transport process. High feed concentration in the feed membrane interface leads to saturation of the membrane phase w.r.t. the available carrier content. Whereas, the factors which govern the capacity to transfer the solute to the strip side like, the diffusion length, membrane strip interfacial area, concentration of strip etc remain limited. Hence beyond a certain concentration of feed, increase in feed concentration will lead to reduced rate of extraction, unless the carrier concentration in the membrane is increased. Similar behavior has been observed by several researchers previously [62-64].

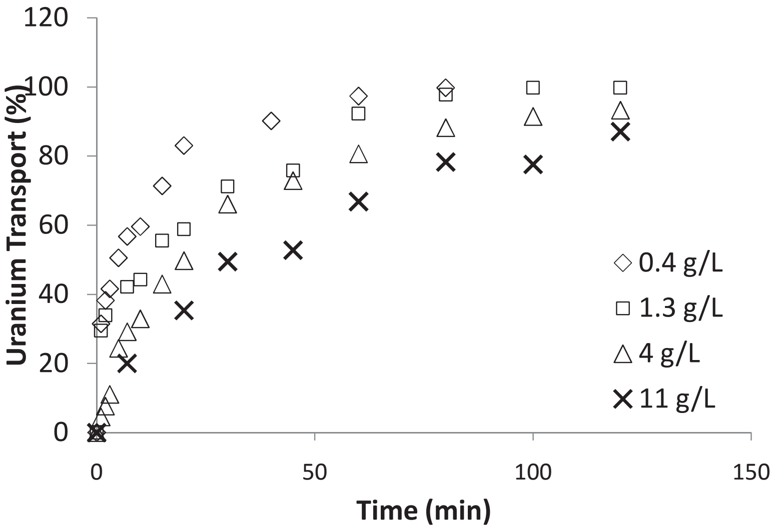

Figure 5.4: Effect of varying feed uranium concentration on percentage extraction; feed: U^{+6} in 1 N nitric acid medium; emulsion: aq/org 1:1, *aq* (1 M Na_2CO_3), *org* 10 % (v/v) TBP in dodecane with 3 % SPAN 80

Effect of varying feed acidity

Effect of variation of feed-acidity is shown in Fig 5.5. It is observed that rate of transport increases with increase in feed-side nitric acid concentration. The reason is as NO_3^- is co-transported ion along with uranium (Eq. 1); it provides driving force for uranyl ion transport. Although experiments are not conducted with acidity beyond 3 N owing to possible deterioration of polypropylene fibers, it seems that on further increasing the feed acidity $TBP.HNO_3$ type complexes may compete with $UO_2(NO_3)_2.2TBP$ leading to decrease in uranium transport [65].

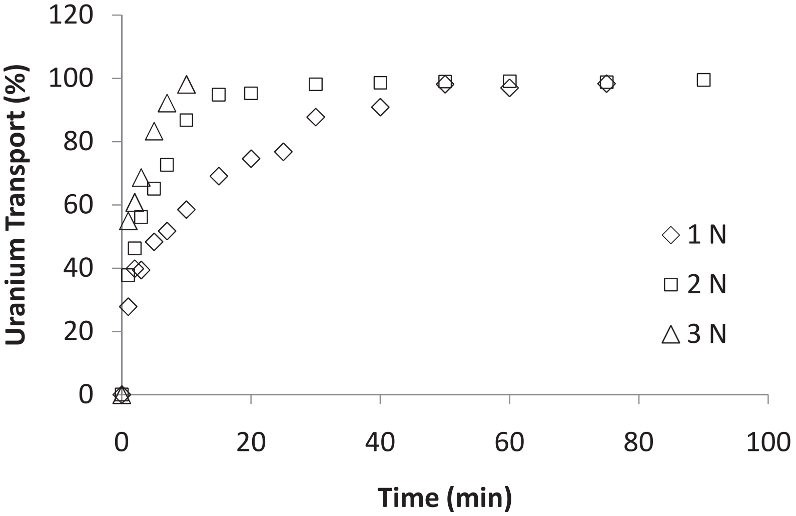

Figure 5.5: Effect of varying feed acidity on percentage extraction; feed: 0.4 g/L U^{+6} in nitric acid medium; HFDLM: aq/org 2:1, aq (1 M Na_2CO_3), org (10 % TBP in dodecane)

Effect of varying aqueous to organic ratio in shell-side

Aqueous to organic ratio is varied in dispersion and results are presented in Fig 5.6. It has been observed that increasing aqueous to organic ratio will increase the extraction of uranium from feed to strip. This is due to reduced diffusion length of membrane phase and more interfacial area of strippant available for unit volume of organic, which leads to faster removal of solute from the organic phase by rapid diffusion and stripping, which enhances extraction.

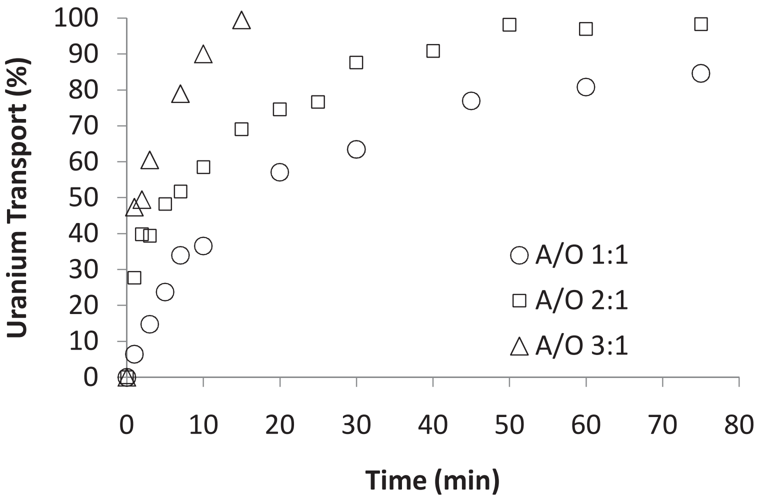

Figure 5.6: Effect of varying aq:org ratio (in emulsion) on percentage extraction; feed: 0.4 g/L U^{+6} in 1 N nitric acid medium; HFDLM: aq (1 M Na_2CO_3), org (10 % TBP in dodecane)

Effect of presence of surfactant

Effect of presence of surfactant has been seen by adding 3 % v/v sorbitan monooleate (SPAN 80) in dispersion of strippant and organic for both 10% and 30% TBP. It is observed (Fig 5.7) that the performance of system without surfactant is marginally poorer than system with surfactant using 10% v/v TBP in the membrane phase; while a comparable performance of both is obtained at higher carrier loading (30% v/v TBP). The reason for this may be attributed to high interfacial area of strippant per unit volume of organic in presence of surfactant, which leads to better recovery of solute in case of 10% TBP. While for 30% TBP, increased concentration of carrier enhances the extraction and counterbalances the effect of less internal membrane strip interfacial.

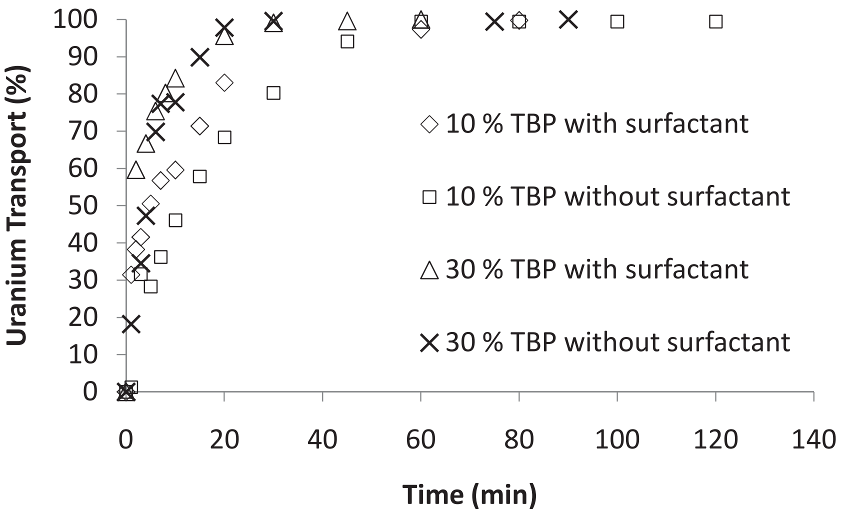

Figure 5.7: Effect of presence of surfactant; feed: 0.4 g/L U^{+6} in 1 N nitric acid medium; dispersion: aq/org 1:1, aq (1 M Na_2CO_3), org (TBP in dodecane); surfactant: 3 % v/v SPAN 80

Transport behavior of U^{+6} using Uranium Waste (UNRS)

After preliminary studies with UNPS solution, the performance of DLM for actual waste stream, UNRS has been tested. Accordingly, experiments are being conducted with solvent extraction raffinate of plant which contains uranium in nitrate form along with other metal ions majorly Al, Fe, Cr and Mg (composition of raffinate given above). TBP in various concentrations dissolved in dodecane was utilized as carrier agent. 1 M sodium bi carbonate solution was used as strippant. Flow rate was kept as 200 ml/min in both lumen and shell side. Volume of feed and dispersion was taken as 1000 ml. Fig 5.8 shows transport behavior of uranium both from feed to membrane and from membrane to strip. It was found that with increase in carrier concentration, extraction of uranium increases. The reason is concentration of TBP in the organic at any point of time at the pore interface is more for 30 % TBP than for 10 %. Stripping was also efficient for 30 % TBP. The partition coefficient of both extraction and stripping are given in Table 5.3; similar results are found for UNPS and given above.

Uranyl ion flux [{U^{+6} transported (g/L) x 238^{-1} (gmole/g) x Volume of feed (0.5 L)}/ {Extraction area (m^2) x time (hr)}] has been found as 1 $x10^{-3}$ moles/m^2-hr, while it was 3.4 $x10^{-3}$ moles /m^2-hr for pure solution. Reason might be lower distribution coefficient (K_d = 4.99) of uranium in case of waste as compared to pure solution.

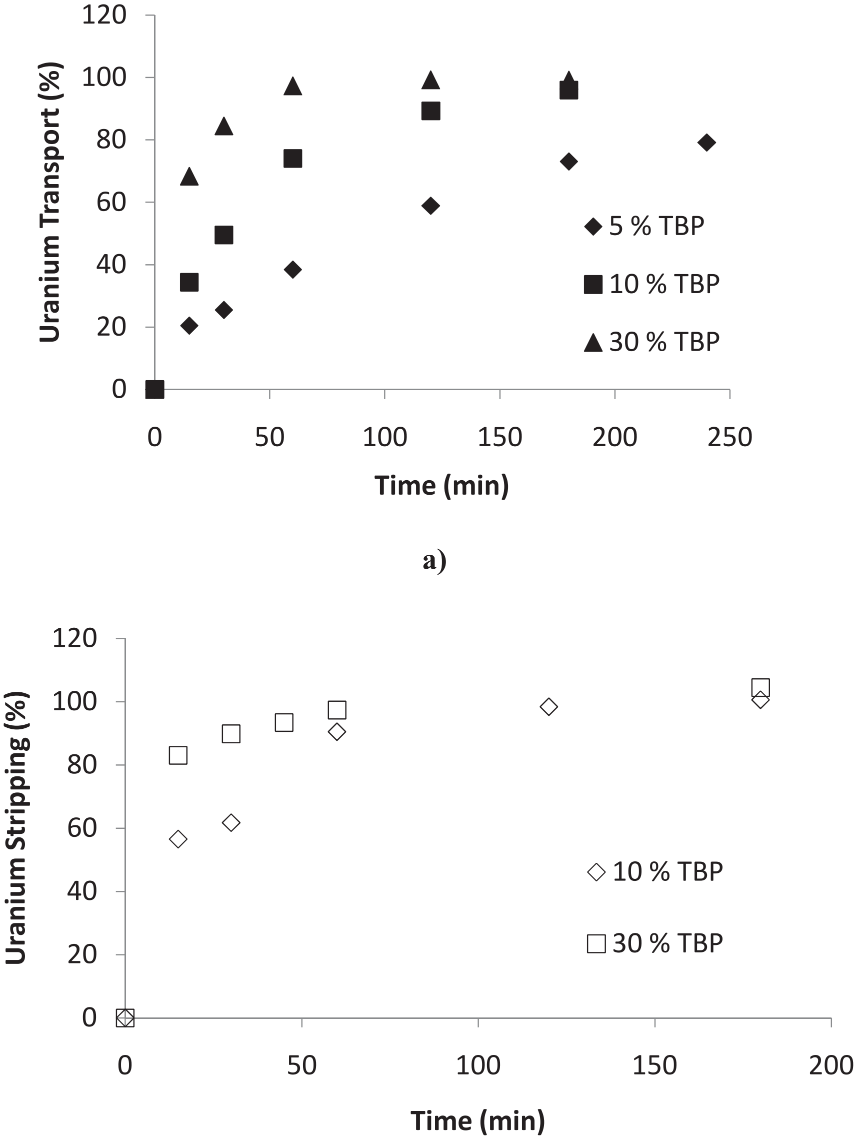

a)

b)

Figure 5.8: Transport behavior of uranium with time using UNRS; dispersion: aq/org 1:1, aq (1 M $NaHCO_3$), org (TBP in dodecane); flow rate: 200 ml/min

Choice of strippant: Among 0.01-N nitric acid, 1-M Na_2CO_3 and 1-M $NaHCO_3$, sodium bicarbonate was chosen as the strippant as it gives faster and more efficient stripping compared to nitric acid. TBP as a carrier for uranium, co extracts nitric acid. As the permeation process proceeds, there is gradual build up of nitric acid in the strip phase, which does not favour the de-complexation of the Uranium-TBP complex at the strip boundary. Use of a dilute alkali like Na_2CO_3 or $NaHCO_3$ promotes de-complexation by instant stripping, which in turn enhances extraction at the feed boundary by fast generation of free carrier. Both Na_2CO_3 and $NaHCO_3$ as strippant are performing virtually the same, while being a milder alkali compared to Na_2CO_3, possibility of losing uranium by precipitation during stripping is less for $NaHCO_3$ and so used. Percent extraction after 3 hrs is 96% and 80% for $NaHCO_3$ and HNO_3, respectively. Complete stripping was achieved with $NaHCO_3$, while it was 80 % for HNO_3. The reason being stripping by nitric acid is equilibrium based, while for sodium bicarbonate, it is reaction based and hence, is faster. Equilibrium data generated for different strippant were also showing the same trend (Table 5.3).

Model prediction

For computation of simulation, mass-transfer resistances of aqueous feed film and of organic membrane are estimated using Eq 3 by evaluating the aqueous feed film thickness, d_{aq} and diffusivity of metal complex, d_{org} through Eq 4 and 5, respectively [5, 29].

$$\Delta_{aq} = \frac{R\,\varepsilon\, d_{aq}}{\left(R - d_{aq}\right) D_{aq}} \;\&\; \Delta_{org} = \frac{d_{org}\,\tau}{D_{org}} \tag{3}$$

$$Sh = \frac{R}{d_{aq}} = 1.62\left(\frac{4R^2 v}{LD_{aq}}\right)^{1/3} \tag{4}$$

$$D_{org} = \frac{k_b T}{6\pi\eta R_c}\left[1 + \frac{9R_c}{4d_P}\ln\left(\frac{2R_c}{d_P}\right) - 1.54\left(\frac{2R_c}{d_P}\right)\right] \quad \text{for} \left(\frac{2\,R_c}{d_p}\right) < 0.2 \tag{5}$$

where, v, η, R_c and d_p denote feed flow velocity, viscosity of membrane, molecular radius of solute complex and pore-diameter of micro-porous fiber. Viscosity of the membrane η is calculated by $1/\eta = (w_1/\eta_1) + (w_2/\eta_2)$ [66] using viscosity of TBP (η_1) as 3.38 cp [67] and of dodecane (η_2) as 1.34 cp [68-69] at 25 ˚C. Parameters used in simulation are presented in Table 5.4; and generated equilibrium data used for simulation is given in Table 5.2 and 5.3, respectively for UNPS and UNRS. Percent deviation [70] between model prediction and data is calculated as,

$$\text{Deviation}(\%) = \frac{100}{p}\sum_{m=1}^{p}\left(\frac{\left|y_{\text{Expt},m} - y_{\text{Pred},m}\right|}{y_{\text{Expt},m}}\right) \tag{6}$$

Where, *p* stands for number of data points and *y* represents data values.

Table 5.4: Parameters used for simulation

Parameter	***Value***	
k_b (J/K)	1.38×10^{-23}	
T (K)	298	
D_{aq} (cm^2/s)	6×10^{-6} [60]	
R_c (cm)	12.86×10^{-8} [25]	
Viscosity of membrane liquid, η (cP); metal complex diffusivity, D_{org} (cm^2/s); membrane resistance, Δ_{org} (s/cm)	5 % v/v TBP	1.39; 0.87×10^{-6}; 11497
	10 % v/v TBP	1.45; 0.84×10^{-6}; 11964
	30 % v/v TBP	1.71; 0.71×10^{-6}; 14073

Feed flow velocity, v (cm/s); aqueous film thickness, d_{aq} (cm); aqueous film resistance, Δ_{aq} (s/cm)	200 ml/min	0.74; 4.41×10^{-3}; 349
	400 ml/min	1.47; 3.51×10^{-3}; 330
	800 ml/min	2.95; 2.78×10^{-3}; 241

Simulation has been generated for transport of uranium at different feed flow rates for both 10 % and 30 % TBP as carrier; Δ_{aq} at a particular flow rate is used accordingly from Table 5.4. Simulation shows that on increasing in flow rate, metal transport increases accordingly; which is according to expected trend because as flow rate increases, Δ_{aq} decreases leads to increase in transport. In the operating range of the hollow fiber module in use, increase in flow rate leads to minor increase in the uranium transport as the controlling resistance is in the membrane side.

The present work shows potential of application of dispersed liquid membrane system in HF contactor to recovery of uranium from actual raffinate streams of Uranium Metal Plant. DLM in hollow fiber contactor, with the sodium carbonate/ bicarbonate as strip phase dispersed in 10% TBP in dodecane as the organic extractant provides complete recovery of uranium from dilute feed solution. The process shows good stability during operation with low consumption of organic. While the process is efficient due to high surface area for extraction as well as stripping, the energy consumption is low due to mild agitation for dispersion and ease of phase disengagement after pertraction.

The developed model is able to predict the transport of uranium in HFDLM system under various operating conditions. The film resistance values have been estimated independently using physical properties of system, contactor characteristics and hydrodynamic conditions. The model is unique in simplicity and versatility. It will be useful for generation of data for scale up and design of the system.

Thus, dispersion liquid membrane in Hollow-fiber module (HFDLM) seems to be a promising configuration in terms of stability, simplicity and cost of operation for treatment of such kind of lean wastes. Sustained studies are required on material and geometry of lumens and structural configuration of Hollow Fiber contactor in order to establish its applicability for wider range of aqueous and organic streams.

Appendix

For Dispersed Phase (Sodium Carbonate (Strippant)):

$\rho = 1000$ Kg/m^3

$\sigma = 72.8 \times 10^{-3}$ N/m

For Continuous Phase (30% TBP in DD (Organic)):

$\rho = 817.50$ Kg/m^3

(where, $\rho_{TBP} = 975$ Kg/m^3, $\rho_{DD} = 750$ Kg/m^3 at 25°C)

Impeller Dia = 35 mm

n = 3000 rpm = 3000/60 rev/s = 50 rev/s

For Dispersion (Aq: org 1:1):

$\rho = 0.5\,(1000) + 0.5\,(817.5) = 908.75$ Kg/m^3

To find the Drop Size,

$We = \rho_c n^2 D_a^3 / \sigma = (817.5) \times (50)^2 \times (0.035)^3 / (72.8 \times 10^{-3}) = 1203.65$

Volume fraction of dispersed phase in the system, $\psi = 0.5$

Now $\overline{D_S} / D_a = 0.058(1+5.4\psi)\, We^{-0.6}$ [69] $= 0.058\,(1+5.4(0.5)) / (1203.65\text{^}0.6) = 3.043 \times 10^{-3}$

Hence, Sauter mean Diameter $\overline{D_S}$ is, $3.043 \times 10^{-3} \times 35$ mm = 0.1065 mm

Therefore, strippant droplets created are of the order of 0.1 mm.

CHAPTER 6

DISPERSION LIQUID MEMBRANE IN HOLLOW FIBER CONTACTOR: SCALE UP ASPECTS

Introduction

Effective removal and recovery of U^{+6} from raffinate stream of uranium solvent extraction plant is one of the major challenges in nuclear industry. For a typical plant output of 2000 T of U/day, huge quantities of lean raffinate streams are generated. Acidic raffinate generated contains uranium along with other base metals. It is very much desirable to recover all the uranium from such lean solutions both in view of resource utilization and stringent environmental regulations [71-72]. HFDLM (Hollow Fiber Dispersed Liquid Membrane) (Figure 6.1), through use of advanced process and equipment, has proved its potential to produce aqueous raffinate almost free of uranium [33] which can be recycled in the plant as process stream or disposed safely with minimum processing. The hollow fiber contactor, as equipment, has distinct advantages such as very high specific surface area, which leads to compact systems with lower plant profiles, small foot prints and lighter weights. Due to non-dispersive contact, phase flow rates can be controlled without flooding limitations. Due to modular design, it is easy to scale up.

Tri-n-butyl phosphate, known commonly as TBP, is an established carrier agent for entire nuclear fuel cycle and has been so chosen. In uranium purification plant, uranyl nitrate impure solution is put through TBP extraction process in which only uranyl ion gets extracted in organic phase and the impurities are left behind, which remains in acidic raffinate.

Similarly, while recovering uranium from acidic raffinate using HFDLM, the TBP selectively complexes with uranyl ion and the other impurities are left behind. Sodium bi carbonate being an efficient strippant for recovery of uranium from nitrate medium, a dispersion of $NaHCO_3$–TBP/ Dodecane has been used.

Although, few studies on scale up of membrane extractors are reported, where copper recovery from spent ammoniacal etchant [24], degassing [25], hexanol separation from water [26] and recovery of radio-strontium from acidic feeds [27] has been discussed, recovery of uranium from the above raffinate on larger scale is studied for the first time. The objective of this work is to show application of HFDLM technique for recovery of uranium from given raffinate on larger scale.

A developed mathematical model [33, 73, and 74] has been extended to attend the scale-up of hollow fiber contactors both in number and size. The major parameters of the model include a geometric parameter, a hydrodynamic parameter, three mass transfer coefficients, k_{aqf} , k_{org}, k_{aqs} for feed, organic and strip films and equilibrium parameters K_{df} and K_{ds} at feed and strip interface. The simulation utilizes the parameters of the model including K_{eq} to predict the transport of uranium from feed to strip both with lumen length and with time under various operating conditions. Along with extraction it is also able to predict the stripping performance. Model can be used to understand the performance of contactors of various sizes in a common and unified way. These all may be the basis for scale up of commercial facility for treating such kind of raffinate.

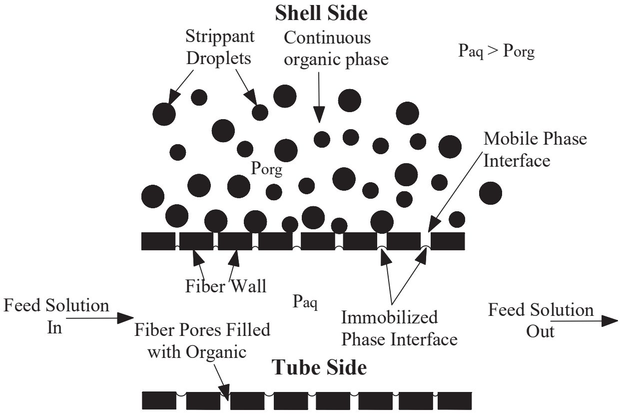

Figure 6.1: An enlarged view of the HFDLM

Experimental

Materials

The extractant solution was prepared by dissolving required amount of Tri-n-butyl phosphate in n-dodecane, which is kindly obtained from Heavy Water Board, Mumbai. Uranium metal plant (UMP) raffinate was obtained from Uranium Extraction Division, BARC and used after filtration. Typical composition of the raffinate is given as following: Uranium(U): 0.68 g/L, Aluminium(Al): 0.4 g/L, Boron(B): 0.04 g/L, Chromium(Cr): 7.2 mg/L, Iron(Fe): 0.5 gm/L, Magnesium(Mg): 0.14 g/L, Manganese(Mn): 10 mg/L, Nickel(Ni): 5 mg/L, Nitric acid: 1-2 M. Sodium bicarbonate solution used as strippant was prepared by dissolving the required amount of it in distilled water. Isopropyl alcohol was used for cleaning of the membrane contactor. All chemicals used were of A.R. Grade.

Methods

Solvent extraction studies

The extraction of U^{+6} using TBP as the extractant from nitric acid medium can be represented by the following equilibrium reaction [75],

$$UO_2^{2+}(aq) + 2\,NO_3^-(aq) + 2\,TBP(org) \xleftrightarrow{K_{eq}} UO_2(NO_3)_2.2TBP(org) \tag{1}$$

Concentrations at interface are related as per Eq. 2, considering fast chemical reaction,

$$K_{eq} = \frac{\left[UO_2(NO_3)_2.2TBP\right]_{org}}{\left[UO_2^{2+}\right]_{aq}\left[NO_3^-\right]_{aq}^2\left[TBP\right]_{org}^2} = \frac{K_{df}}{\left[NO_3^-\right]^2\left[TBP\right]^2} \tag{2}$$

K_{eq} stands for equilibrium constant and K_{df} is the distribution coefficient of uranium at feed-membrane interface, which is equal to $[UO_2(NO_3)_2.2TBP]_{org}/\ [UO_2^{+2}]_{aq}$. The equilibrium distribution data of U for various TBP concentrations and for different strippants have been generated through independent experiments, presented elsewhere [33]. In a set of batch experiments, the K_d values are obtained at constant $[NO_3^-]$ and variable $[TBP]$. The K_{eq} for U^{+6} with TBP in dodecane is calculated from K_{df} values. A log-log plot is drawn of distribution coefficient and carrier concentration (refer Fig 6.2). By the intercept value of linear regression (R^2 = 0.997) from that plot and using the Eq 2, the value of equilibrium constant, K_{eq} has been calculated as 4.75 M^{-4}. The value of K_{eq} is used as an input in model.

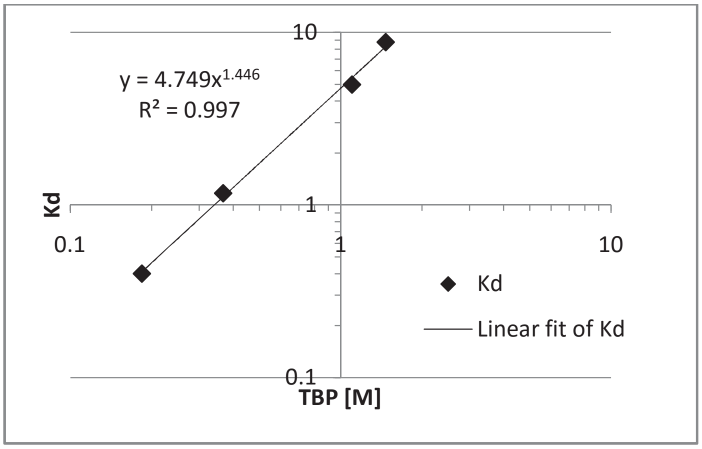

Figure 6.2: Variation of K_{df} with the carrier concentration, TBP in M, feed: U Raffinate in 1 N nitrate medium

Supported liquid membrane with strip dispersion (HFDLM)

A typical HFDLM system mainly comprises a hollow-fiber module, a feed solution reservoir, a feed pump, a dispersion reservoir, a dispersion pump and an agitator for the dispersion reservoir (for dispersing strip phase into organic) (Figure 6.3). An aqueous strippant is dispersed in an organic membrane separately in a reservoir using a high speed agitator (REMI make: RQT-127 /D) at 3000 rpm. As membranes are not wetted by dispersed phase, the organic continuum is ensured by keeping impeller in organic phase.

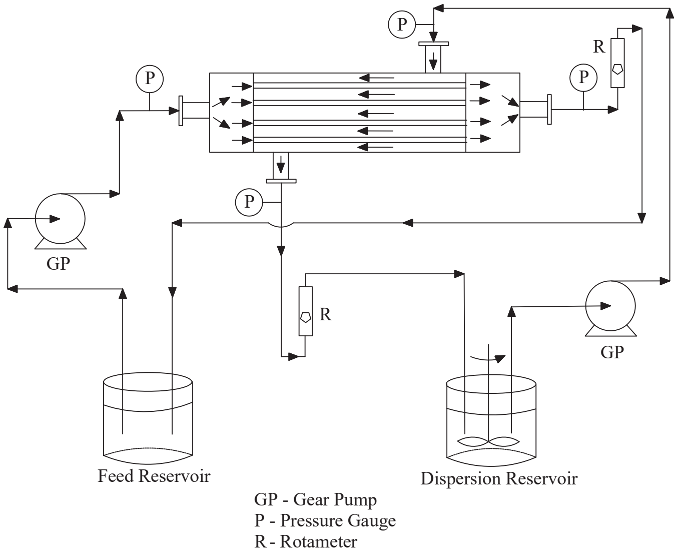

Figure 6.3: Schematic of HFDLM with flow diagram of experimental apparatus

The hollow-fiber modules (LiquiCel® 2.5x8” and 4x13” X50) used in the present investigations were purchased from Membrana, Germany. Dimensional details for the contactors tested are given in Table 6.1. For all the experiments, the feed solution was passed through the lumen side, while the dispersion was passed through the shell side of the module in re-circulating mode, unless otherwise stated. The volume of both feed and dispersion were taken as 1000 ml (for 2.5x8” contactor) and 2000 ml (for 4x13” contactor). The flow rates of both the shell and tube side were maintained constant at 200 ml/min (for 2.5x8” contactor) and 1000 ml/min (for 4x13” contactor). A schematic diagram of hollow fiber contactor is shown in Figure 6.4. Details of experiments are presented elsewhere [33]. At the end of the experiment, the agitator for the strip dispersion is turned off and the dispersion disengages into two phases, the lean organic solution and the loaded strip solution. Phase separation is instantaneous. The loaded strip solution can be precipitated and dried to get nuclear pure uranium.

Table 6.1: Dimensional details for the contactors tested

Contactor size designator	2.5x8	4x13
Effective surface area (m^2)	1.4	8.1
Number of fibers	10,000	30,000
Effective fiber length (m)	0.15	0.25
Average cartridge i.d. (m)	0.022	0.032
Average cartridge o.d. (m)	0.050	0.085
Priming Volume Shell side (l)	0.40	1.26
Priming Volume lumen side (l)	0.15	0.61
Fiber material	polypropylene	
Fiber internal diameter (μm)	220	
Fiber outer diameter (μm)	300	
Fiber wall thickness (μm)	40	
Effective pore size (μm)	0.05	
Porosity (%)	40	
tortousity	2	

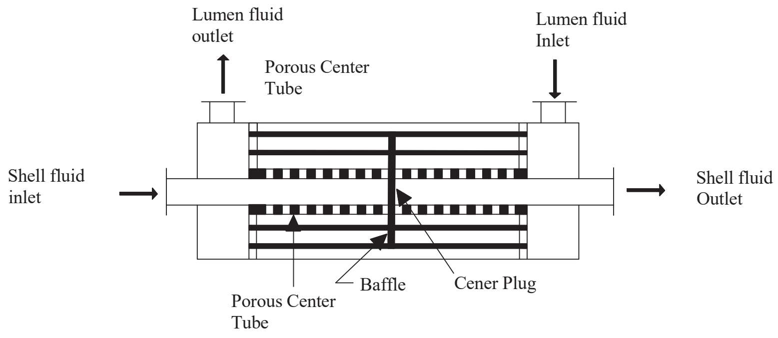

Figure 6.4: Schematic of hollow fiber membrane contactor

The permeation of uranium through the liquid membrane was measured through analysis of uranium content in the aqueous solutions (non-active) using colorimetry with Jasco V-550 UV-VIS spectrophotometer. Amount of uranium transported from feed to strip is estimated by periodically sampling the feed as well as the strip solution and analyzing uranium using colorimetry (wavelength was kept as 578 nm with bromo-PADAP dye as a coloring agent) [24]. All the data are generated at least in duplicate and the accepted data are within ±5%.

Viscosity measurements

Viscosity data for 100% TBP, pure dodecane and their combinations in 5%, 10%, 20%, 30% and 40% TBP in dodecane are measured with BROOKFIELD LVDV-II + pro cone and plate type viscometer and presented in Table 6.2. From regression ($R^2 = 0.99$) of generated data, viscosity of liquid membrane can be estimated from $\eta = 1.318 \exp\{9.074E\text{-}03\ (\%TBP\ v/v)\}$ at a given volume percent of carrier agent. Data are essential for estimating the diffusivity of metal complex in organic membrane.

Table 6.2: Effect on viscosity of liquid membrane with variation in TBP concentration measured at 25 ˚C; diluent is dodecane

		Viscosity, cP
Pure component	TBP	3.35
	Dodecane	1.38
TBP % v/v (M)	5 (0.18)	1.38
	10 (0.37)	1.45
	30 (1.10)	1.65
	40 (1.47)	1.84

Results and discussion

Evaluation of mass transfer coefficients

The mass transfer resistance is related to the reciprocal of individual mass transfer coefficient by the following equation,

$$\zeta = \frac{K_{df}}{k_{aqf} A_1} + \frac{1}{k_{org} A_{A,lm}} + \frac{K_{ds}}{k_{aqs} A_2} \tag{3}$$

Assuming that the stripping reaction is instantaneous at the membrane strip interface (Data of K_{ds} is of the order of 10^{-2}), the contribution of the shell side aqueous phase resistance is neglected. Therefore, Eq 3 can be reduced as following,

$$\zeta = \frac{K_{df}}{k_{aqf} A_1} + \frac{1}{k_{org} A_{A,lm}} \tag{4}$$

The effect of carrier concentration on the transport of uranium from acidic raffinate was investigated and the results are presented [33]. The permeation of U^{+6} increased with the carrier concentration due to increased distribution coefficient value. The data of C/C_o vs. t at different carrier concentrations are fitted to Eq 16 to estimate the ζ values. K_{df} is taken from batch experiments. Then, a plot of ζ vs. K_{df} is drawn. By the slope and intercept value of linear regression ($R^2 = 0.999$) from that plot and using the Eq 20, the values of k_{aqf} and k_{org} were calculated as 1.43×10^{-3} and 5.57×10^{-5} cm/s, respectively. The value of k_{aqf} was found to be higher than k_{org} by order of 2, indicating that the membrane mass transfer is the rate controlling step. The D_{org} ($= k_{org}\, d_{org}\, \tau$) for the present system was calculated to be 5.57×10^{-7} cm^2/s, where d_{org} is fiber wall thickness and τ is tortuosity of solid support.

For diffusion process with fast chemical reaction under laminar flow, the mass transfer coefficient inside the fibers is commonly described by the Leveque equation Eq 5 [5, 76].

$$\mathrm{Sh} = 1.62\left(\frac{4R_i^{\,2}v}{LD_{aq}}\right)^{1/3} \tag{5}$$

where, *Sh* is the Sherwood number ($kd_i/D_{aq;}$ k mass transfer coefficient, d_i fiber inner diameter), R_i *is* the internal radius of fiber, v is the linear flow velocity of the feed solution through fiber, *L* is the effective length of fiber and D_{aq} is the aqueous diffusion coefficient. Using the Leveque relation and k_{aqf}, the value of D_{aq} was estimated as 1.61×10^{-5} cm^2/s. Similar value of D_{aq} as 1.4×10^{-5} cm^2/s is reported [28, 77].

Membrane phase diffusivity of metal-carrier complex is calculated theoretically by Stokes-Einstein equation for porous media Eq 6 [29],

$$D_{org} = \frac{k_b T}{6\pi\eta R_c}\left[1 + \frac{9R_c}{4d_p}\ln\left(\frac{2R_c}{d_p}\right) - 1.54\left(\frac{2R_c}{d_p}\right)\right] \qquad \text{for}\left(\frac{2\,R_c}{d_p}\right) < 0.2 \tag{6}$$

where, k_b is the Boltzmann constant, 1.38×10^{-23} J/K, Temperature is 298 K, d_p is pore-diameter of fiber, 0.05 μm, R_c denotes molecular radius of U-TBP complex, 13×10^{-8} cm [78] and η is viscosity of membrane phase (refer Table 6.2). The value of D_{org} calculated by the above equation is 7.34×10^{-7} cm^2/s. The calculated value is in agreement with that obtained experimentally. Similar values are reported elsewhere [79, 46].

Transport of Uranium from acidic raffinate of uranium processing plant

Effect of variation in system parameters on transport rate of U^{+6} using plant raffinate is reported below with HFC 2.5 x 8” of specific area 900 m^2/m^3.

Carrier concentration: The composition of organic membrane has a significant effect on facilitated transport of metal ion. The flux is expected to increase with increase in carrier concentration, because it enhances the formation of U-TBP complex at the feed-membrane interface, resulting in increased rate of extraction of uranyl ion. However, with increasing carrier concentration, viscosity of membrane phase also increases. These two competing factors lead to an optimum in transport flux of U as a function of carrier concentration at 30% v/v TBP. Figure 6.5 summarizes the data for uranium flux vs. TBP concentration in membrane. The flux value is obtained by moles transported/area/time. Mass transfer area is taken as $10^4 * 2\pi R_{Alm} L\varepsilon = 0.4862\ m^2$.

Strippant: Figure 6.6 shows the 1 M sodium bicarbonate as the most efficient strippant as it gives more than 96 % permeation of U (VI). Lower concentrations than 1 M of $NaHCO_3$ have underperformed as shown. As the acid concentration in the strip solution increased with time, it suppresses the dissociation of metal-carrier complex at the membrane strip interface, thereby reducing the transport rate of U (VI). Use of a dilute alkali like $NaHCO_3$ promotes de-complexation by instant stripping, which in turn enhances extraction at the feed boundary by fast generation of free carrier. Distill water is performing better than 0.01 N nitric acid, delivering uranium transport as 81% and 79%, respectively. It is in accordance with the expected trend through $K_{d\ stripping}$, which is 0.04, 0.29 and 0.34, respectively for 1 M $NaHCO_3$, Distill water and 0.01 N HNO_3. Sample of strip phase has been collected from dispersion reservoir at regular time intervals and analyzed for uranium. Complete stripping was achieved with 1 M $NaHCO_3$, while it was 79% and 61% for distill water and nitric acid, respectively (refer Figure 6.6 b).

A/O ratio in dispersion: Prediction has been made for varying A/O ratio in dispersion as 2.33, 1.5, 1, 0.66 and 0.43 and percent extraction is found as 99.14, 98.46, 97.56, 96.48 and 95.24, respectively. It shows increase in rate of transport with increasing A/O. The reason is the diffusional path length of metal-carrier complex to achieve a strip droplet decreases with increase in A/O. Having simulation in hand, trials are taken only with A/O 1 and 2.33 with the aim of reduction in organic requirement. Organic is required as a continuous phase for constant replenishment of washed organic of membrane pores to increase the membrane lifetime, so A/O of dispersion can't be increased beyond 2.33 without using surfactants. Dispersion A/O as 2.33 leads to 97 % U transport in 1 hr. In Figure 6.7, it can be seen that transport of uranium virtually remains same as aqueous to organic ratio in dispersion is increased from 1 to 2.33. With A/O 2.33, reduction in organic requirement has been achieved for same uranium removal; however strip concentration factor is more for A/O 1.

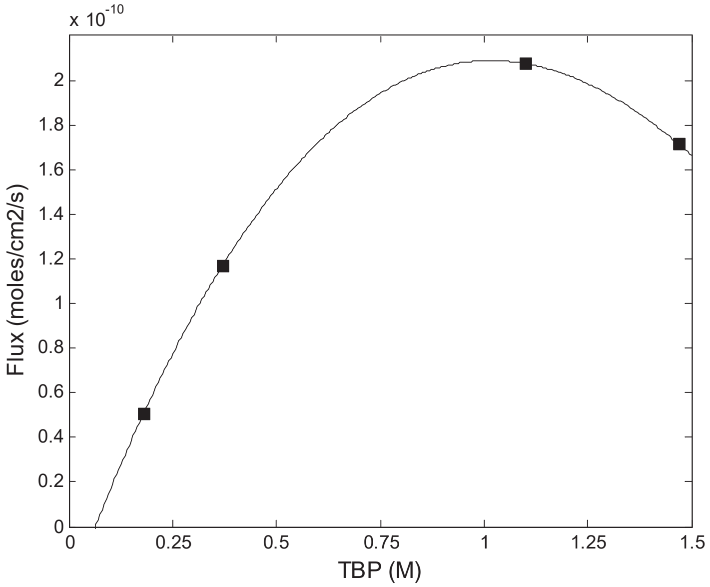

Figure 6.5: Effect of carrier concentration on flux of uranium transport; ■ – data; feed: U Raffinate; *dispersion*: strip/org 1:1, strip (1 M NaHCO$_3$), org (TBP in dodecane); *flow rate*: 200 ml/min

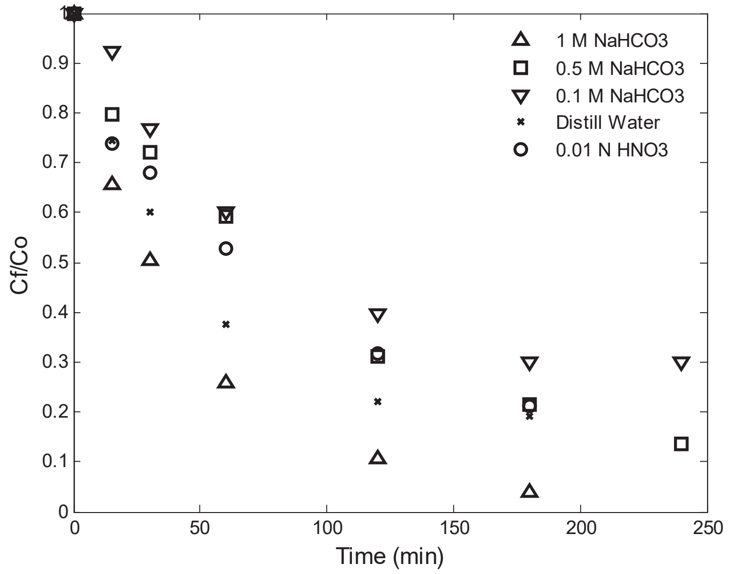

(a)

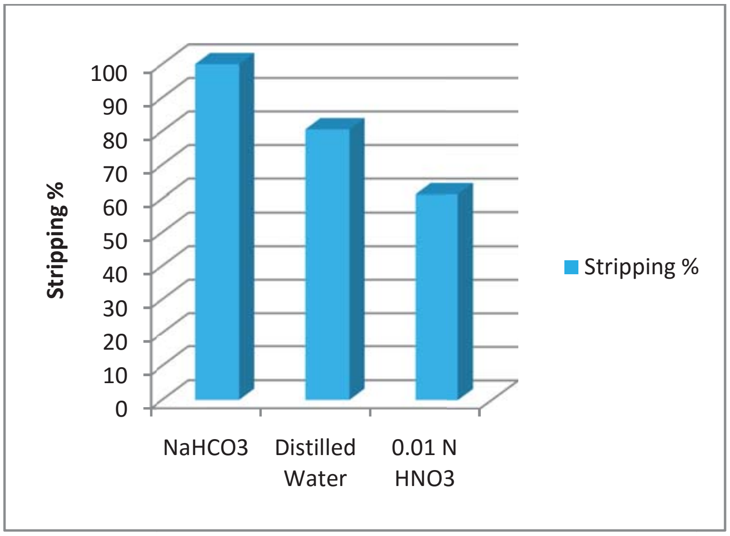

(b)

Figure 6.6: Effect of variation in strippant on transport rate, (a) Extraction, (b) Stripping; *feed*: U Raffinate; *dispersion*: strip (varying), org (10% TBP v/v in dodecane), A/O 1; *flow rate*: 200 ml/min

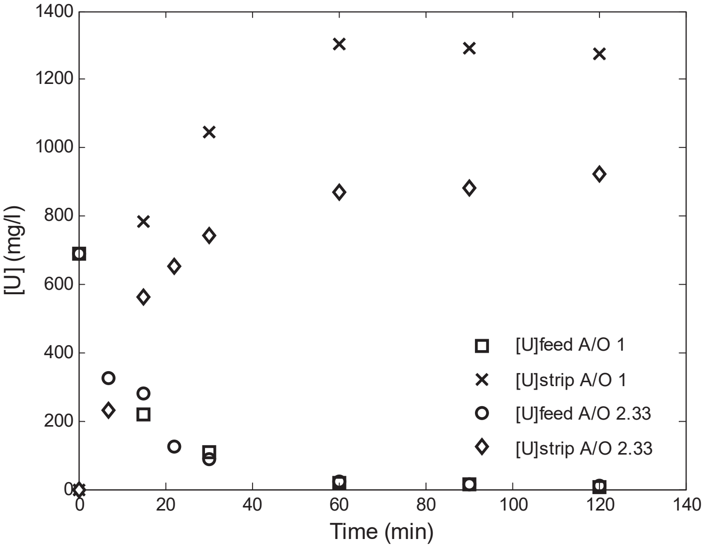

Figure 6.7: Effect of variation in organic fraction of dispersion on transport rate; *feed*: Uranium raffinate; *dispersion*: strip (1 M $NaHCO_3$), org (30% TBP v/v in dodecane), A/O (varying); *flow rate*: 200 ml/min

Transport of uranium along contactor length at different TBP concentrations

Figure 6.8 shows the lumen and shell concentrations of uranium along contactor length during single-passage of feed and strip solutions through hollow fiber contactor 2.5x8” at different TBP concentrations. It is assumed that at any z, concentrations are invariant with radial distance. Samples are collected at the end of the hollow fiber after single pass and analyzed for uranium. Data are shown by symbols in the Figure below. For simulation at a given carrier concentration, model equations have been used to get the variation of C_f and C_s with lumen length, z along the hollow fiber contactor and shown by smooth line. Initial condition is taken as (C_{fo} = 2.6e-03 M, C_{so} = 0) at z = 0. Model ties in well with the data. Further, both the feed and strip solutions are re-circulated two more times from lumen and shell with 30 % TBP and data are reported at z =30 and 45 cm (Effective fiber length in a module is 15 cm).

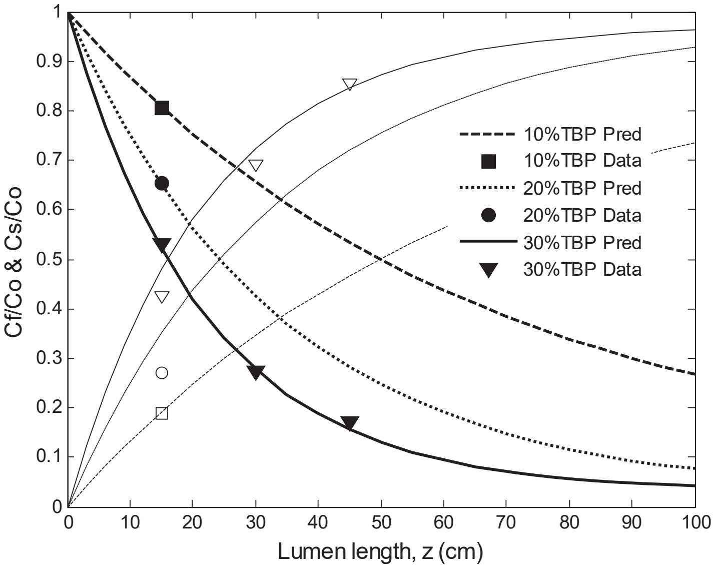

Figure 6.8: Transport of Uranium with lumen length at different carrier concentrations, *feed*: uranium raffinate; *dispersion*: aq/org 1:1, aq (1 M $NaHCO_3$), org (TBP in dodecane); *flow rate*: 200 ml/min

Number multiplication of Hollow fiber contactor 2.5x8"

Figure 6.9 (a) shows three 2.5x8" contactors combined in series, where feed and strip solutions are passed along the length in single-pass mode. Here, lean feed in contactor 3, encounters the fresh strippant; while fresh feed of contactor 1, found loaded strip. Individual contactor gave almost the same extraction as 57 % using 30% TBP, while stripping was 51, 79 and 90 % for HFC I, II and III. Figure 6.9 (b) shows the flux vs. log mean concentration difference, ΔC_{lm}. ΔC_{lm} is evaluated for each contactor by Eq 7, given below. The slope of the linear regression gives the overall mass transfer coefficient value for the process as 1.55e-02 cm/s. Overall extraction of uranium after passing the solutions through three contactors in series is achieved as 92 %, which is already predicted by the model in Figure 6.9 (refer the smooth line of C_f/C_o at z = 45 cm). Individual contactor efficiency is also calculated through actual transport per module divided by transport if equilibrium is achieved between two phases in contact. It is seen that efficiency remains virtually the same for each contactor as 60%.

$$\Delta C_{lm}=\frac{\left(C_{f_{in}}-C_{s_{out}}\right)-\left(C_{f_{out}}-C_{s_{\text{in}}}\right)}{\ln\left(\dfrac{C_{f_{in}}-C_{s_{out}}}{C_{f_{out}}-C_{s_{\text{in}}}}\right)} \tag{7}$$

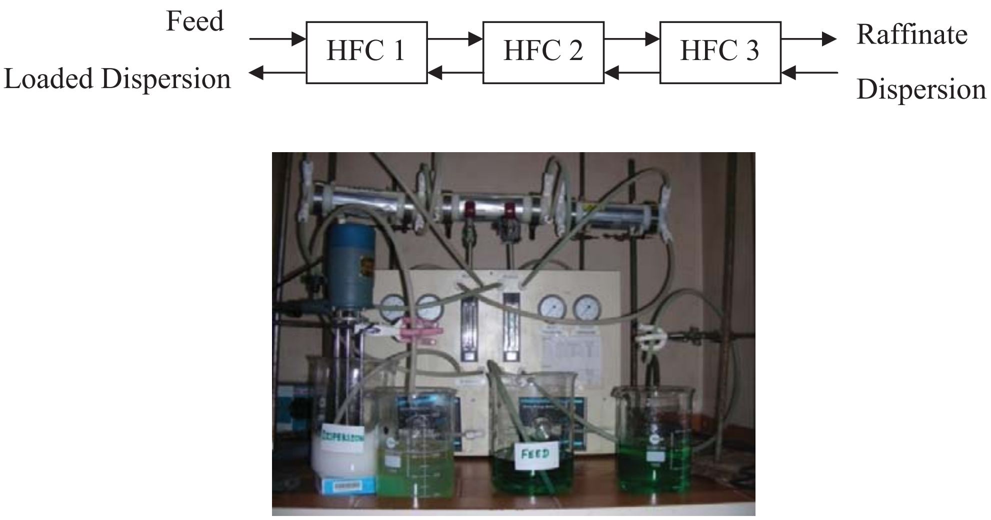

(a)

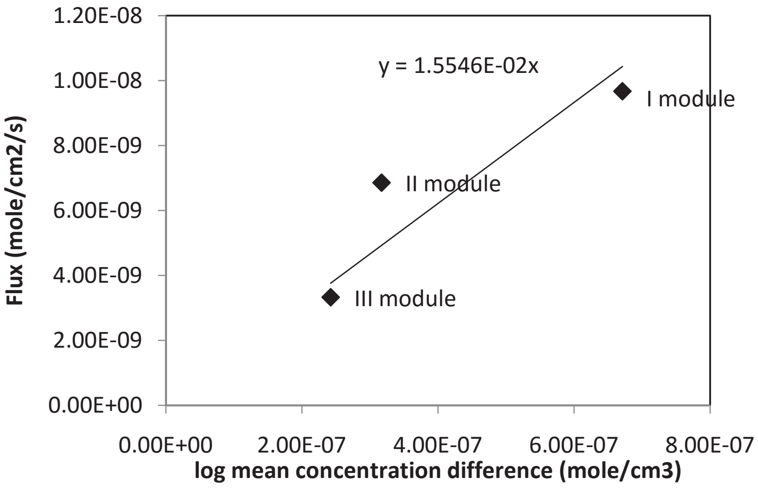

(b)

Figure 6.9: Series multiplication of hollow fiber contactor, 2.5x8" (interfacial area 0.54 m^2): (a) Schematic of series combination of contactors (b) flux vs. ΔC_{lm}; *feed*: U

raffinate; *dispersion*: aq/org 1:1, aq (1 M $NaHCO_3$), org (30 % v/v TBP in dodecane); *flow rate*: 200 ml/min

Effect of agitation speed: Figure 6.10 presents the data showing the effect of agitation speed of dispersion on uranium transport with the three 2.5x8" contactors combined in series. It has been observed that with increase in agitation speed from 3000 to 5000 rpm, due to continuous decrease in drop size, mass transfer improves. Further, on increasing speed to 6000 rpm, mass transport decreases. Reason might be the formation of rigid spheres like drops, which hinders the mass transfer. Hence, optimum speed of dispersion preparation may be selected as 5000 rpm. It can be seen that concentration of uranium in the source solution has been brought down below 0.05 g/l using three such contactors in series.

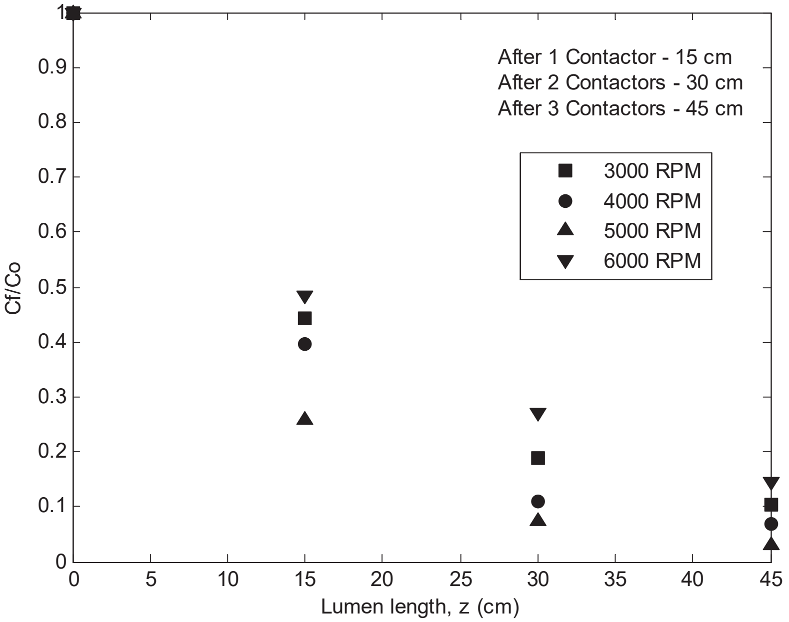

Figure 6.10: Series multiplication of hollow fiber contactor, 2.5x8": Effect of variation in speed of dispersification on Uranium transport; *feed*: U raffinate; *dispersion*: aq/org 1:1, aq (1 M $NaHCO_3$), org (30 % v/v TBP in dodecane); *flow rate*: 200 ml/min

Number multiplication of Hollow fiber contactor 4x13"

A larger HFC 4x13" having specific area 1300 m^2/m^3 (MT area 2.43 m^2, hold up volume 1.87 L) is employed for removal of uranium from waste. Figure 6.11 shows the transport of uranium along lumen length for the array of four 4x13" HFC's combined in series and operated in single pass mode. Smooth line represents the prediction of decrease in feed concentration, C_f/Co; experimental data are shown by symbols. Mass transfer coefficients evaluated from data generated with HFC 2.5x8" are used here for simulation. For each contactor 4x13", effective fiber length is 25 cm and feed flow velocity is 1.23 cm/s. Flux was 6.1e-05 $mol/m^2/s$. Efficiency of module was calculated as 89%. It is found that placing four 4x13" HFC's in series will lead to more than 98 % transport of uranium from feed to strip in single pass mode. It can be seen that the prediction ties in well with the data. Hence, by the model developed, transport performance of such a contactor of any size can be estimated at its effective fiber length for a given carrier concentration.

Figure 6.12 shows the prediction for varying carrier concentrations for re-circulating mode. More than 98 % uranium is transported from feed to strip in 10 minutes with the use of 30 % TBP as carrier agent. Data tie in well with the prediction. Developed model could be used to understand the performance of contactor of any size with known properties in a common and unified way.

The present work shows the successful number and size scale-up of HFDLM system to recovery of uranium from actual raffinate streams of uranium metal plant. Process mass transfer coefficient of uranium was experimentally found to be 2.174e-02 cm/s, which was in good agreement with the predicted value (2.49e-02 cm/s) from model. The magnitude of transport coefficient for aqueous film is found to be higher than the organic membrane phase by order of 2. Hence, the solute transport is membrane diffusion controlled. More than 98 % transport of uranium was obtained from lean source solution in 10 minutes with the use of 30 %

TBP as carrier agent. Model is able to predict the rate of transport of a cation from feed to strip through immobilized liquid membrane with varying process (DLM) parameters like carrier concentration, flow rates of feed and strip i.e. treat ratio, A/O ratio of dispersion, feed side concentrations of metal ion and acidity, strippant and volume of feed and with varying equipment (HFC) parameters like, specific area m^2/m^3, hold up volume, fiber MOC, porosity, tortousity, fiber length, fiber inner diameter, its wall thickness and number of fibers. The present modeling showed it’s utility for optimization and scale-up of the process by limited experimental trial runs.

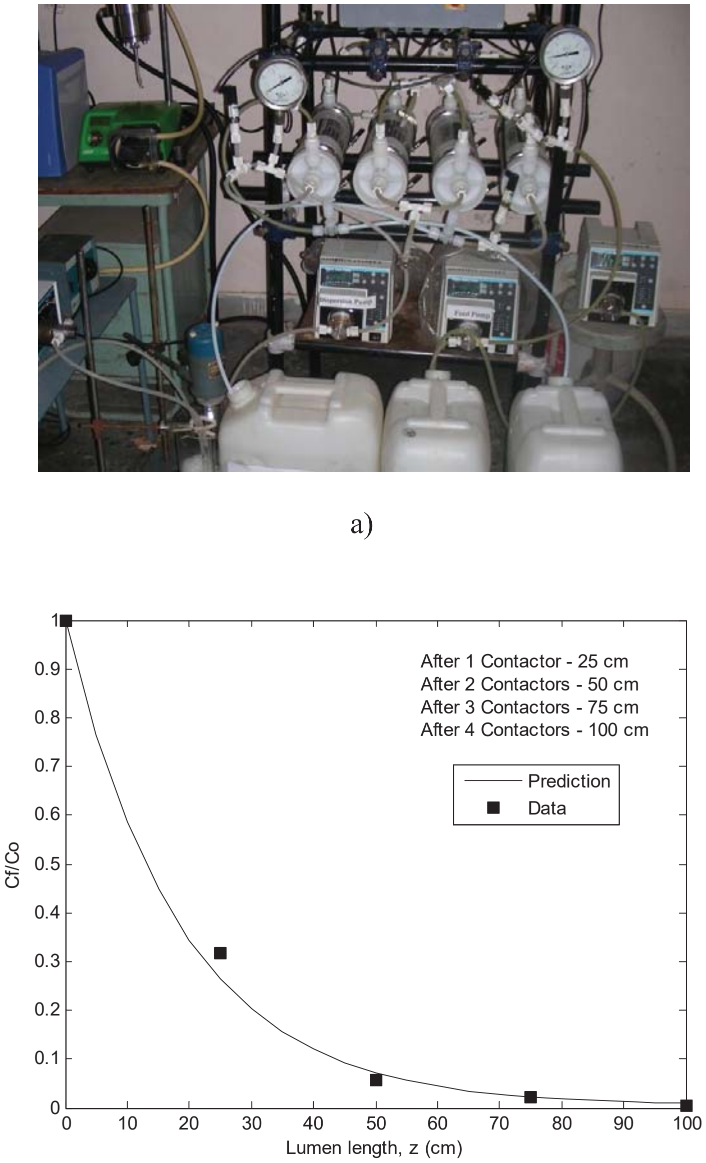

a)

b)

Figure 6.11: Series multiplication of hollow fiber contactor, 4x13" (interfacial area 2.54 m^2): a) photograph of experimental set up, b) Transport of uranium with lumen length; *feed*: U raffinate; *dispersion*: aq/org 1:1, aq (1 M $NaHCO_3$), org (30 % v/v TBP in dodecane); *flow rate*: 1000 ml/min

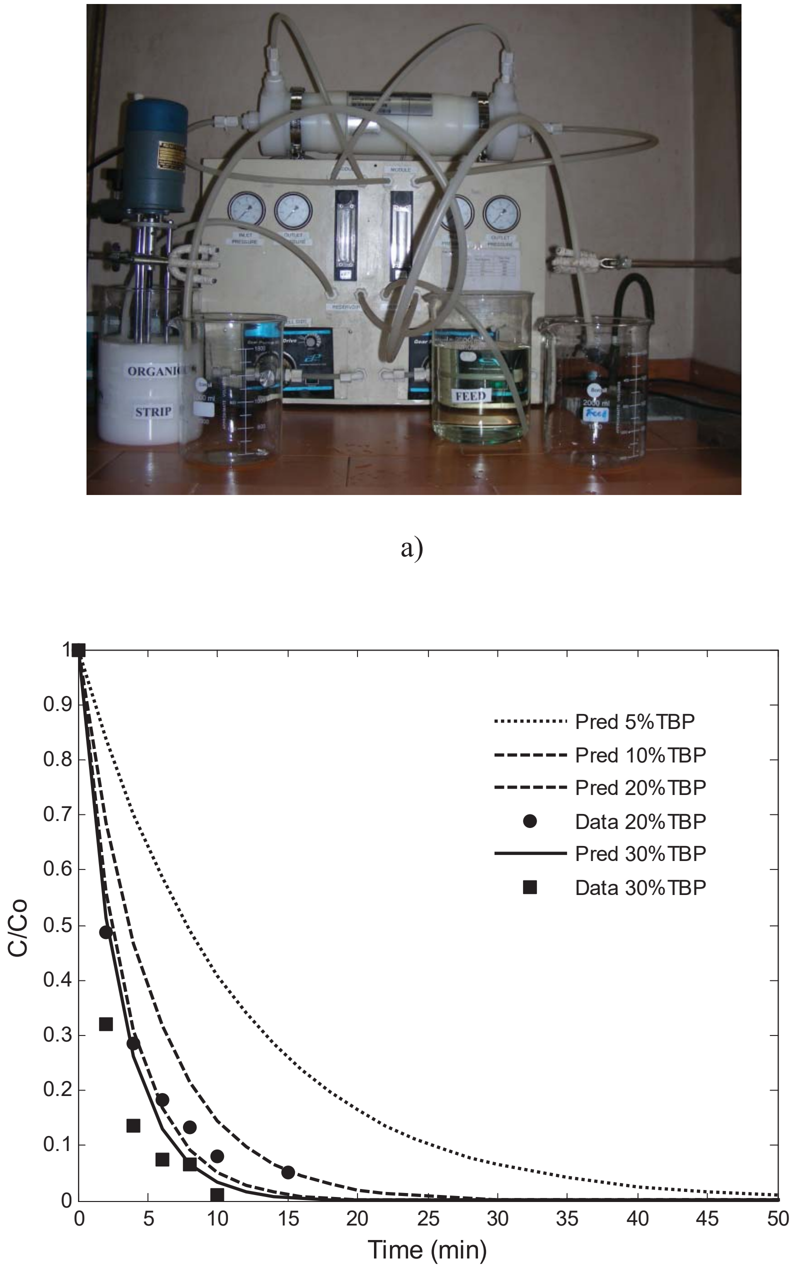

a)

b)

Figure 6.12: a) Photograph of large scale HFDLM facility with contactor 4x13”

b) Transport of uranium with time using contactor 4x13” at different carrier concentrations; *feed*: U Raffinate; *dispersion*: strip/org 1:1, strip (1 M NaHCO$_3$), org (TBP in dodecane); *flow rate* (shell and tube side): 1000 ml/min, *Volume of feed and dispersion* = 2000 ml

CONCLUSION

We concluded that after a certain drop diameter, the rate of coalescence of drops becomes equal to the rate of their breakage. Effect of surfactant becomes negligible in this region. At carrier concentration of 10 % v/v, both the ligands TiAP and TBP have the same interfacial tension and yet, smaller water drops produced with TiAP. This is due to the fact that the branched iso amyl chains of TiAP produce greater steric hindrance to coalescence than the linear chains of TBP. It is seen that with increase in the concentration of TBP, the drop diameter increases. This is because of possible displacement of SPAN80 by TBP due to their high concentration. Since, TBP is not as effective as SPAN80 to prevent drop coalescence, due to its shorter hydrocarbon chains, the drop size increases as concentration of TBP in the solution increases. A similar behavior is also observed with TiAP.

The drop diameter decreases with increase in concentration of SPAN80 until a threshold concentration is reached, beyond which increase in SPAN80 has no effect on drop diameter. The concentration of SPAN80 needed to reach the threshold increases with increase in the concentration of the carrier. Higher, is the concentration of the carrier, greater is the concentration of the surfactant needed to displace it and hence the threshold value is higher. Both TBP and TiAP show similar trend.

A mathematical model has been developed for estimation of the wetted length of the fiber pore. Developed model is not system specific and can be used for prediction of extraction rate of other ions and other types of polymeric membranes. It is found that 40 % of the pore length is wetted by the organic phase in polysulfone contactor. Similarly, for polypropylene contactor, consisting hydrophobic polypropylene lumen, α is estimated to be 1.1. This implies that in the case of polypropylene membrane, the entire length of the pore is wetted by the organic phase. Polypropylene module is found to exhibit greater extent of extraction than polysulfone. This is because, the fiber wall thickness of PP lumen is one order of magnitude less than that of the PS lumen. Hence, the reduction in the rate of diffusion of uranium ions due to higher value of α in PP lumen is overcompensated by its shorter pore length. It has also been understood that for polymeric membranes with higher ε/τ, extraction of solute will be less dependent on the fraction of the pore length wetted by the organic membrane phase. The model has been utilized to predict the performance of PS and PP hollow fiber contactor, respectively, on their scale up. The magnitude of transport coefficient for aqueous film is found to be one order of magnitude higher than the organic membrane phase. Hence, the solute transport is membrane diffusion controlled.

Efficacy of TiAP as a carrier for extraction of U(VI) from acidic plant raffinate has been evaluated in comparison to TBP. On the positive side, TiAP has a greater affinity for U(VI) compared to TBP with dodecane as solvent. On the negative side, TiAP has a higher propensity to extract nitric acid into dodecane, which reduces the driving force for extraction. These two factors appear to balance each other when the extraction is performed on a uranium plant raffinate containing 1.5 M nitric acid using hollow fiber extractor, where both TBP and TiAP perform almost identically. However, there are many lean uranium streams which have low acidity and we expect TiAP to perform better than TBP in those cases. In addition, considering the other advantages of TiAP over TBP viz. lower aqueous solubility and low rates of degradation on exposure to radiation, we can conclude that TiAP is a promising carrier in dispersion liquid membrane process for recovery/enrichment of U(VI) from acidic raffinates of uranium refining plants.

The present work also shows potential of application of dispersed liquid membrane system in HF contactor to recovery of uranium from actual raffinate streams of Uranium Metal Plant. DLM in hollow fiber contactor, with the sodium carbonate/ bicarbonate as strip phase dispersed in 10% TBP in dodecane as the organic extractant provides complete recovery of uranium from dilute feed solution. The process shows good stability during operation with low consumption of organic. While the process is efficient due to high surface area for extraction as well as stripping, the energy consumption is low due to mild agitation for dispersion and ease of phase disengagement after pertraction.

The developed model is able to predict the transport of uranium in HFDLM system under various operating conditions. The film resistance values have been estimated independently using physical properties of system, contactor characteristics and hydrodynamic conditions. The model is unique in simplicity and versatility. It will be useful for generation of data for scale up and design of the system.

Thus, dispersion liquid membrane in Hollow-fiber module (HFDLM) seems to be a promising configuration in terms of stability, simplicity and cost of operation for treatment of such kind of lean wastes. Sustained studies are required on material and geometry of lumens and structural configuration of Hollow Fiber contactor in order to establish its applicability for wider range of aqueous and organic streams.

The present work also shows the successful number and size scale-up of HFDLM system to recovery of uranium from actual raffinate streams of uranium metal plant. Process mass transfer coefficient of uranium was experimentally found to be 2.174e-02 cm/s, which was in good agreement with the predicted value (2.49e-02 cm/s) from model. The magnitude of transport coefficient for aqueous film is found to be higher than the organic membrane phase by order of 2. Hence, the solute transport is membrane diffusion controlled. More than 98 % transport of uranium was obtained from lean source solution in 10 minutes with the use of 30 % TBP as carrier agent. Model is able to predict the rate of transport of a cation from feed to strip through immobilized liquid membrane with varying process (DLM) parameters like carrier concentration, flow rates of feed and strip i.e. treat ratio, A/O ratio of dispersion, feed side concentrations of metal ion and acidity, strippant and volume of feed and with varying equipment (HFC) parameters like, specific area m^2/m^3, hold up volume, fiber MOC, porosity, tortousity, fiber length, fiber inner diameter, its wall thickness and number of fibers. The present modeling showed it's utility for optimization and scale-up of the process by limited experimental trial runs.

NOMENCLATURE

a_1, $a_2$and a_{lm} *inner, outer and log mean area of fiber lumen,respectively,cm^2*

C_f *concentration of UO_2^{2+}in feed phase, M*

C_o *concentration of UO_2^{2+}in organic phase, M*

C_s *concentration of UO_2^{2+}in strip phase, M*

C_{if} *concentration of UO_2^{2+} at aqueous side of feed-membrane interface, M*

C_{io} *concentration of UO_2^{2+}atorganic side of feed-membrane interface, M*

C_{is} *concentration of UO_2^{2+} at membrane-strip interface, M*

d_f *feed film thickness, cm*

d_o *organic film thickness, cm*

d_s *strip film thickness, cm*

D_f *distribution coefficient of UO_2^{2+}between feed and membrane phases*

D_s *distribution coefficient of UO_2^{2+}between membrane and strip phases*

$\mathscr{D}_f$ *diffusion coefficient of UO_2^{2+} in the aqueous phase cm^2/s*

$\mathscr{D}_o$ *diffusion coefficient of $UO_2(NO_3)_2$.2TBP complex in the organic membrane, cm^2/s*

J *flux of UO_2^{2+}through the liquid membrane present in pores, mol/cm^2-s*

k_f *mass transfer coefficient on feed side, cm/s*

k_o *mass transfer coefficient through membrane phase, cm/s*

k_s *mass transfer coefficient between membrane phase and strip droplet, cm/s*

l *effective length of the fiber lumen, cm*

n_f *total number of hollow fibers in the contactor*

PP *polypropylene*

PS *polysulfone*

r_1 *inner radius of fiber, cm*

r_2 *outer radius of fiber, cm*

v *linear feed velocity, cm·s^{-1}*

$\dot{V}$ *volumetric flow rate, cm^3/s*

z *length measured along axis of fiber, cm*

L *fiber wall thickness or pore length, cm*

L_f *fiber wall thickness wetted by aqueous feed solution, cm*

L_o *fiber wall thickness wetted by organic membrane liquid, cm*

α *fraction of the pore length wetted by the organic membrane phase*

ε *porosity of hollow fiber*

τ *tortuosity of hollow fiber*

DLM *dispersion liquid membrane*

HF *hollow fiber*

TBP *Tri-n-butyl phosphate*

TiAP *Tri iso amyl phosphate*

Appendix A

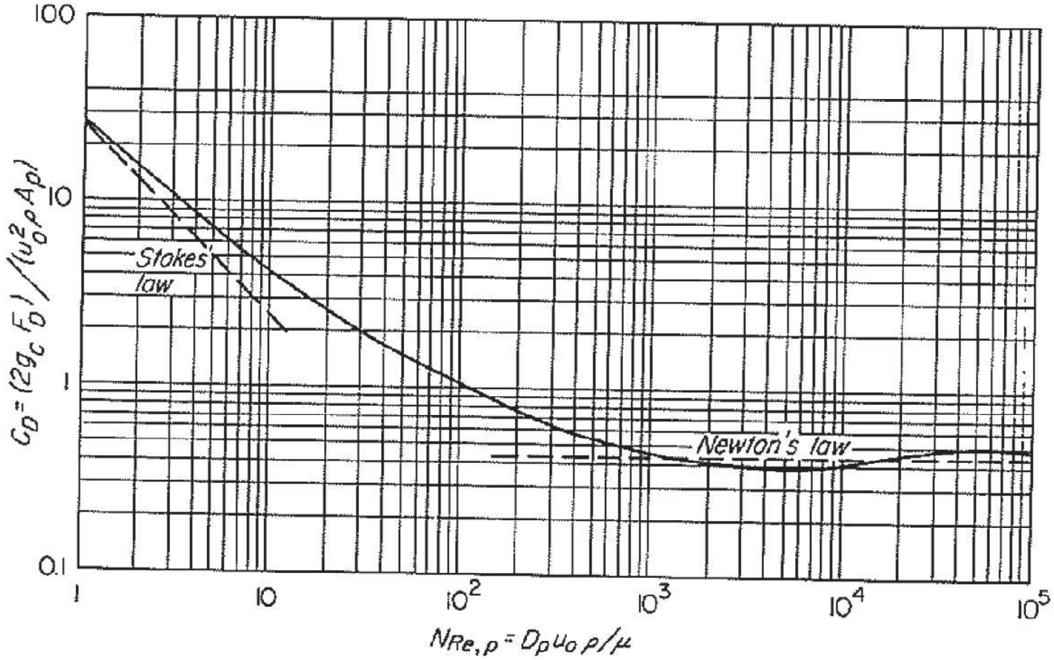

Figure A: drag coefficient versus reynolds number (unit operations of chemical engineering, McCabe Smith, 5th edition, pg 158)

REFERENCES

[1] M.M. Hedges, Uranium exploration and production: a review of innovation, Transactions of the Institutions of Mining and Metallurgy, Section B, 117(2), 2008, pp. 51-54.

[2] H.C. Hayworth, W.S. Ho, W.A. Burns, N.N. Li, Extraction of uranium from wet process phosphoric acid by liquid membranes, Sep. Sci. Technol., 18, 1983, pp. 493-521.

[3] X.J. Yang, A.G. Fane, K. Soldenhoff, Comparison of liquid membrane processes for metal separations: permeability, stability, and selectivity, Ind. Eng. Chem. Res., 42, 2003, pp. 392-403.

[4] S.E. Kentish, G.W. Stevens, Innovations in separations technology for the recycling and re-use of liquid waste streams, Chem. Eng. J., 84, 2001, pp. 149-159.

[5] A. Gabelman, S-T.Hwang, Hollow-fiber membrane contactors, J. Membr. Sci., 159, 1999, pp. 61-106.

[6] K.K. Sirkar, Membranes, phase interfaces, and separations: novel techniques and membranes – an overview, Ind. Eng. Chem. Res., 47, 2008, pp. 5250-5266.

[7] W.S.W. Ho, T.K. Poddar, New Membrane Technology for removal and recovery of chromium for waste waters, Environ. Prog., 20, 2001, pp. 44.

[8] S-Y.B. Hu, J.M. Wiencek, Emulsion-liquid-membrane extraction of copper using a hollow-fiber contactor, AICHE J., 44, 1998, pp. 570-581.

[9] G.E. Charles, S.G. Mason, The coalescence of liquid drops with flat liquid/liquid interfaces, Journal of Colloid Science, 15, 1960, pp. 236-267.

[10] O. Reynolds, On the theory of lubrication and its application to Mr. Beauchamp's towers experiments, Phil. Trans. R. Soc. Lond., 177, 1886, pp. 157.

[11] T. Gillespie, E.K. Rideal, The coalescence of drops at an oil-water interface, Transactions of the Faraday Society, 52, 1956, pp. 173-183.

[12] P. Ghosh, V.A. Juvekar, Analysis of the drop-rest phenomenon, Trans. I. Chem. E., 80, 2002, pp. 715-728.

[13] O. Mengual, G. Meunier, I. Cayre, K. Puech, P. Snabre, Characterization of instability of concentrated dispersions by a new optical analyzer: The Turbiscan MA 1000, Colloids Surf., A: Physicochem.Eng. Aspects., 152, 1999, pp. 111-123.

[14] O. Mengual, G. Meunier, I. Cayre, K. Puech, P. Snabre, Turbiscan MA 2000: multiple light scattering measurement for concentration emulsion and suspension instability analysis, Talanta, 50, 1999, pp. 445- 456.

[15] C. Bordes, F. Garcia, P. Snabre, C. Frances, Online characterization of particle size during an ultrafine wet grinder process, Powder Technol., 128, 2002, pp. 218-228.

[16] C. Lemarchand, P. Convreur, C. Vauthier, D. Costantini, R. Gref, Study of emulsion stabilization by graft co- polymer using the optical analyzer Turbiscan, Int. J. Pharm., 254, 2003, pp. 77-82.

[17] A. Abbas, D. Nobbs, J.A. Romagnoli, Investigation on on-line optical particle characterization in reaction and cooling crystallization systems, Current state of art. Meas. Sci. Technol., 13, 2002, pp. 349-356.

[18] J. Liu, X.F. Huang, L.J. Lu, M.X. Li, J.C. Xu, H.P. Deng, Turbiscan Lab Expert analysis of the biological demulsification of a water-in-oil emulsion by two biodemulsifiers, J. Hazard. Mater., 190, 2011, pp. 214-221.

[19] S.H. Hasan, J.P. Shukla, Tri-iso-amyl phosphate (TAP): An alternative extractant to tri-butyl phosphate (TBP) for reactor fuel processing, J. Radioanal. Nucl. Chem., 258(3), 2003, pp. 563-573.

[20] A. Suresh, C.V.S. Brahmmananda Rao, B. Srinivasulu, N.L. Sreenivasan, S. Subramaniam, K.N. Sabharwal, N. Sivaraman, T.G. Srinivasan, R. Natarajan, P.R. Vasudeva

Rao, Development of alternate extractants for separation of actinides, Energy Procedia., 39, 2013, pp. 120-126.

[21] T.K. Sahoo, T.G. Srinivasan, Effect of temperature on the extraction of uranium by TiAP/n-dodecane, Desalination and Water Treatment, 12, 2009, pp. 40-44.

[22] A. Sengupta, R. Basu, K.K. Sirkar, Separation of solutes from aqueous solutions by contained liquid membranes, AICHE J., 34(10), 1988, pp. 1698-1708.

[23] R. Prasad, S. Khare, A. Sengupta, K.K. Sirkar, Novel liquid-in-pore configurations in membrane solvent extraction, AICHE J., 36(10), 1990, pp. 1592-1596.

[24] Q. Yang, N.M. Kocherginsky, Copper recovery and spent ammoniacal etchant regeneration based on hollow fiber supported liquid membrane technology: from bench-scale to pilot-scale tests, J. Membr. Sci., 286, 2006, pp. 301-309.

[25] A. Sengupta, P.A. Peterson, B.D. Miller, J. Schneider, Jr.C.W. Fulk, Large-scale application of membrane contactors for gas transfer from or to ultrapure water, Separ. Purif. Technol., 14, 1998, pp. 189-200.

[26] A.F. Seibert, J.R. Fair, Scale-up of hollow fiber extractors, Separ. Sci. Technol., 32 (1-4), 1997, pp. 573-583.

[27] P. Kandwal, S.A. Ansari, P.K. Mohapatra, A highly efficient supported liquid membrane system for near quantitative recovery of radio-strontium from acidic feeds. Part II: Scale up and mass transfer modeling in hollow fiber configuration, Journal of Membrane Science, 405-406, 2012, pp. 85-91.

[28] Christie J. Geankoplis, Transport processes and unit operations, Prentice Hall of India, 3rd ed., 2002, pp. 400-412.

[29] E.L. Cussler, Diffusion-Mass transfer in fluid systems, Cambridge University Press: New York, 1st ed., 1988.

[30] Formulaction, Stability of pigment inkjet inks, Application paper, 1-5, 2009.

[31] A.Z. Tasic, B.D. Djordjevic, D.K. Grozdanic, N. Radojkovic, Use of mixing rules in predicting refractive indices and specific refractivities for some binary liquid mixtures, J. Chem. Eng. Data., 37, 1992, pp. 310-313.

[32] S.C. Roy, J.V. Sonawane, N.S. Rathore, A.K. Pabby, P. Janardan, R.D. Changrani, P.K. Dey, S.R. Bharadwaj, Pseudo-Emulsion based hollow fiber strip dispersion technique: optimization, modelling and application of PEHFSD for recovery of U(VI) from process effluent, Sep. Sci. Technol., 43, 2008, pp. 3305-3332.

[33] S. Dixit, S. Mukhopadhyay, S. Govalkar, K.T. Shenoy, H. Rao, S.K. Ghosh, A mathematical model for pertraction of uranium in hollow fiber contactor using TBP, Desalination and Water Treatment, 38, 2012, pp. 195-206.

[34] N.M. Kocherginsky, Q. Yang, L. Seelam, Recent advances in supported liquid membrane technology, Sep. Purif. Technol., 53, 2007, pp. 171-177.

[35] A.K. Dinkar, P.K. Mohapatra, A. Dakshinamoorthy, V.K. Manchanda, Transport of Americium(III) across SLM containing CMPO as the carrier extractant, Desalination and Water Treatment, 12, 2009, pp. 73-78.

[36] Surekha Chowta, P.K. Mohapatra, B.S. Tomar, K.M. Michael, A. Dakshinamoorthy, V.K. Manchanda, Pre-concentration of Americium(III) from low acid solutions using an emulsion liquid membrane containing PC-88A as the carrier extractant, Desalination and Water Treatment, 12, 2009, pp. 62-67.

[37] C. Hill, J-F. Dozol, H. Rouquette, S. Eymard, B. Tournois, Study of the stability of some supported liquid membranes, J. Membr. Sci., 114, 1996, pp. 73-80.

[38] F.F. Zha, A.G. Fane, C.J.D. Fell, Effect of surface tension gradients on stability of supported liquid membranes, J. Membr. Sci., 107, 1995, pp. 75-86.

[39] P.R. Danesi, L. Reichley-Yinger, P.G. Rickert, Lifetime of supported liquid membranes: the influence of interfacial properties, chemical composition and water transport on the long-term stability of the membranes, J. Membr. Sci., 31, 1987, pp. 117-145.

[40] R. Klaassen, A.E. Jansen, The membrane contactor: environmental applications and possibilities, Environ. Prog., 20, 2001, pp. 37.

[41] Y. Lv, X. Yu, S. Tu, J. Yan, E. Dahlquist, Wetting of polypropylene hollow fiber membrane contactors, J. Membr. Sci., 362, 2010, pp. 444-452.

[42] M. R. Esfahani, H. A. Stretz, M. J. M. Wells, Comparing humic acid and protein fouling on polysulfone ultrafiltration membranes: Adsorption and reversibility, J. Water Process Engineering, 6, 2015, pp. 83-92.

[43] M. R. Esfahani, J. L. Tyler, H. A. Stretz, M. J. M. Wells, Effects of a dual nanofiller, nano-TiO2 and MWCNT, for polysulfone-based nano composite membranes for water purification, Desalination, 372, 2015, pp. 47-56.

[44] S. Mukhopadhyay, S. K. Ghosh, V. A. Juvekar, Mathematical model for swelling in a liquid emulsion membrane system, Desalination, 232, 2008, pp. 110-127.

[45] W. Davis, Jr., J. Mrochek, R. R. Judkins, Thermodynamics of the two-phase system: water-uranyl nitrate- tributyl phosphate-Amsco 125-82, J. Inorg. Nucl. Chem., 32, 1970, pp. 1689.

[46] N.S. Rathore, J.V. Sonawane, Anil Kumar, A.K. Venugopalan, R.K. Singh, D.D. Bajpai, J.P. Shukla, Hollow fiber supported liquid membrane: a novel technique for separation and recovery of plutonium from aqueous acidic wastes, J. Membr. Sci., 189, 2001, pp. 119.

[47] A. Ghazi, Al-Enezi, M.S.E. Abdo, Mass transfer measurements around a single cylinder in cross flow at low reynolds numbers, Chemie Ingenieur Technik, 63, 1991, pp. 381-384.

[48] S. Dixit, S. Mukhopadhyay, K.T. Shenoy, V. A. Juvekar, A Process intensified technique of Liquid Membrane employed in in-house Hollow Fiber Contactor, Desalination and water treatment, 79, 2017, pp. 40-48

[49] S. Dixit, R. Chinchale, S. Govalkar, S. Mukhopadhyay,K. T. Shenoy, H. Rao, S. K. Ghosh, A mathematical model for size and number scale up of hollow fiber modules for the recovery of uranium from acidic nuclear waste using the DLM technique, Separ. Sci. Technol., 48, 2013, pp. 2444-2453

[50] Rakesh K. Benadict, A. Suresh, PR Vasudeva Rao, Extraction and stripping behavior of tri-iso-amyl phosphate and tri-n-butyl phosphate in n-dodecane with U(VI) in nitric acid media, Radiochim. Acta., 102(7), 2014, pp. 619-628.

[51] S.V. Bagawde, P.R. Vasudeva Rao, V.V. Ramakrishna, S.K. Patil, The effect of temperature on the extraction of uranium (VI) from nitric acid by tri-n-butyl phosphate, J. Inorg. Nucl. Chem., 40, 1978, pp. 1913-1918.

[52] T.K. Rout, D.K. Sengupta, G. Kaur, S. Kumar, Enhanced removal of dissolved metal ions in radioactive effluents by flocculation, International Journal of Mineral Processing, 80(2-4), 2006, pp. 215-222.

[53] J.M. Wiencek, S-Y. Hu, Emulsion liquid membrane extraction in a hollow-fiber contactor, Chem. Eng. Technol., 23, 2000, pp. 551-553.

[54] J.V. Sonawane, A.K. Pabby, A.M. Sastre, Au(I) extraction by LIX-79/n-heptane using the pseudo-emulsion-based hollow-fiber strip dispersion (PEHFSD) technique, J. Membr. Sci., 300, 2007, pp. 147-155.

[55] J.V. Sonawane, A.K. Pabby, A.M. Sastre, Pseudo-emulsion based hollow fiber strip dispersion: a novel methodology for gold recovery, AICHE J., 54(2), 2008, pp. 453-463.

[56] F.J. Alguacil, M. Alonso, F.A. Lopez, A. Lopez-Delgado, Application of pseudo-emulsion based hollow fiber strip dispersion (PEHFSD) for recovery of Cr(III) from alkaline solutions, Separ. Purif. Technol., 66, 2009, pp. 586-590.

[57] R. Gonzalez, A. Cerpa, F.J. Alguacil, Nickel(II) removal by mixtures of Acorga M5640 and DP8R in pseudo-emulsion based hollow fiber with strip dispersion technology, Chemosphere, 81 (9), 2010, pp. 1164-1169.

[58] J.V. Sonawane, A.K. Pabby, A.M. Sastre, Pseudo-emulsion based hollow fiber strip dispersion (PEHFSD) technique for permeation of Cr(VI) using cyanex-923 as carrier, Journal of Hazardous Materials, 174, 2010, pp. 541-547.

[59] F.J. Alguacil, M. Alonso, F.A. Lopez, A. Lopez-Delgado, I. Padilla, H. Tayibi, Pseudo-emulsion based hollow-fiber with strip dispersion pertraction of iron(III) using $(PJMTH^+)_2$ (SO_4^{2-}) ionic liquid as carrier, Chemical Engineering Journal, 157, 2010, pp. 366-372.

[60] H. Matsuoka, M. Aizawa, S. Suzuki, Uphill transport of uranium across a liquid membrane, J. Membr. Sci., 7, 1985, pp. 11.

[61] T. Huang, C. Huang, The mechanism of transport of uranyl nitrate across a solid supported liquid membrane using tributyl phosphate as mobile carrier, J. Membr. Sci., 29, 1986, pp. 295.

[62] E.A. Fouad, H.-J. Bart, Emulsion liquid membrane extraction of zinc by a hollow-fiber contactor, J. Membr. Sci., 307, 2008, pp. 156-168.

[63] M. Reis, A. Teresa, Jorge M. R. Carvalho, Modelling of zinc extractions from sulfate solutions with bis (2-ethylhexyl) thiophosphoric acid by emulsion liquid membranes, J. Membr. Sci., 237, 2004, pp. 97-107.

[64] S.C. Lee, B.S. Ahn, W.K. Lee, Mathematical modelling of silver extraction by an emulsion liquid membrane process, J. Membr. Sci., 114, 1996, pp. 171-185.

[65] J.P. Shukla, S.K. Misra, Carrier-mediated transport of uranyl ions across tributyl phosphate-dodecane liquid membranes, J. Membr. Sci., 64, 1991, pp. 93.

[66] R.K. Sinnott, Coulson & Richardson's Chemical Engineering Vol. 6 Chemical Engineering Design, Butterworth-Heinemann, Oxford, 3rd ed., 1999.

[67] N. Swain, D. Panda, S.K. Singh, V. Chakravortty, Viscosity and density of tri-n-butyl phosphate + benzene + o-xylene from 30 ^{0}C to 45 ^{0}C, J. Chem. Eng. Data, 42, 1997, pp. 1235.

[68] P.E. Liley, G.H. Thomson, D.G. Friend, T.E. Daubert, E. Buck, in: R.H. Perry, D.W. Green, J.O. Maloney (Eds.), Perry's Chemical Engineer's Handbook, McGraw Hill, U. S. A., 1997, pp. 7-374.

[69] W.L. McCabe, J.C. Smith, P. Harriott, Unit Operations of Chemical Engineering, McGraw Hill, U. S. A., 7th ed., 2005, pp. 278.

[70] S. Dixit, A. Khanna, Y.S. Sistla, S. Mukhopadhyay, P.K. Bhattacharya, Modeling and prediction of removal of metal ions from aqueous solution through facilitated transport, Int. J. Environmental Engineering, 2, 2010, pp. 73-91.

[71] N. Mortimer, Uranium resource economics: An application of energy analysis, Resources Policy, 6(1), 1980, pp. 19-32.

[72] D. Melo, W. Burkart, Uranium: Environmental pollution and health effects. Encyclopedia of environmental health, 2011, pp. 526-533.

[73] P. Kandwal, S. Dixit, S. Mukhopadhyay, P.K. Mohapatra, Mass transport modeling of Cs(I) through hollow fiber supported liquid membrane containing calix-[4]-bis(2,3-naptho)-crown-6 as the mobile carrier, Chemical Engineering Journal, 174(1), 2011, pp. 110-116.

[74] P. Kandwal, S. Dixit, S. Mukhopadhyay, P.K. Mohapatra, V.K. Manchanda, Mathematical modeling of Cs(I) transport through flat sheet supported liquid membrane using calix-[4]-bis(2,3-naptho)-18-crown-6 as the mobile carrier, Desalination, 278(1–3), 2011, pp. 405-411.

[75] A. Apelblat, M. Faraggi, Extraction in the system: uranyl nitrate - nitric acid- tributyl phosphate - diluents, J. Nuclear Energy, 20, 1966, pp. 55.

[76] G.R.M. Breembroek, A. van Straalen, G.J. Witkamp, G.M. van. Rosmalen, Extraction of cadmium and copper using hollow fiber supported liquid membranes, J. Membr. Sci., 146, 1998, pp. 185-195.

[77] S. Panja, P.K. Mohapatra, P. Kandwal, S.C. Tripathi, Uranium (VI) pertraction across a supported liquid membrane containing a branched diglycolamide carrier extractant: Part III mass transfer modeling, Desalination, 285, 2012, pp. 213-218.

[78] K. Ohwada, T. Ishihara, Infra-red spectrophotometry of uranyl nitrate/ tri-n-butyl phosphate in organic solvents, J. inorg. nucl. Chem., 28, 1966, pp. 2343-2345.

[79] P. R. Danesi, E. P. Horwitz, P. G. Rickert, Rate and mechanism of facilitated americium (III) transport through a supported liquid membrane containing a bifunctional organophosphorous mobile carrier, J. Phys. Chem., 87, 1983, pp. 4708.

Thesis Highlight

Name of the student: Smita Mishra
Name of the CI: BARC, Mumbai **Enrolment No.**: ENGG01201004017
Thesis Title: Mass transfer and coalescence in liquid-liquid systems with relevance to dispersion liquid membrane in hollow fiber contactor
Discipline: Engineering Sciences **Sub-area of discipline**: Chemical Engineering
Date of viva voce: 9/10/2018

1. Processes involving facilitated transport through dispersion liquid membranes, in hollow fiber contactors, are advantageous over conventional processes for separation of valuable metals from lean streams. In liquid membrane based transport process, fraction of the pore length wetted by the organic liquid membrane phase is important in deciding the rate of extraction. A mathematical model has been developed for determining the rate of transport through the membrane and the extent of extraction through the contactor as a function of the fraction of the pore length wetted by the organic membrane phase. The data has been generated for extraction of uranium from nitric acid in countercurrent once-through mode using hollow fiber dispersion liquid membrane.

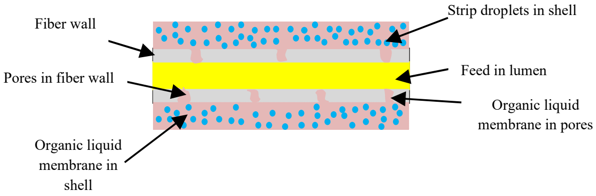

Figure 1

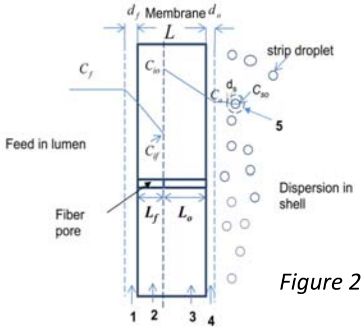

Figure 2

Figure 1: An enlarged view of the dispersion liquid membrane in hollow fiber contactor
Figure 2: Schematic representation of transport of metal ion through the hollow fiber membrane; 1- diffusion film at feed-membrane interface, 2-region of the pore filled with feed solution, 3-region of the pore filled with organic liquid, 4- diffusion film at organic membrane interface, 5-diffusion film at strip-organic interface

2. Low rates of coalescence are desirable to achieve high stability of dispersion in dispersion liquid membrane processes. The rate of drop-coalescence depends on the nature and concentration of the adsorbed species at the drop-organic phase interface. When the organic phase contains more than one surface active species, there would be competition among them to occupy interface. Moreover, different surface active species, depending on the structure of their hydrophobic tail, have different ability to prevent coalescence. In the present work, two different techniques have been used to study stability of emulsion. In the first, time of fall of drop of aqueous phase through an organic pool and its coalescence with its bulk phase has been studied with a typical liquid-liquid extraction system. The second technique involves use of an optical instrument 'Turbiscan Online' to characterize the liquid dispersions using multiple light scattering. Based on these studies, it was possible to arrive at the optimal formulation of the dispersion and method of emulsification.

Figure 3: Schematic of the experimental facility and video image of the drop resting at the interface